DEVELOPMENTS IN AND APPLICATIONS OF CAPILLARY ELECTROPHORESIS INDUCTIVELY COUPLED PLASMA MASS SPECTROMETRY

By Karen Anne Taylor

A Doctoral Thesis submitted in partial fulfilment
of the requirements for the award of Doctor of Philosophy of
Loughborough University

August 1999

ACKNOWLEDGEMENTS

ABSTRACT

This project has set out to design and optimise a robust and efficient interface for capillary electrophoresis-inductively coupled plasma mass spectrometry (CE-ICP-MS) and to investigate the application of the technique in elemental speciation studies.

An interface was constructed using a commercial microconcentric nebuliser (MCN) and a cyclonic spray chamber. The cyclonic spray chamber was designed specifically to provide rapid sample response and washout and to minimise sample dispersion. Isoforms of the heavy metal binding protein, metallothionein, were separated and the bound metals detected to characterise the interface. Suction from the self-aspirating nebuliser was identified as the principal factor controlling electrophoretic resolution. To maintain resolution, two methods for counterbalancing the nebuliser suction were investigated. In the first method an optimised make-up flow was employed, and in the second a negative pressure was applied to the buffer vial during the separation. The negative pressure method was preferred because it did not significantly compromise sensitivity. The MCN was found to be prone to regular blocking which compromised the analytical precision of the system.

A second interface was constructed using a glass MicroMist nebuliser. The MicroMist nebuliser was found to be less prone to blocking than the MCN and significantly improved the precision of the system to less than 4.3 % RSD. The MicroMist nebuliser did, however, provide a lower sensitivity. The advantage of employing an electroosmotic flow marker to correct for migration time drifts was demonstrated.

A CE-ICP-MS method was developed for the speciation of selenium in selenium enriched yeasts and nutritional supplements. Selenoamino acids and inorganic selenium species were separated, as anions, under strong electroosmotic flow conditions. Methods to enhance the selenium sensitivity were investigated. A proteolytic enzyme extraction method was employed and the effect of the mass of enzyme and extraction temperature on the extraction efficiency was investigated. The chemical form of selenium present in the samples varied; inorganic selenate was identified as the chemical form of selenium in two of the samples, and for one sample selenomethionine was the predominant form of selenium. For one selenium enriched yeast sample, a matrix effect hindered the speciation.

Selenium speciation in the selenium enriched yeasts and nutritional supplements was also undertaken using anion exchange HPLC-ICP-MS to allow a comparison of the two speciation techniques.

CONTENTS

PRESENTATIONS AND PUBLICATIONS

CHAPTER ONE

Research Background and Rationale

1.0 INTRODUCTION

The role of trace metals in environmental and biological systems has been the focus of much research over the past few decades. This research has led to the realisation that information on a metal, based uniquely on its total concentration, does not provide a valid representation of its chemical, biological and toxicological activity. The potentially harmful effects of the speciation (i.e. chemical form) of trace metals in toxicology were recognised after the death of 50 residents of a fishing village in Japan who suffered from the biomethylation of mercury in their food.[1] The spillage of tetraalkyl lead in the Mediterranean highlighted the dangers of organic forms of lead[2] and extinction of the oyster population in the Arcachon Bay in France stimulated interest in the possible release of butyltins from antifouling paints.[3]

Elemental speciation can be termed as the identification and quantification of the different oxidation states and/or chemical forms of a given element. Significant progress has been made in elemental speciation by the direct coupling of chromatographic separation techniques to powerful elemental detectors such as inductively coupled plasma mass spectrometry (ICP-MS). The use of chromatography hyphenated with ICP-MS has been comprehensively reviewed by several authors.[4-8] Speciation analysis in a variety of matrices has been undertaken using ICP-MS hyphenated with gas chromatography (GC),[9-12] supercritical fluid chromatography (SFC)[13,14] and

1

the various modes of high performance liquid chromatography (HPLC).[15-20]

The coupling of HPLC to ICP-MS is relatively simple and can be accomplished with a piece of tubing connecting the analytical column to the nebuliser. The hyphenated technique offers all the advantages of ICP-MS i.e. low limits of detection, wide linear dynamic range and ability to perform isotopic analyses, but does, however, suffer from a number of limitations:

♦ It is often necessary to compromise the chromatographic conditions for effective compatibility between the mobile phase and ICP-MS. Mobile phases with a high salt content can block the nebuliser, and erode the sampler and skimmer cones thereby influencing the ion beam and sensitivity. Mobile phases containing high levels of organic solvent can cause plasma instability, increased reflected power values and may deposit carbon on the sampler cone.

♦ Identification of species is by retention behaviour alone and is thus dependent upon *a priori* information and the availability of standards.

♦ Depending upon the mode of HPLC, it may only be possible to determine one chemical form i e. anionic, cationic, polar, non-polar.

♦ LC separations can be slow and poorly resolved.

♦ Interactions between analytes and the stationary phase may destroy or shift the equilibrium, resulting in inaccurate speciation information. This may be particularly problematic for labile complexes where the free and associated forms have different affinities for the stationary phase.

The limitations of HPLC-ICP-MS and the ever increasing demand for accurate speciation information has led to the investigation of capillary electrophoresis-ICP-MS as a potential elemental speciation technique. Capillary electrophoresis (CE) is a separation technique often used as a complimentary technique to LC, but offering a number of advantages in terms of: high efficiency and resolution; speed; small sample volumes (nl); minimal reagent consumption; use of aqueous buffers; and the ability to separate anions, cations and neutral species in one electrophoretic run. In addition, CE may also hold unique promise in terms of speciation by exerting minimal disturbance on the existing equilibrium between analytes thus reducing the possibility of speciation changes during the separation process. The principal drawback of CE is its low sensitivity consequent upon the small sample sizes employed. This is further exacerbated when coupled to flow through detectors by the dilution incurred in transporting the analyte to the detector.

1.1 CAPILLARY ELECTROPHORESIS-ICP-MS

Olesik and co-workers[21] published the first research on CE-ICP-MS in 1995. It was evident from this first publication that the fundamental challenge and key to the analytical success of CE-ICP-MS was in the design of the interface. For effective compatibility with CE, the interface must have a low dead volume, be able to facilitate low flow rates, provide a high analyte transport efficiency and provision must be made for grounding of the capillary.

Olesik *et al.*[21] developed an interface comprising of a concentric glass nebuliser (Meinhard) and a purpose built conical spray chamber. The end of the capillary was inserted inside the nebuliser central tube and grounding was achieved by conducting silver paint applied to the end 5 cm of the capillary. The silver paint proved not to be ideal due to sample contamination. A natural aspiration rate of 2 ml min^{-1} was measured in the interface due to the suction generated by the nebuliser. This was the cause of significant band broadening due to induced laminar flow within the capillary.

Tomlinson *et al.*[22] used an interface similar to that described by Olesik *et al.*[21] Their initial investigations involved applying pressure to the capillary after the electrophoretic separation was accomplished. This approach, however, was not successful because the laminar flow induced by the pressure resulted in a loss of resolution. The group later adapted a glass frit nebuliser to provide electrophoretic separation all the way to the nebuliser. Grounding of the capillary was achieved by the use of a buffer solution which flowed around the capillary forming a coaxial sheath. It was found that the flow rate of the buffer solution had significant effect on the behaviour of the nebuliser; slow flow rates caused pulsing and a high background, whilst higher flow rates diluted the sample. The interface was successfully used to separate lead compounds, however the glass frit nebuliser was not ideal as an interface because of regular clogging and its complex design.

Liu et al.[23] used a direct injection nebuliser (DIN) in a CE-ICP-MS interface where the separation capillary was placed concentrically inside the sample introduction capillary of the DIN. The sample was directly nebulised into the torch thus providing 100 % analyte transport efficiency and accommodating low sample flow rates (10 - 100 μl min^{-1}). Grounding of the capillary was achieved by the use of a coaxial sheath of make-up solution. The make-up solution and EOF were combined inside a 1 mm long section of the DIN sample introduction capillary before nebulisation. Nebuliser suction was not observed, band broadening was minimal and excellent peak shapes were observed. A DIN, designed to operate at solution flow rates of 1 - 15 μl min^{-1}, has also been used in a CE-ICP-MS interface designed by Tangen et al.[24]

Lu et al.[25] developed a concentric glass nebuliser/conical spray chamber interface, similar to that used by the Olesik group. The separation capillary was inserted into the central glass tube of the nebuliser approximately 2 cm from the tip. A second fused silica capillary was inserted coaxially into the nebuliser around the separation capillary so that it reached only as far as the nebuliser gas tube joint. A coaxial sheath of make-up solution provided the electrical continuity. A unique feature of the interface was the variable position of the separation capillary inside the nebuliser. The position of the capillary had a significant influence on signal intensity, resolution and migration time. Signal intensity increased, migration times shortened and resolution was compromised as the capillary was inserted further into the nebuliser. The loss in resolution was due to an increase in the nebuliser suction. It was suggested that the

suction could be counterbalanced by applying a negative pressure to the buffer

vial during the separation. The interface was used to separate the metal binding

proteins, metallothionein and ferritin. Detection limits were in the sub pg

range.

A CE-ICP-MS interface incorporating an ultrasonic nebuliser (USN) was

designed by Lu and Barnes.[26] The sample uptake tube of the commercial USN

was modified to accommodate the separation capillary assembly. The capillary

ground path was provided using a coaxial sheath flow. As described in the

previous interface designed by Lu et al.[25] the position of the separation

capillary was variable inside the nebuliser. However, contrary to the previous

interface, the capillary position did not have a significant effect on the

electrophoretic separation. Further, suction on the capillary as a result of the

nebuliser gas flow observed with the pneumatic nebuliser interface was not

present. The interface was characterised by the separation of metallothioneins

and overall the USN was found to offer improved resolution and sensitivity

compared to the concentric nebuliser interface.[25]

Michalke and Schramel[27] used an interface based on a modified Meinhard

nebuliser where the exact positioning of the separation capillary within the

nebuliser was crucial. A coaxial sheath flow provided the electrical contact and

no detectable suction was identified. The interface was used to separate

selenium and platinum species.

Two different interfaces (one based on a modified concentric nebuliser and low volume cyclone spray chamber, another based on a standard cross-flow nebuliser and Scott-type spray chamber) were described by Majidi and Miller-Ihli.[28] A coaxial sheath buffer flow was employed for grounding the capillary and also to satisfy the liquid flow requirements of the nebulisers. To minimise nebuliser suction and maintain electrophoretic resolution, the pressure differential at the inlet of the cross-flow nebuliser was measured using a water filled manometer. It was found that the nebuliser suction could be controlled by varying the nebuliser gas flow rate. At < 0.7 l min^{-1} a positive pressure at the inlet of the nebuliser was generated, at 0.7 l min^{-1} no pressure differential was observed and at > 0.7 l min^{-1} a negative pressure due to the nebuliser suction was measured. However, since the nebulisation efficiency is directly related to the nebuliser gas flow rate, a compromise exists between sensitivity and resolution. Isoforms of metallothionein were separated using the system and detection limits for Cd in rabbit metallothionein were 2.36 and 0 21 μg ml^{-1} for the concentric and cross-flow nebulisers, respectively.

Van Holderbeke et al.[29] evaluated two different microconcentric nebulisers, a MCN-100 and MicroMist, for use in a CE-ICP-MS interface. The design of the interface was very similar to previous designs[25,30] with a sheath flow providing the ground path. Nebuliser suction was minimised by increasing the sheath flow rate which gave rise to a back pressure in the liquid carrying central tube of the nebuliser. It was noted that for different nebuliser types and even for different nebulisers of the same type, a different suction flow was observed.

7

Thus, it was necessary to optimise the sheath flow rate for each individual nebuliser. A comparison of the two microconcentric nebulisers found that the MCN was more vulnerable to blocking by crystallisation of the buffer salt, was less sensitive to matrix effects and had a slightly lower transport efficiency than the MicroMist nebuliser. The interface was used to separate arsenic species in standards solutions, mineral water, soil leachate and urine.

1.2 PRESENT STUDY

The objectives of the present study were:

♦ To design a CE-ICP-MS interface that conserves the inherent resolution of CE whilst maximising the sensitivity. In addition, the interface must be both analytically and mechanically robust, and simple enough to allow quick installation without modification of the standard ICP torch.

♦ To design and optimise a rapid washout, low dead volume spray chamber suitable for use with the low solution flow rates employed in CE.

♦ To fully characterise and optimise the interface with respect to both CE and ICP-MS operating conditions.

♦ To investigate the application of CE-ICP-MS to elemental speciation studies, with particular reference to the speciation of nutritionally important elements.

REFERENCES

[1] U. Forstner and G. T. W. Wittmann, *Metal Pollution in the Aquatic Environment*, 1983, Springer, Heidelberg.

[2] M. Branica and Z. Konrad, *Lead in the Marine Environment*, 1980, Pergamon, Oxford.

[3] C. Alzieu, J. Sanjuan, P. Michel, M. Borel and J. P. Dreno, *Mar. Pollut. Bull*, 1989, **20**, 22.

[4] S. J. Hill, M. J. Bloxham and P. J. Worsfold, *J. Anal. At Spectrom*, 1993, **8**, 499.

[5] F. A. Byrdy and J. A. Caruso, *Environ. Sci. Technol.*, 1994, **28**, 528A.

[6] K. Sutton, R. M. C. Sutton and J. A Caruso, *J Chromatogr A*, 1997, **789**, 85.

[7] R. Lobinski, *Appl. Spectrosc.*, 1997, **51**, 261A.

[8] G. K. Zoorob, J. W. McKiernan and J. A. Caruso, *Mikrochim. Acta*, 1998, **128**, 145.

[9] A. Prange and E. Jantzen, *J Anal. At. Spectrom*, 1995, **10**, 105.

[10] E. Blake, M. W. Raynor and D. Cornell, *J. High Resolut. Chromatogr.*, 1995, **18**, 33.

[11] H. Tao, T. Murakami, M. Tominaga and A. Miyazaki, *J Anal. At. Spectrom*, 1998, **13**, 1085.

[12] S. Slaets, F. Adams, I. Pereiro and R. Lobinski, *J. Anal At. Spectrom.*, 1999, **14**, 851.

[13] T. De Smaele, L. Moens, R. Dams and P. Sandra, *Fresenius' J Anal. Chem*, 1996, **355**, 778.

[14]U. T. Kumar, N. P. Vela and J. A. Caruso, *J. Chromatogr. Sci*, 1995, **33**, 606.

[15]C. Barnowski, N. Jakubowski, D. Stuewer and J. A. C. Broekaert, *J. Anal. At Spectrom.*, 1997, **12**, 1155.

[16]S. M. Bird, H. Ge, P. C. Uden, J. F. Tyson, E. Block and E. Denoyer, *J. Chromatogr A*, 1997, **789**, 349.

[17]W. Chao and S. Jiang, *J Anal. At. Spectrom.*, 1998, **13**, 1337.

[18]B. P. Jackson and W. P. Miller, *J. Anal. At Spectrom*, 1998, **13**, 1107.

[19]J. Szpunar, P. Pellerin, A. Makarov, T. Doco, P. Williams and R. Lobinski, *J Anal. At. Spectrom*, 1999, **14**, 639.

[20]E. H. Evans, S. Chenery, A. Fisher, J. Marshall, K. Sutton, *J. Anal. At. Spectrom*, 1999, **14**, 977.

[21]J. W. Olesik, J. A. Kinzer and S. V. Olesik, *Anal Chem*, 1995, **67**, 1.

[22]M. J. Tomlinson, L. Lin and J. A. Caruso, *Analyst*, 1995, **120**, 583.

[23]Y. Liu, V. Lopez-Avilia, J. J. Zhu, D. R. Wiederin and W.F. Beckert, *Anal Chem.*, 1995, **67**, 2020.

[24]A. Tangen, W. Lund, B. Joefsson and H. Borg, *J. Chromatogr A*, 1998, **826**, 87.

[25]Q. Lu, S. M. Bird and R. M. Barnes, *Anal Chem.*, 1995, **67**, 2949.

[26]Q. Lu and R. M. Barnes, *Microchemical J.*, 1996, **54**, 129.

[27]B. Michalke and P. Schramel, *Fresenius' J. Anal. Chem*, 1997, **357**, 594.

[28]V. Majidi and N. J. Miller-Ihli, *Analyst*, 1998, **123**, 803.

[29]M. Van Holderbeke, Y. Zhao, F. Vanhaecke, L. Moens, R. Dams and P. Sandra, *J. Anal. At. Spectrom.*, 1999, **14**, 229.

[30]J. A. Kinzer, J. W. Olesik and S. V. Olesik, *Anal. Chem.*, 1996, 68, 3250.

CHAPTER TWO

Capillary Electrophoresis

2.0 INTRODUCTION

Electrophoresis is defined as the migration of charged particles through a solution under the influence of an electric field.[1] Electrophoresis as a separation technique was introduced by Tiselius in 1930.[2] By placing protein mixtures between buffer solutions in a tube and applying an electric field, he found that sample components migrated in a direction and at a rate determined by their charge and mobility. Tiselius noted that the major problem with free solution electrophoresis was that of Joule heating and, for this reason, electrophoresis has been traditionally performed in anti-convective media such as polyacrylamide or agarose gels.

The first demonstration of electrophoretic separation in an open tube or capillary can be credited to Hjerten[3] who, in 1967, demonstrated free solution electrophoresis in 3 mm id tubing. Later, in 1974, Virtanen[4] described the advantages of using smaller diameter capillaries and achieved the separation of alkali cations by free solution electrophoresis in 200 - 500 µm id Pyrex tubing. In 1981, a pioneering paper by Jorgenson and Lukacs[5] provided the first example of high separation efficiency CE where efficiencies in excess of 400000 theoretical plates were obtained using 75 µm id capillary. Following the work by Jorgenson and Lukacs, a rapid growth in the development of CE led to the advent of commercial CE instrumentation in 1989.

2.1 ELECTROPHORETIC MOBILITY

In CE, ions are separated according to their differential velocity in an applied

electric field. The velocity of an ion when subjected to an applied field can be

given by Equation 2.1,

$$v = \mu_e E$$
(Eqn. 2 1)

where, v is the ion velocity, μ_e is the electrophoretic mobility and E is the

electric field strength. The electrophoretic mobility, for a given ion and

medium, is a constant which is characteristic of that ion. The mobility is

determined by the electric force that the ion experiences, balanced by its

frictional drag through the medium. The electric force (F_E) experienced by an

ion of charge q is given by Equation 2.2,

$$F_E = qE$$
(Eqn. 2.2)

and the frictional force (F_F) experienced by a spherical ion is given by Equation

2.3,

$$F_F = -6\pi\eta r v$$
(Eqn. 2.3)

where, η is the solution viscosity and r is the ionic radius. During

electrophoresis, an ion will reach a constant steady state velocity when the

balance of these forces is attained. At this point, the forces are equal but

opposite thus

$$qE = 6\pi\eta r v$$
(Eqn. 2.4)

By solving for velocity and substituting equation 2.4 into equation 2.1, the mobility of an ion is now given by Equation 2.5,

$$\mu_e = \frac{q}{6\pi\eta r}$$
(Eqn. 2.5)

From Equation 2.5 it is evident that the electrophoretic mobility of an ion is governed by two principal factors, charge and size. Because mobility is directly related to charge, a calculated value of the electrophoretic mobility can be determined directly from the degree of dissociation of the ion. A generalised acid-base equilibrium involving an acid BH^+ and it conjugate base B may be written as,

$$B + H^+ \rightleftharpoons BH^+$$

$$\alpha \qquad\qquad 1-\alpha$$
(Eqn 2.6)
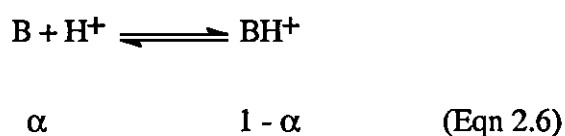
where, α is the degree of dissociation. In a buffer solution, the relative amounts of the acid and base are given by the Henderson - Hasselbach equation:

$$pH = pK_a + \log\frac{\alpha}{1-\alpha}$$
(Eqn. 2.7)

which may be rewritten as

$$\alpha = \left[1 + 10^{(pKa-pH)}\right]^{-1}$$
(Eqn. 2.8)

where, pKa is the acid dissociation constant. The electrophoretic mobility of an ion can therefore be calculated using Equation 2.9,

$$\mu_e = \alpha\mu_B + (1-\alpha)\mu_{BH^+} = (1-\alpha)\mu_{BH^+} \qquad \text{(Eqn. 2.9)}$$

where, μ_{BH^+} and μ_B are the mobilities of the acid and base, respectively.

2.2 ELECTROOSMOTIC FLOW

One of the fundamental processes that drives CE is the electroosmotic flow

(EOF). Electroosmotic flow is the bulk flow of liquid in the capillary and

originates from the electrophoretic movement of the hydrated part of the

electric double layer at the capillary wall.[6] The fused silica capillaries typically

used in CE have ionisable silanol groups at the capillary surface. At pH > 2 the

silanol groups are deprotonated and buffer cations closest to the capillary wall

are attracted as counterions and form an immobile layer (~ 3 - 500 nm wide)

known as the Stern layer. Beyond this is a diffuse mobile layer of cations

which, upon the application of a voltage, migrate in the direction of the

cathode. Since the cations are solvated by water molecules the result is an

overall bulk flow of solution towards the cathode. The potential across the

layers is known as the zeta potential[3] and is given by the Helmholtz equation

(Equation 2.10),

$$\zeta = \frac{4\pi\eta\mu_{eo}}{\varepsilon} \qquad \text{(Eqn. 2.10)}$$

where, ζ is the zeta potential, μ_{eo} is the electroosmotic mobility, ε is the

dielectric constant.

The zeta potential is essentially determined by the surface charge on the

capillary wall and since this charge is strongly pH dependent, the magnitude of

the EOF can be controlled by the pH of the buffer. The zeta potential is also

dependent upon the applied voltage and the ionic strength of the buffer.

Increased ionic strength results in double layer compression, decreased zeta

potential and reduced EOF. An increase in the applied voltage causes the zeta

potential to increase thus increasing the EOF. The magnitude of the EOF can

be expressed by Equation 2.11,

$$\mu_{eo} = \frac{\varepsilon\zeta}{\eta} \qquad\qquad \text{(Eqn. 2.11)}$$

EOF allows the separation of anions, cations and neutral species in one

electrophoretic run since it causes migration of nearly all species, regardless of

charge, in one direction. Under normal conditions (that is, where the capillary

surface is negatively charged) anions will be flushed towards the cathode since

the EOF mobility can be sufficiently high to overcome the electrophoretic

mobility of anions towards the anode. This process is depicted in Fig. 2.1.

A unique feature of electroosmotic flow, that permits the high efficiency of CE,

is its plug-like or flat velocity flow profile. The driving force of the EOF is

uniformly distributed along the entire length of the capillary and, as a result,

there is no pressure drop within the capillary. The flow velocity is therefore

uniform across the capillary except very close to the walls where the flow rate

approaches zero (Fig 2 2). This flat flow profile is beneficial because it does

not directly contribute to the dispersion of solute zones. This is in contrast to
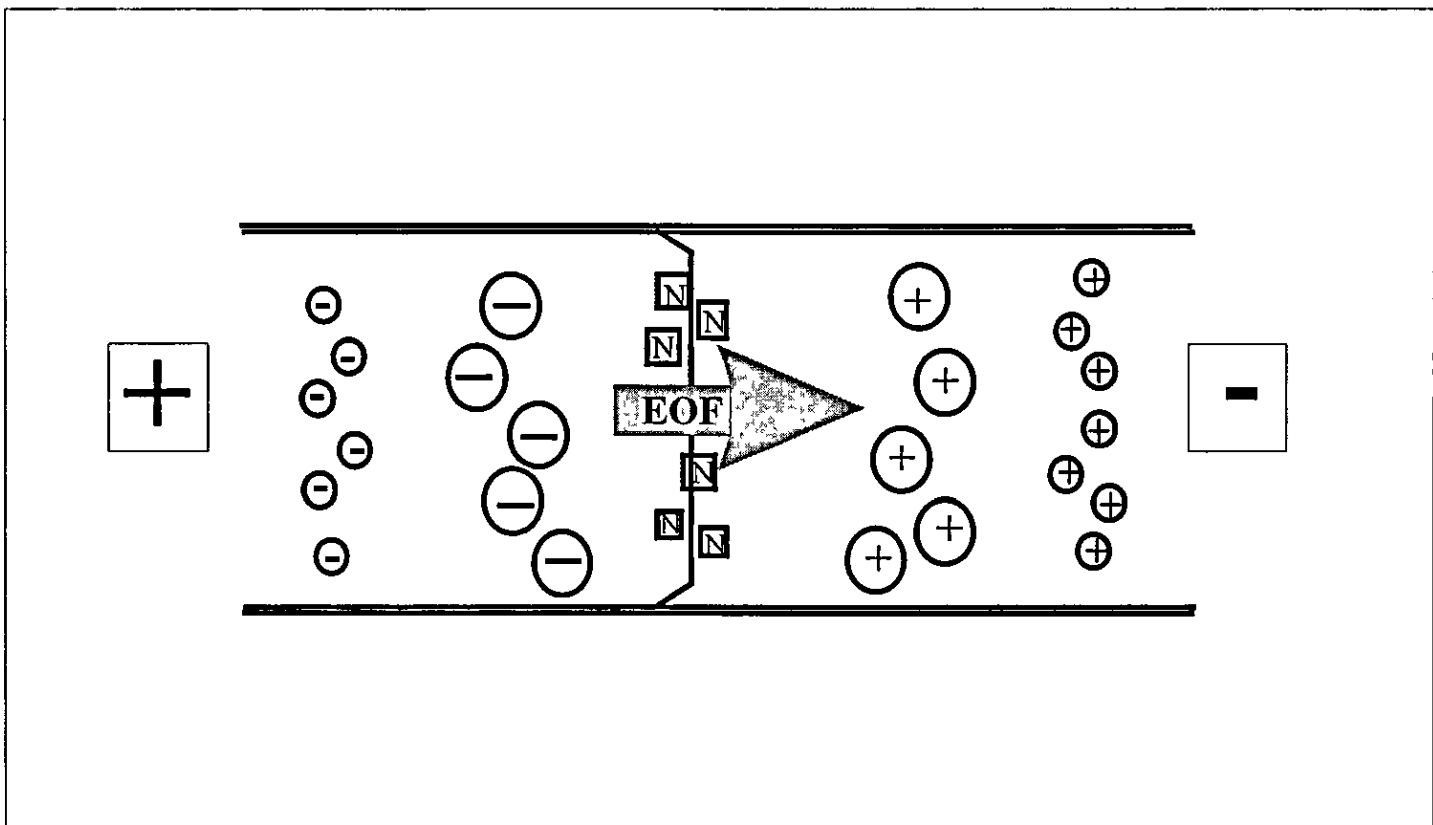
Figure 2.1 Differential solute migration in CE in a fused silica capillary.

pressure-driven systems such as in liquid chromatography where the frictional

forces at the liquid-solid interfaces result in substantial pressure drop and

laminar flow.

EOF
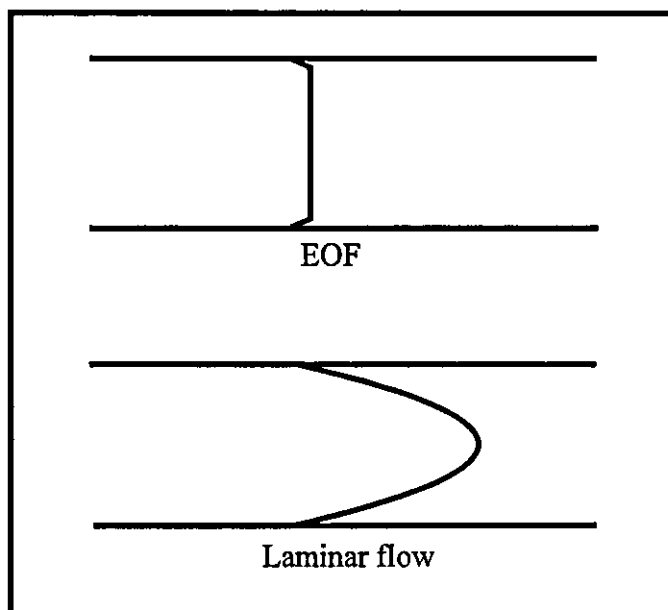
Laminar flow

Figure 2.2. Velocity flow profiles of EOF and laminar flow.

2.3 EFFICIENCY AND RESOLUTION

The absence of laminar flow in CE eliminates dispersion due to radial

diffusion. Similarly, the use of open-tubular capillaries of small id minimises

resistance to mass transfer related dispersion. Thus, the major contributor to

dispersion and band broadening in CE is longitudinal or molecular diffusion.

The width of a peak, described as the variance (σ^2) is therefore related to

molecular diffusion[7,8] according to Equation 2.12,

$$\sigma^2 = 2\,D\,t = \frac{2\,D\,L^2}{\mu_e V} \qquad \text{(Eqn. 2.12)}$$

where, D is the diffusion coefficient, t is the migration time, L is the capillary

length and V is the applied voltage. The peak efficiency, expressed in number

of theoretical plates (N) is given by,

$$N = \frac{L^2}{\sigma^2} = \frac{\mu_e V}{2D}$$

(Eqn. 2.13)

From Equation 2.13, it can be seen that the efficiency is dependent upon

voltage but is independent of capillary length. In addition, efficiency will be

greatest for large molecules such as proteins which have low diffusion

coefficients. The number of theoretical plates can also be determined directly

from an electropherogram using Equation 2.14,

$$N = 5.54 \left(\frac{t}{w_{1/2}} \right)^2$$

(Eqn. 2.14)

where, $w_{1/2}$ is the peak width at half peak height.

The ultimate goal in CE is resolution of sample components. Resolution of two

zones is defined as[5,9]

$$R = \frac{\left(\mu_{ep1} - \mu_{ep2} \right) \left\{ V / \left[L D \left(\mu_{ep} + \mu_{eo} \right) \right] \right\}^{1/2}}{4\sqrt{2}}$$

(Eqn. 2.15)

where, μ_{ep} is the mean electrophoretic mobility of the two solutes of mobilities

μ_{ep1} and μ_{ep2}. According to Equation 2.15, increasing the voltage is not an

effective method for improving resolution because of the square root

relationship. To double the resolution, the voltage must be quadrupled which

may lead to excessive Joule heating.

Separation in CE is primarily driven by efficiency, not selectivity. This is in

contrast to liquid chromatography where the opposite is true. Due to the very

sharp solute zones, small differences in solute mobility (< 0.05 % in some

cases) are often sufficient for complete resolution.[10] The resolution can also be

expressed with respect to efficiency,

$$R = \frac{1}{4}N^{1/2}\left(\frac{\Delta t}{t}\right)$$
(Eqn. 2.16)

2.3.1 Factors Affecting Efficiency

Whilst longitudinal diffusion is the principal source of dispersion in CE, a

number of other factors can also contribute to dispersion. A summary of the

sources of band broadening and dispersion in CE is presented in Table 2.1. It is

fortunate that these factors are usually controllable by careful selection of

electrophoretic conditions.

Joule Heating

The heat generated by the passage of electrical current through an electrolyte

solution is known as Joule heat. Excessive Joule heating is detrimental in CE

since it leads to intracapillary temperature gradients, local changes in viscosity

and ultimately compromised efficiency. For the types of capillary used in CE,

heat must be dissipated at the interfaces between buffer and the fused silica

Source	Comment
Longitudinal diffusion	• Defines fundamental limit of efficiency • Solutes with lower diffusion coefficients form narrower zones
Joule heating	• Leads to temperature gradients and laminar flow
Injection plug length	• Injection plug length should be less than the dispersion caused by diffusion, approximately 1 to 2 % of the total capillary length
Solute-wall interactions	• Interaction of solute with capillary walls often leads to peak tailing
Electromigration	• Solutes with higher conductivities than the run buffer result in fronted peaks • Solutes with lower conductivities than the run buffer result in tailing peaks
Unlevel buffer vials	• Generates laminar flow

Table 2.1. Sources of band broadening in CE.

wall, between the fused silica and the polyimide coating and between the polyimide coating and the surroundings. The centre of the capillary will be hotter than the periphery and, since the viscosity of most fluids is inversely proportional to the temperature, the viscosity of the buffer at the centre of the capillary will be lower than that near the walls. Thus, zone deformation occurs and the velocity flow profile tends to that of laminar flow. In addition to intracapillary temperature gradients, Joule heating can also cause a gradual

temperature rise in the capillary which leads to changes in viscosity and ultimately imprecise migration times.

The contribution of Joule heating to dispersion has been extensively studied by several authors.[11-14] Losses in efficiency arising from Joule heating effects can be minimised by employing low field strengths, low ionic strength buffers and small id capillaries, typically 50 μm. Most commercial CE instruments also have forced air or liquid cooling systems to minimise heating effects.[15,16]

Electromigration

Electromigration dispersion arises as a result of differences in sample zone and run buffer conductivities. This phenomena, also known as electrophoretic dispersion,[17] electrokinetic dispersion,[18] electrodispersive effects[19] and concentration overload,[20] leads to asymmetric peak shapes. An analyte X will provide a fronting peak if its mobility (μ_x) is greater than the mobility of the buffer co-ion (μ_{bge}), and a tailing peak if $\mu_x < \mu_{bge}$.[17,21] When the solute zone has a higher mobility (that is higher conductivity) than that of the run buffer the front edge of the solute zone, which diffuses in the direction of migration, encounters a higher field strength when entering the buffer zone. This causes the diffusing solute to accelerate away from the solute zone and results in zone fronting. As the solutes at the trailing edge diffuse into the run buffer they also encounter a higher field but in the same direction of migration and thus accelerate back into the solute zone leaving the trailing edge sharp. Similar reasoning accounts for the peak tailing observed when $\mu_x < \mu_{bge}$.

Peak shape distortions arising as a result of electromigration can only be eliminated by matching the run buffer and sample conductivities.

Solute-Wall Interactions

Interactions between solutes and the capillary surface silanol groups are detrimental in CE. Depending on the extent of the interaction, peak tailing and even irreversible adsorption of the solute can occur. Peak distortion of non-adsorbing species may also result as the wall pollution causes disruption of the electrical double layer with concomitant non-uniformity in the axial disruption of the zeta potential; this is particularly true in the first few centimetres of capillary where the bulk of the irreversible adsorption occurs. Adsorption is especially problematic for proteins and peptides because these species possess numerous cationic sites and hydrophobic moieties. The nature of protein-wall interactions has been investigated by Zhao *et al.*[22] The theoretical plate height (H) affected by adsorption deteriorates such that,

$$H \propto v, v_{eo}, t_{ad}, (C^2 - C^3) \qquad \text{(Eqn. 2.17)}$$

where, t_{ad} is the mean residence time of the adsorbed solute and C is the fractional concentration of the free solute.

In order to reduce solute-wall interactions, a number of strategies have been employed. By increasing the concentration of the buffer, interactions are reduced due to a reduction in the effective surface charge, however this approach is limited by the increased current and subsequent Joule heating.[23,24]

Alternatively, zwitterionic salts with low conductivities can be added to the buffer at relatively high concentrations without adverse heating effects.[25]

Operation at extreme pH has also been successful in reducing interactions. At low pH (< 2-3) the silanol groups are protonated and uncharged, whilst at high pH (> 9-10) both the wall and sample will be deprotonated and anionic thus interactions will be limited by charge repulsion. A further method employed to alleviate adsorption effects is modification of the capillary wall, either by permanent covalently bonded or physically adhered phases, or by dynamic deactivation using buffer additives (see Section 2.4.1).

2.4 BUFFER COMPOSITION

The nature of the buffer is of fundamental importance in an electrophoretic separation since it determines both the magnitude and direction of the EOF and the migration behaviour of solutes. The suitability of a buffer depends upon a number of factors including, the solubility and stability of analytes, effect of pH and ionic strength, influence of buffer ions on electromigration, and heat generation.[26]

The buffer pH has a substantial effect upon the magnitude and direction of the EOF and the degree of ionisation of solutes. The EOF velocity increases with increasing pH, reaching an optimum around pH 9. The utilisation of a high pH and strong EOF allows the separation of anions, cations and neutral species in one electrophoretic run. Alterations in pH are particularly useful for

zwitterionic species such as peptides and proteins. The pH determines the

charge and therefore direction of migration of zwitterionic species. At a pH

equal to the isoelectric point (pI) a zwitterionic solute will have no net charge;

above the pI it will carry a negative charge and below it will be positive.

Buffer pH can also be used to optimise separations by maximising the

difference in charge status between ionisable analytes.[27,28] If the pKa values of

the analytes are known, the charge status of each analyte at different pH's can

be calculated using the Henderson-Hasselbach equation (Equation 2.8).

The ionic strength of the buffer influences the EOF velocity and the

electrophoretic mobility of solutes.[29] It has been shown that in general the

observed mobility of a solute is inversely related to the buffer concentration[30]

approximately given by,

$$\mu_e \approx \frac{e}{3 \times 10^7 |Z| \eta \sqrt{C}}$$
(Eqn. 2.18)

where, e is the excess charge in solution per unit area, Z is the effective charge

of the ion and C is the molar concentration. Ions in solution are surrounded by

a layer of counter-ions which migrate in a direction opposite to the central ion.

Since the counter-ions are solvated, a viscous drag is experienced by the central

ion which retards its migration.[31] This effect, known as the electrophoresis

effect, is increased with increasing concentration of counter-ions.

2.4.1 Buffer Additives

Buffer additives are employed in CE in order to perform one or more of the following functions; modify the electrophoretic mobility of solutes, modify the direction and magnitude of the EOF, solubilise analytes, reduce or eliminate solute-wall interactions. A wide variety of additives are currently used, the most common of which are given in Table 2.2.

Surfactants (anionic, cationic, zwitterionic and non-ionic) are among the most widely used buffer additives, particularly in micellar electrokinetic chromatography (MEKC). At concentrations below the critical micelle concentration (CMC) monomer ionic surfactant molceules can act as solubilising agents for hydrophobic solutes, as ion-pairing reagents or as wall modifiers   The interaction of the solute with the surfactant can occur either via ionic interactions with the charged end of the surfactant or through hydrophobic interactions between the alkyl chain and hydrophobic moieties of the solute. Surfactants can also be used to adsorb onto the capillary wall modifying the EOF and also limiting solute-wall interactions. Depending upon the charge of the surfactant, the EOF can be increased, reduced or reversed. Surfactant concentrations above the CMC are employed in MEKC (see Section 2 5.1) to separate both neutral and charged solutes.

The addition of organic solvents to the buffer permits the analysis of solutes that are not normally aqueous soluble and also reduces the magnitude of the EOF. The EOF reduction is more significant with increasing concentration of

Additive	Example	Function
Surfactants	Anionic SDS Cationic CTAB	• EOF modification • Solubilise hydrophobic solutes • Above CMC used in MEKC • Ion pairing
Zwitterionic substances	MES, Tris, CHAPS	• Alter selectivity of proteins
Organic modifiers	Methanol, acetonitrile	• Modify EOF • Alter selectivity • Solubiliser
Metal ions	Cu^{2+}, K^+, Na^+, Ca^{2+}	• Alter selectivity
Linear hydrophobic polymers	Methyl cellulose, polyacrylamide	• Reduce EOF • Allow size selectivity • Minimise adsorption
Complexing buffers	Borate	• Carbohydrate and phenolic compounds separation
Chiral selectors	Cyclodextrins, crown ethers, bile salts	• Chiral separations • Solubilisation of hydrophobic solutes
Quaternary amines	Diaminopropane	• EOF reversal • Ion pairing

Table 2.2. Buffer additives in CE.

27

organic solvent and with alcohol chain length[1]. Alcohols have the greatest use

in MEKC where they are employed to alter the selectivity of a separation.

Sodium tetraborate and boric acid are commonly used buffers in CE, however

at high concentrations they have also been used to facilitate the separation of

carbohydrates and phenolic compounds due to borate complexation with the

receptive hydroxyl groups.[32]

Attempts to provide more size selectivity in CE have relied upon the addition

of dilute polymer solutions to the buffer.[33] These polymer solutions generally

act by forming a solubilised, mobilised entangled network within the buffer

which effectively acts as a molecular sieve and retards larger solutes as they

pass through

The separation of structural, positional and stereo isomers can be carried out by

the inclusion of chiral selectors into CE buffers. Chiral resolution is achieved

by stereoselective interactions between the solute and chiral selector. The most

widely used chiral selectors are cyclodextrins. Cyclodextrins are cyclic chiral

carbohydrates consisting of a hollow truncated cone with a central hydrophobic

cavity. Chiral selectivity results from inclusion of a hydrophobic portion of the

solute into the cavity and also from hydrogen bonding interactions with

secondary chiral hydroxyl groups on the circumference of the cyclodextrin.

The nature of the interactions between cyclodextrins and chiral solutes has been

investigated by a number of workers.[34-36] Chiral selectivity and resolution can

be altered by changing the type of cyclodextrin, the cyclodextrin concentration,

and the temperature

2.5 SEPARATION MODES

2.5.1 Micellar Electrokinetic Chromatography (MEKC)

MEKC is a hybrid of electrophoresis and liquid chromatography, and was

introduced in 1984 by Terabe and co-workers.[37] MEKC greatly extents the

capabilities of CE since it can separate both neutral and charged solutes. The

separation is accomplished by the use of surfactants in the run buffer, the most

common of which is sodium dodecyl sulphate (SDS). At concentrations above

the CMC the surfactant molecules organise, to lower the free energy of the

system, into aggregates known as micelles. Micelles are essentially spherical

with the hydrophobic tails of the surfactant oriented towards the centre to avoid

interaction with the hydrophilic buffer, and the charged head groups oriented

towards the buffer. The micelles, depending upon their charge, will migrate

either with or against the EOF.

Neutral solutes are separated on the basis of their chromatographic partitioning

between the micellar pseudostationary phase and buffer. Solutes migrate with a

velocity that is dependent upon the distribution coefficient of the micellar

solubilisation. The ratio of the total moles of solute in the micelle to those in

the buffer is given by the capacity factor (k'),

$$k' = \frac{(t_r - t_0)}{t_0\left(1 - \frac{t_r}{t_m}\right)} = K\left(\frac{V_s}{V_m}\right) \qquad \text{(Eqn. 2.19)}$$

where, t_r is the migration time of the solute, t_0 is the migration time of

unretained solute moving at the EOF rate, t_m is the micelle migration time, K is

the partition coefficient, V_s is the volume of the micellar phase and V_m is the

volume of the buffer.

Selectivity in MEKC can be altered by varying the physical nature (that is, size,

charge, geometry) of the micelle by using different surfactants. In addition,

variations in pH, buffer concentration, temperature and the use of buffer

additives can alter selectivity in MEKC.

2.5.2 Capillary Isoelectric Focusing (CIEF)

In CIEF, ampholytic species such as peptides and proteins are separated on the

basis of their isoelectric points (pI values). Sample ions are mixed with carrier

ampholytes that span the desired pH range, and the mixture is loaded onto the

EOF suppressed capillary. The anodic end of the capillary is placed into an

acidic solution and the cathodic end into a basic solution. Upon the application

of a voltage, a pH gradient is formed and the sample ions focus concurrently at

a pH where they become electrically neutral (at their pI). Focused sample

zones are then mobilised towards the detector by either application of a

pressure or by adding a salt solution to exploit the principle of

electroneutrality.[10]

2.5.3 Capillary Isotachophoresis (CITP)

CITP is a moving boundary electrophoretic technique where a combination of two buffers is used to create a state in which separated zones all move at the same velocity. The discrete samples zones are sandwiched between a leading electrolyte which has a mobility greater than any of the sample components, and a terminating electrolyte whose mobility is less than the sample components. A steady state velocity develops in CITP since the electric field varies in each zone. The field is self-adjusting to maintain constant velocity, with the lowest field across the zone with the highest mobility. This phenomenon maintains very sharp boundaries between discrete zones and thus leads to a very high separation efficiency and resolution.

2.5.4 Capillary Gel Electrophoresis (CGE)

In CGE, separations are carried out in gel filled capillaries which act as a molecular sieve and produce size-based separations. The gel acts as an anti-convective medium, minimising solute diffusion, and preventing solute-wall adsorption thus very high efficiencies can be achieved. The technique, however, is only applicable to charged solutes due to the suppression of the EOF. Large biomolecules such as DNA oligomers and proteins are the most amenable analytes for CGE.

2.5.5 Capillary Electrochromatography (CEC)

CEC was first demonstrated in 1974 by Pretorius et al.[38] as a hybrid separation technique combining the stationary phase of liquid chromatography with the

31

electrically driven mobile phase of CE. In CEC, the capillary is packed with a HPLC type stationary phase and the separation mechanism becomes that of HPLC partitioning in combination with electrophoretic mobility. The technique offers very high efficiency and resolution as a result of the electroosmotic driven flow and small diameter stationary phase particles (< 3 µm). However, a drawback of the technique is the difficulty of obtaining adequate and reproducible EOF. CEC can separate both charged and neutral species and has been used increasingly in the pharmaceutical industry for the analysis of neutral products and related impurities.[39-41]

2.6 METAL SPECIATION APPLICATIONS

The realisation that CE may offer unique advantages over HPLC in terms of speciation, by exerting minimal disturbance on the existing equilibrium between analytes, has led to increased application of the technique for speciation studies. CE, in combination with both UV and element specific detectors, has been used for the speciation of individual metals, and for the characterisation of metal ion interactions with biological and naturally occurring macromolecules. A comprehensive review of the application of CE to metal speciation studies has been published by Dabek-Zlotorzynska et al.[42]

CE has been used for the speciation of selenium in: tap water,[43] human milk,[44,45] bacterial suspensions,[46] and serum;[45] arsenic in: urine,[47,48] coal fly ash,[49] tin mining water,[50] soil leachate[48] and ground water;[51] mercury in: marine samples[52] and contaminated sediments;[53] tin in: sea sand[54] and soil;[55] lead in: soil[55] and

drain water[56] and platinum in: soil[57-59] and serum[60]. CE has also been used for

the characterisation of metalloproteins[61-63] and metal complexes of

pharmaceutical interest,[64] and in metal-chelate studies.[65,66]

REFERENCES

[1]S. F. Y. Li, *Capillary Electrophoresis, Principles, Practice and Applications,* Journal of Chromatography Library Vol. 52, 1992, Elsevier, Amsterdam.

[2]A. Tiselius, *Trans. Faraday Soc.,* 1937, **33**, 524.

[3]S. Hjerten, *Chromatogr. Rev.,* 1967, **9**, 122.

[4]R. Virtanen, *Acta Polytech. Scand.,* 1974, **123**, 1.

[5]J. W. Jorgenson and K. D. Lukacs, *Anal. Chem.,* 1981, **53**, 1298.

[6]B. L. Karger and F. Foret, *Capillary Electrophoresis Technology,* Chromatographic Science Series, Vol. 64, 1993, Marcel Dekker Inc., New York.

[7]S. Hjerten, *Electrophoresis,* 1991, **11**, 665.

[8]R. A. Wallingford and A. G. Ewing, *Adv. Chromatogr.,* 1989, **29**, 1.

[9]J. W. Jorgenson and K. D. Lukacs, *Science*, 1983, **222**, 266.

[10]D. N. Heiger, *High Performance Capillary Electrophoresis*, 1992, Hewlett-Packard, France.

[11]F. Foret, M. Deml and P. Bocek, *J. Chromatogr.,* 1988, **452**, 601.

[12]E. Grushka, R. McCormick and J. Kirkland, *Anal. Chem.,* 1989, **61**, 241.

[13]J. H. Knox, *Chromatographia,* 1988, **26**, 329.

[14]A. E. Jones and E. Grushka, *J. Chromatogr.,* 1989, **466**, 219.

[15]D. M. Goodall, D. K. Lloyd and S. J. Williams, *LC-GC (Int.),* 1990, **3**, 28.

[16]W. G. Kuhr and C. A. Monnig, *Anal. Chem.,* 1992, **64**, 389R

[17]W. Thormann, *Electrophoresis,* 1983, **4**, 383.

[18]G. O. Roberts, P. H. Rhodes and R. S. Snyder. *J Chromatogr.,* 1989, **480**, 35.

[19]J. L. Beckers, *Electrophoresis*, 1995, **16**, 1987.

[20]H. Poppe, *Anal Chem*, 1992, **64**, 1980.

[21]F. E. P. Mikkers, F. M. Everaerts and T. P. Verheggen, *J Chromatogr*, 1979, **169**, 1.

[22]Z. Zhao, A. Malik and L. L. Milton, *Anal. Chem*, 1993, **65**, 2747.

[23]J. S. Green and J. W. Jorgenson, *J. Chromatogr.*, 1989, **478**, 63.

[24]F. A. Chen, L. Kelly, R. Palmieri, R. Biehler and H. E. Schwartz, *J. Liq Chromatogr.*, 1992, **15**, 1143.

[25]M. M. Bushey and J. W. Jorgenson, *J. Chromatogr*, 1989, **480**, 301.

[26]K. Altria, T. Kelly and B. Clark, *LC-GC*, 1996, **10**, 408.

[27]S. A. C. Wren, *Microcol Sep*, 1991, **3**, 147.

[28]A. G. McKillop, R. M. Smith, R. C. Rowe and S. A. C. Wren, *J Chromatogr A*, 1996, **730**, 321.

[29]D. Li, S. Fu and C. A. Lucy, *Anal. Chem*, 1999, **71**, 687.

[30]H. Issaq, G. Atamna, G. Muschik and G. Janini, *Chromatographia*, 1991, **32**, 155.

[31]P. D. Grossman and J. C. Colburn, *Capillary Electrophoresis-Theory and Practice*, 1992, Academic Press Inc., London.

[32]S. Honda, *J. Chromatogr. A*, 1996, **720**, **337.**

[33]W. A. MacCrehan, H. T. Rasmussen and D. M. Northop, *J. Liq Chromatogr.*, 1992, **15**, 1063.

[34]S. A. C Wren and R. C. Rowe, *J. Chromatogr*, 1992, **603**, 363.

[35]S. A. C Wren, R. C. Rowe and R. S. Payne, *Electrophoresis*, 1994, **15**, 774.

[36]S. G. Penn, E. T. Bergstrom, D. M. Goodall and J. S. Loran, *Anal. Chem.,* 1994, **66**, 2866.

[37]S. Terabe, K. Otsuka, K. Ichikawa, A. Tsuchiya and T. Ando, *Anal. Chem.,* 1984, **56**, 111.

[38]V. Pretorius, B. J. Hopkins and J. D. Schielie, *J. Chromatogr.,* 1974, **99**, 23.

[39]J. Wang, D. E. Schaufelberger and N. C. Guzman, *J. Chromatogr. Sci.,* 1998, **36**, 155.

[40]J. H. Miyawa, D. K. Lloyd and M. S. Alasandro, *J. High Resolut. Chromatogr.,* 1998, **21**, 161.

[41]M. Euerby, C. M. Johnson, K. D. Bartle, P. Myers and S. Roulin, *Anal. Commun.,* 1996, **33**, 403.

[42]E. Dabek-Zlotorzynska, E. P. C. Lai and A. R. Timberbaev, *Anal. Chim. Acta,* 1998, **359**, 1.

[43]K. Li and S. F. Y. Li, *Analyst,* 1995, **120**, 361.

[44]B. Michalke, *Fresenius' J. Anal. Chem.,* 1995, **351**, 670.

[45]B. Michalke and P. Schramel, *J. Chromatogr. A,* 1998, **807**, 341.

[46]E. B. Walker, J. C. Walker, S. E. Zuagg and R. Davidson, *J. Chromatogr. A,* 1996, **745**, 111.

[47]B. Wildman, P. E. Jackson, W. R. Jones and P. G. J. Alden, *J. Chromatogr. A,* 1991, **546**, 459.

[48]M. Van Holderbeke, Y. Zhao, F. Vanhaecke, L. Moens, R. Dams and P. Sandra, *J. Anal. At. Spectrom.,* 1999, **14**, 229.

[49]L. Lin, J. Wang and J. Caruso, *J. Chromatogr. Sci.,* 1995, **33**, 177.

[50]D. Schlegel, J. Mattusch and R. Wennrich, *Fresenius' J. Anal. Chem*, 1996, **354**, 535.

[51]Y. M. Huang and C. W. Whang, *Electrophoresis*, 1998, **19**, 2140.

[52]A. M. C. Diaz, R. A. Lorenzo-Ferreira and R. Cela-Torrijos, *Microchim Acta*, 1996, **123**, 73.

[53]E. P. C. Lai and E. Dabek-Zlotorzynska, *Am. Environ. Lab.*, 1996, **6**, 1.

[54]K. S. Whang and C. W. Whang, *Electrophoresis*, 1997, **18**, 241.

[55]K. Li and S. F. Y. Li, *J. Chromatogr. Sci*, 1995, **33**, 309.

[56]C. L. Ng, H. K. Lee and S. F. Y. Li, *J. Chromatogr. A*, 1993, **652**, 547.

[57]B. Michalke and P. Schramel, *Fresenius' J Anal Chem*, 1997, **357**, 594.

[58]B. Michalke, S. Lustig and P. Schramel, *Electrophoresis*, 1997, **18**, 196.

[59]S. Lustig, J. Dekimpe, R. Cornelis, P. Schramel and B. Michalke, *Electrophoresis*, 1999, **20**, 1627.

[60]C. Vogt and G. Werner, *J. Chromatogr A*, 1994, **686**, 325.

[61]Q. H. Lu and R. M. Barnes, *Microchem J*, 1996, **54**, 129.

[62]K. A. Taylor, B. L. Sharp, D. J. Lewis and H. M. Crews, *J. Anal. At. Spectrom*, 1998, **13**, 1095.

[63]M. P. Richards and J. H. Beattie, *J. Chromatogr A*, 1993, **648**, 459.

[64]H. Wittrisch, S. Conradi, E. Rohde, J. Vogt and C. Vogt, *J Chromatogr A*, 1997, **781**, 407.

[65]A. Timerbaev, O. Semenova and G. Bonn, *Chromatographia*, 1994, **38**, 255.

[66]W. Buchberger and S. Mulleder, *Mikrochimica Acta*, 1995, **119**, 103.

CHAPTER THREE

Inductively Coupled Plasma Mass Spectrometry

3.0 INTRODUCTION

Inductively coupled plasma mass spectrometry (ICP-MS) is the most powerful analytical technique for the determination of trace and ultra-trace elements in a variety of matrices. The analytical advantages of the technique include extremely low limits of detection, wide linear dynamic range, high sample throughput, ability to perform isotope dilution analyses and the ease with which it can be combined with different types of sample introduction system.

The first known fundamental and applied research into the use of an inductively coupled plasma as a vaporisation, atomisation and excitation source was conducted by Babat in 1941.[1] About 20 years later, Reed[2] extended Babat's work and described methods of maintaining argon plasmas in open vessels (torches). Reed operated an ICP in a quartz tube using a single flow of argon gas and anticipated the application of an ICP in atomic emission spectrometry (AES) by injecting powders into the discharge. The application of the ICP to analysis was pioneered in the 1960's by the Greenfield[3] and Fassel[4] groups.

The initial development of ICP-MS, in the 1970's, was brought about by the realisation that the analysis of trace elements in rock samples using ICP-AES was severely limited by spectral interferences from high matrix levels. In 1975,

Gray[5] demonstrated the extraction of ions from a DC plasma through a pinhole sized sampling orifice into a pumped vacuum system leading to a quadrupole mass analyser. However, as a result of the poor degree of ionisation, poor dissociation of sample molecules and severe matrix effects in the DC plasma, alternative plasma sources were investigated including the microwave induced plasma (MIP) and the ICP. The development work on ICP-MS was undertaken in parallel by Gray and Date in the UK and Houk, Fassel and co-workers in the USA, with the first commercial instrument reaching the market in 1984.[6]

3.1 THE INDUCTIVELY COUPLED PLASMA

An inductively coupled plasma (ICP) is formed when energy is transferred to a gas (most commonly argon) by means of an induction coil. The plasma is generated inside and at the open end of a series of concentric fused silica tubes known as a torch. The most commonly used torch, based on the Scott-Fassel design,[7] has an outer tube (for the coolant gas flow) encircled by 2-4 turns of a water or gas cooled copper induction coil. The coolant gas flow enters the torch tangentially and swirls upwards effectively protecting the tube walls from the very hot plasma and providing the plasma sustaining gas. Within the outer tube are two concentric tubes (for the auxiliary and nebuliser gas flows) which terminate approximately 25 mm from the open end of the outer tube.

When a RF current is supplied to the induction coil, a magnetic field is established within the torch. Argon gas passing through the coil is seeded with free electrons generated by a spark from a Tesla coil, and is subsequently

ionised. The free electrons and argon ions absorb energy from the alternating magnetic field (known as inductive coupling) and are accelerated in circular orbits around the magnetic field lines. Collisions between the accelerating argon ions and electrons yield an avalanche of charged particles and, once the electrons reach the ionisation potential of argon, collisional ionisation occurs. At atmospheric pressure the mean free path of the electrons is small ($\sim 10^{-3}$ mm) thus the rate of collision is high and an intense self-sustaining plasma is formed.

The skin-depth effect[8] occurring in RF induction heating ensures that most of the energy is coupled to the outer or induction region of the plasma, thus leading to a temperature as high as 10000 K. The cool nebuliser gas flow punches a central channel through the centre of the plasma and results in the plasma adopting a toroidal or doughnut shape. Gas in the central channel is heated mainly by radiation and conduction from the surrounding plasma and therefore has a lower temperature of between 5000 K and 7000 K (Figure 3.1).
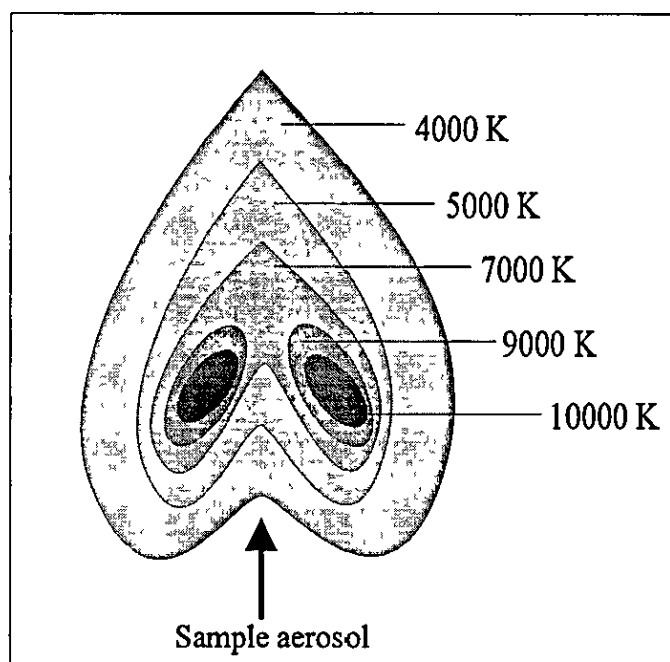
Figure 3.1. Temperature distribution in an ICP.

3.1.1 Ionisation Mechanisms

Analyte species are subjected to a relatively long residence time in the very hot,

inert plasma and undergo complete dissociation and atomisation, and almost

complete ionisation. The degree of ionisation of an element is dependent upon

the ionisation conditions in the plasma, which are dominated by the major

constituents (usually Ar, H, O, and electrons) and the ionisation constant and

partition functions for the atom concerned.[6] The degree of ionisation of an

element in an ICP can be calculated using the Saha equation,

$$\frac{M^+}{M} = \frac{1}{n_e}\left(\frac{2\pi m_e k\, T}{h^2}\right)^{3/2}\frac{Q^+}{Q}\,e^{-\left(\frac{IP}{kT}\right)} \qquad \text{(Eqn. 3.1)}$$

where, n_e is the electron density, m_e is the mass of the electron, k is the

Boltzmann constant, T is the temperature, h is Planck's constant, Q^+ and Q are

the partition functions of the ion and neutral atom respectively, and IP is the

ionisation potential of the element.

The mechanisms by which energy is transferred or by which ionisation occurs

in the ICP are still not fully understood and remain the focus of research. The

major ionisation mechanism is considered to be that of electron collision, with

neutral or excited argon atoms. Additionally, when the excitation energy of a

metastable state of atom A is greater than the ionisation energy of atom B

Penning ionisation[9] may occur, where

$$A^m + B \rightarrow A + B^+ + e \qquad \text{(Eqn. 3.2)}$$

In an argon ICP this process would be,

$$Ar^m + B \rightarrow Ar + B^+ + e \qquad \text{(Eqn. 3.3)}$$

Metastable argon may also act as a source of ions (with a low effective

ionisation potential) as follows,

$$Ar^m + e \rightarrow Ar^+ + 2e \qquad \text{(Eqn. 3.4)}$$

Water vapour in the aerosol is known to play an important part in the ionisation

of analyte atoms by causing the heat capacity of the aerosol to increase. As a

result of the high temperature gradient and magnetohydrodynamic (MHD)

thrust, energetic Ar and Ar^+ species migrate towards the aerosol channel. Houk

et al.[10] suggested that the transfer of energy at the boundary between the

nebuliser gas and the plasma occurs by collisions such as,

$$Ar^+ + H_2O \rightarrow ArH^+ + OH \qquad\qquad (Eqn.\ 3.5)$$

The OH species are then involved in the transfer of energy to the analyte atoms.

The presence of water vapour in the aerosol contributes significantly to the

electron population in the central channel of the plasma.[6] In a dry plasma $n_{Ar^+} =$

$n_e = 1 \times 10^{15}$ cm^{-3}, however if a nebulised solution is introduced additional

electrons are contributed by the ionisation of O and H from the solvent. At a

nebuliser gas flow rate of 1 ml min^{-1} and a transport efficiency of 1 %, the

populations of H$^+$ and O$^+$ are about 2×10^{14} cm^{-3} and 1×10^{14} cm^{-3}, respectively.

Thus, the electron population increases so that n_e is approximately 1.3×10^{15}

cm^{-3}.

3.2 SAMPLE INTRODUCTION

Sample introduction into the ICP is a critical part of the analytical process and

is most commonly carried out by means of pneumatic nebulisation. Liquid

samples are converted into a polydisperse aerosol by a nebuliser and are

carried, in a gas stream, through a spray chamber and into the plasma. The

most commonly used nebulisers are of the pneumatic concentric type,[11] with

the Meinhard[12] and cross-flow[13] being the most popular.

Concentric nebulisers operate at solution flow rates of typically around 1 ml

min[-1] and offer very low analyte transport efficiencies of typically 1 - 2 %.

These nebulisers are compromised in terms of sensitivity when operated at low

solution flow rates. The limited sample volumes available in, for example, the

semi-conductor industry and clinical sciences, and the coupling of ICP-MS

with separation techniques has led to the development of concentric nebulisers

which operate at low solution flow rates. These microconcentric nebulisers

operate at typically below 100 µl min^{-1} and, because their design is optimised at

low flow rates, they offer improved efficiencies and detection limits compared

with conventional concentric nebulisers. Such nebulisers include the high

efficiency nebuliser (HEN),[14-16] microconcentric nebuliser (MCN)[17-20] and the

MicroMist nebuliser (MM)[21].

The primary purpose of the spray chamber in ICP-MS is to remove large

droplets (> 6 µm) from the polydisperse aerosol. The design of the spray

chamber is of crucial importance since it directly influences the analyte

transport efficiency, sample dispersion and memory effects A variety of spray

chamber have been designed for use in ICP-MS including, Scott-type double

pass,[7] vertical rotary,[22,23] cyclonic,[18,24-26] and doughnut shaped.[27] The removal of

larger droplets in spray chambers is accomplished by a variety of processes

including, impact-loss, turbulent, gravitational and centrifugal mechanisms.

The theory and dynamics of spray chambers are detailed in a comprehensive

review by Sharp.[28]

As a consequence of the poor analyte transport efficiencies associated with the use of spray chambers, nebulisers have been designed which directly inject the aerosol into the plasma. Such nebulisers are the direct injection nebuliser (DIN)[29-31] and the direct injection high efficiency nebuliser (DIHEN).[16,32] The avoidance of a spray chamber means that that these nebulisers provide transport efficiencies close to 100 %. However, as more solvent load is introduced into the plasma an increase in spectroscopic interferences may be apparent.

Although nebulisation is the most common method of sample introduction in ICP-MS, other methods are employed. These include electrothermal vaporisation,[33-35] hydride/vapour generation,[36-38] laser ablation[39,40] and slurry nebulisation.[41,42]

3.3 ION EXTRACTION

Ion are extracted into the vacuum system *via* a sampling interface consisting of a sampler and skimmer cone. The plasma tail flame impinges on the aperture (1.0 - 1.2 mm diameter) of a water cooled sampling cone at a distance typically between 8 and 15 mm from the load coil. Sampling cones are typically machined from nickel or platinum and their design is of crucial importance.

When the plasma tail flame interacts with the metal cone it is cooled and a boundary layer of gas forms between the plasma and cone. The temperature of the boundary layer is much lower than that of the bulk plasma and consequently chemical reactions such as oxide formation readily occur. The

diameter of the sampling aperture is $< 10^{-2}$. For argon at 7500 K, $\lambda = 1\,6\,\mu m$, therefore an aperture of > 0.16 mm would provide continuum flow and allow sampling of the bulk plasma.

The region behind the sampling cone, known as the expansion chamber, is evacuated to approximately 2 mbar by means of a rotary pump. With this pressure differential across the aperture the sampled ions expand into the lower pressure region as a supersonic jet and pass through a second cone, known as the skimmer cone. The supersonic jet is a freely expanding region surrounded by shock waves known as the barrel shock and a Mach disc (Fig. 3.2). The shock waves are produced by collisions between fast atoms from the jet and the background gas.[43] To avoid losses of ions due to collisions and scattering, the skimmer cone is situated 5 - 10 mm behind the sampling cone and positioned with its open tip upstream of the Mach disc. The position of the onset of the Mach disc is given by Equation 3.6,

$$X_m = 0.67 D_o (P_o / P_1)^{1/2} \qquad \text{(Eqn. 3.6)}$$

where, X_m is the position of the Mach disc from the sampling orifice along the central axis, D_o is the diameter of the sampling orifice, P_o is the pressure in the ICP and P_1 is the pressure in the extraction chamber.
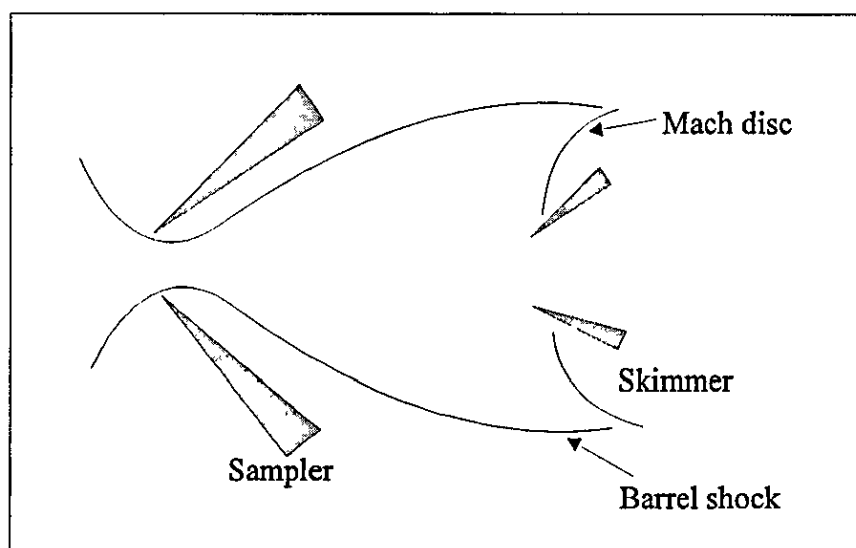
Figure 3.2. Illustration of the shock waves enclosing the supersonic jet in

the expansion chamber.

3.4 ION FOCUSING

After traversing the skimmer, the extracted ions are conveyed to the mass

analyser by an electric field established by a series of ion lenses known as the

ion focusing system. Each lens consists of several electrodes strung together

with a photon stop incorporated in the centre. Ions of different m/z have

different kinetic energies and thus take varying paths through the lens system.

This non-ideal situation means that different ion optical conditions are required

to transmit ions of different m/z thus leading to an uneven sensitivity across the

mass range.

Space-charge effects also lead to non-ideal behaviour in the ion focusing

system of an ICP-MS. In the plasma and in the supersonic jet, the ion current is

balanced by an equal electron current so the beam acts as if it were neutral.

However, as the beam leaves the skimmer, the electric field established by the lenses collects ions and repels electrons. Thus, the electrons are no longer present to confine the ions in a narrow beam and the beam expands greatly due to space-charge effects. This expansion is a major source of ion loss in ICP-MS since it is difficult to collect all the ions leaving the skimmer. In addition, if the same space-charge force acts on all the ions, lighter ions will be deflected the most thus leading to a generally poorer sensitivity for lighter elements.

3.5 MASS ANALYSER

The function of the mass analyser is to separate ions according to their different m/z ratios. The most common mass analysers employed in ICP-MS instruments are of the quadrupole type. A typical quadrupole mass analyser consists of four straight stainless steel or molybdenum rods (12 -18 mm diameter, 20 mm long) suspended parallel to and equidistant from the axis. Opposite pairs of rods are connected together and DC and RF voltages are applied to each pair. The mass resolving power of the quadrupole derives from the intrinsic stability, or instability, of ions when subjected to a particular type of electric field.

Ions are introduced into the quadrupole array at velocities determined by their energy and mass. As the ions proceed down the longitudinal z-axis, they undergo transverse motion in the x- and y-planes perpendicular to the longitudinal axis. The DC fields tend to focus positive ions in the positive plane and defocus them in the negative plane. As the superimposed RF field

becomes negative, ions are accelerated towards the rods with the lighter ions

gaining the greatest velocity (Fig. 3.3). In the following positive half-cycle, the

direction of the ions is reversed and they are accelerated away from the rods.

Ions exhibit oscillations with increasing amplitude until they finally collide

with the rods and are neutralised. By controlling the amplitude of the DC/RF

voltages, the field can be established such that only ions of a given m/z ratio are

transmitted.[44]

The need for enhanced resolution to overcome problematic spectroscopic

interferences has led to the use of magnetic sector mass spectrometers in ICP-

MS.[45-47] In magnetic sector systems, a magnetic field causes ions to be

deflected along curved paths and separated according to their momentum.

Time of flight mass spectrometers (TOF-MS) have also been investigated for

use with an ICP ion source.[48]

3.6 ION DETECTION

The most common ion detectors used in ICP-MS instruments are Channeltron

electron multipliers. Electron multipliers consist of an open, curved glass tube

flared at one end to form a cone. The internal surface of the tube is coated with

a semiconducting material, usually lead oxide. For the detection of positive

ions the cone is biased at a high negative potential (~ - 3 kV) and the collector

electrode, beyond the output end of the tube, is held at ground. The resistance

of the interior coating varies with position along the tube, thus when a voltage

is applied a potential gradient is established.
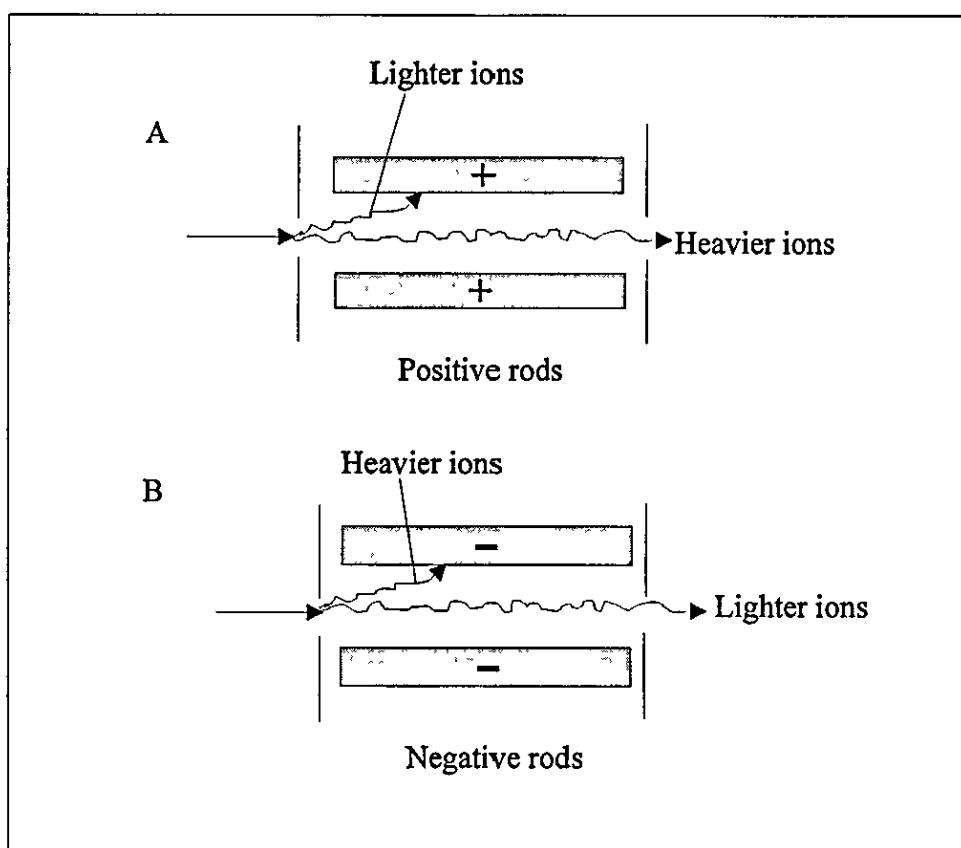
Figure 3.3. Ion separation process in the two rod planes of a quadrupole.

When a positive ion leaves the mass analyser it is attracted to the negative

potential of the cone and will subsequently strike the surface. Upon impact,

one or more secondary electrons are ejected and accelerated down the tube

towards ground potential. These secondary electrons undergo further collisions

with the coating and more secondary electrons are emitted. This process is

repeated many times as the secondary electrons move down the tube towards

the collector electrode. Eventually, the process reaches saturation resulting in a

discrete pulse at the collector containing up to 10^8 electrons. In the normal

mode of operation, pulse counting, these pulses are passed to an amplifier,

through a digital discriminator and are finally counted by a multi channel
analyser.

3.7 INTERFERENCES

Despite the many analytical advantages of ICP-MS, the technique does suffer
from several problematic interferences. These interferences can be broadly
divided into two groups, spectroscopic and non-spectroscopic. A
comprehensive review of interferences in ICP-MS has been published by Evans
and Giglio.[49]

3.7.1 Spectroscopic Interferences

Spectroscopic interferences are caused by atomic or molecular ions having
essentially the same nominal mass as the analyte of interest, thereby causing
erroneously large signals at the m/z of interest. Such interferences originate
from two sources; overlapping isotopes of different elements and polyatomic
ions formed from precursors in the plasma gas, entrained atmospheric gases,
dissolution acids and sample matrix.

Isobaric Overlap

Isobaric overlap, where isotopes having essentially the same m/z are not
resolved by the mass analyser, can exist between elements present in the
sample matrix, in the dissolution acids, or can exist with the plasma gas and its
impurities. Since many elements have at least one, two or three isotopes free
from overlap these interferences, in most cases, can be avoided by correct

isotope selection. However, in some cases accurate measurement of one

isotope is critical and therefore correction for isobaric overlap must be made.

Interference correction can be used or, in a situation where the sample matrix

itself contains the interfering species, a separation technique can be used to

separate the analyte from the interfering matrix. Recently, dynamic reaction or

collision cells have been developed to alleviate spectroscopic interferences

based on promoting different chemical reactions between analyte and

interfering ions.[50]

Polyatomic Ions

A very large number of polyatomic ion species can cause interferences below

80 m/z. The extent of the polyatomic ion formation depends on many factors,

such as extraction geometry, the nature of the acid and sample matrix, the

plasma and nebuliser operating parameters and the specific instrument design.

There has been considerable debate as to the origin of polyatomic ions. The

most likely causes are collisional reactions in the boundary layer[51] and survival

through the plasma itself, particularly with respect to refractory metal oxides.

There are a variety of approaches by which polyatomic ion interferences may

be compensated for. Modification of the sample preparation procedures can

greatly reduce the extent of polyatomic ion formation, in particular avoidance

of HCl, H_2SO_4 and H_3PO_4 acids. Sample introduction methods can also be

selected to reduce such interferences. Methods that introduce a dry sample,

such as laser ablation,[52] hydride generation[53,54] and thermal vaporisation,[55,56]

lead to a reduction in polyatomic species containing O and H. Oxides and

hydroxides can also be reduced by cooling the spray chamber and thereby

condensing the water vapour.[57] The use of alternative gas and mixed gas

plasmas,[58,59] addition of organic solvents[60,61] and cold plasma conditions[62] have

all been successfully used to reduce polyatomic ions. Instrumental conditions

such as the forward power and nebuliser gas flow rate can be optimised to

reduce polyatomic ion formation, but ultimately the best approach is the use of

high resolution mass spectrometers.

3.7.2 Non-Spectroscopic Interferences

Non-spectroscopic interferences are derived from the sample matrix and are

characterised by an enhancement or reduction in analyte signal as a result of

factors influencing the sample transport, ionisation, ion extraction or ion

throughput in the resultant ion beam. Such interferences can be broadly

divided into two categories: (i) physical effects resulting from high levels of

dissolved solid; (ii) matrix induced suppression in the ion beam.

High Levels of Dissolved Solids

Suppression of the analyte signal can be caused by deposition of salt on the

sampler and skimmer cones which substantially affects the sampling process.

To reduce this type of signal suppression, the system can be primed by

allowing the sampling cone to partially clog thereby achieving a pseudo steady-

state where the rate of deposition is equalled by the rate of dissociation.[49]

Matrix Induced Suppression

An excess of a heavy, easily ionisable element in the sample matrix can cause

serious analyte signal suppression. The presence of such matrix elements is

thought to cause a change in the ion transmission which subsequently

suppresses the analyte signal. Several theories have been proposed to accounts

for these effects.[63,64] Gillson *et al.*[65] suggested that space charge effects in the

ion beam play a major role. The most severe effects are caused by heavy

matrix elements with low ionisation potentials (IP's), whilst light analyte

elements with high IP's are most severely affected.

A number of approaches can be employed to overcome the effects of interfering

matrix elements. Internal standardisation can be used to correct for matrix

effects, providing that the analyte and internal standard are closely matched in

both mass and ionisation potential.[66] Methods such as liquid chromatography,

solvent extraction and co-precipitation can be used to separate the analyte from

the interfering matrix, with the additional benefit of analyte pre-concentration.

Matrix matching of samples and standards, and optimisation of the ion lens

settings can also reduce suppression effects.

REFERENCES

[1]G. I. Babat, *J. Inst Electr Eng*, 1947, **94**, 27.

[2]T. B. Reed, *J. Appl. Phys.*, 1963, **34**, 2266.

[3]S. Greenfield, I. Jones and C. T. Berry, *Analyst*, 1964, **89**, 713.

[4]R. H. Wendt and V. A. Fassel, *Anal. Chem*, 1965, **37**, 920.

[5]A. L. Gray, *Analyst*, 1975, **100**, 289.

[6]K. E. Jarvis, A. L. Gray and R. S. Houk, *Handbook of Inductively Coupled Plasma Mass Spectrometry*, 1992, Blackie & Son Ltd., Glasgow.

[7]R. H. Scott, V. A. Fassel, R. N. Kniseley and D. E. Nixon, *Anal Chem*, 1974, **6**, 76.

[8]V. A. Fassel and R. N. Kniseley, *Anal. Chem*, 1974, **46**, 1155A.

[9]P. W. J. M. Boumans, *Spectrochim Acta*, 1982, **37B**, 75.

[10]R. S. Houk, H. J. Svec and V. A. Fassel, *Appl Spectrosc*, 1981, **35**, 380.

[11]B. L. Sharp, *J. Anal. At. Spectrom.*, 1988, **3**, 613.

[12]J. E. Meinhard, *ICP Inf Newsl.*, 1976, **2**, 163.

[13]R. N. Kniseley, H. Amenson, C. C. Butler and V. A. Fassel, *Appl. Spectrosc*, 1974, **28**, 285.

[14]J. A. Kinzer, J. W. Olesik and S. V. Olesik, *Anal. Chem*, 1996, **68**, 3250.

[15]C. B'Hymer, K. L. Sutton and J. A. Caruso, *J Anal At. Spectrom*, 1998, **13**, 855.

[16]J. A. McLean, H. Zhang and A. Montaser, *Anal. Chem.*, 1998, **70**, 1012.

[17]M. Vanhaecke, M. Van Holderbeke, L. Moens and R. Dams, *J. Anal At Spectrom*, 1996, **11**, 543.

[18]T. D. Hettipathirana and D. E. Davey, *J Anal. At. Spectrom.*, 1998, **13**, 483.

[19]M. De Wit and R. Blust, *J. Anal. At. Spectrom*, 1998, **13**, 515.

[20]S. A. Baker and N. J. MillerIhli, *Appl. Spectrosc.*, 1999, **53**, 471.

[21]M. Van Holderbeke, Y. Zhao, F. Vanhaecke, L. Moens, R. Dams and P. Sandra, *J Anal. At. Spectrom*, 1999, **14**, 229.

[22]M. Wu and G. M. Hieftje, *Appl. Spectrosc*, 1992, **12**, 1261.

[23]M. Wu, Y. Madrid, J. A. Auxier and G. M. Hieftje, *Anal Chim Acta*, 1994, **286**, 155.

[24]T. D. Hettipathirana and D. E. Davey, *Appl. Spectrosc.*, 1996, **50**, 1015.

[25]C. Rivas, L. Ebdon and S. J. Hill, *J. Anal. At. Spectrom.*, 1996, **11**, 1147.

[26]K. A. Taylor, B. L. Sharp, D. J. Lewis and H. M. Crews, *J. Anal. At. Spectrom.*, 1998, **13**, 1095.

[27]J. Lui, B. L. Huang and X. J. Zeng, *Spectrochim Acta*, 1998, **53**, 1469.

[28]B. L. Sharp, *J. Anal At. Spectrom*, 1988, **3**, 939.

[29]J. L. Todoli and J. M. Mermet, *J. Anal. At Spectrom*, 1998, **13**, 727.

[30]A. Tangen, W. Lund, B. Josefsson and H. Borg, *J. Chromatogr. A*, 1998, **826**, 87.

[31]Y. Lui, V. Lopez-Avilia, J. J. Zhu, D. R. Wiederin and W. F. Beckert, *Anal. Chem*, 1995, **67**, 2020.

[32]J. A. McLean, M. G. Minnich, L. A. Iacone, H. Lui and A. Montaser, *J Anal. At. Spectrom.*, 1998, **13**, 829.

[33]J. B. Truscott, L. Bromley, P. Jones, E. H. Evans, J. Turner and B. Fairman, *J. Anal. At. Spectrom.*, 1999, **14**, 627.

[34]D. Pozebon, V. L. Dressler and A. J. Curtius, *J. Anal. At. Spectrom.*, 1998, **10**, 1101.

[35]S. J. Santosa, S. Tanaka, and K. Yamanaka, *Fresenius' J. Anal. Chem*, 1997, **357**, 1122.

[36]D. Beauchemin, *J. Anal. At. Spectrom.*, 1998, **13**, 1.

[37]T. Wilke, H. Wildner and G. Wuensch, *J. Anal At. Spectrom*, 1997, **12**, 1083.

[38]M. L. Magnuson, J. T. Creed and C. A. Brockhoff, *Analyst*, 1997, **122**, 1057.

[39]B. J. Masters and B. L. Sharp, *Anal Commun*, 1997, **34**, 237.

[40]R. J. Watling, *J. Anal. At. Spectrom*, 1998, **9**, 917.

[41]L. Ebdon , M. Foulkes and K. Sutton, *J. Anal At. Spectrom*, 1997, **2**, 213.

[42]S. Chen and S. Jiang, *J. Anal. At. Spectrom*, 1998, **10**, 1113.

[43]A. L. Gray, *J. Anal At Spectrom*, 1989, **4**, 371.

[44]H. H. Willard, L. L. Merritt, J. A. Dean and F. A. Settle, *Instrumental Methods of Analysis,* 1988, Wadsworth Publishing Company, California.

[45]N. M. Reed, R. O. Cairns, R. C. Hutton and Y. Takaku, *J Anal At Spectrom.,* 1994, **9**, 881.

[46]I. Rodushkin, F. Odman and S. Branth, *Fresenius' J. Anal. Chem.,* 1999, **364**, 338.

[47]A. T. Townsend and R. Edwards, *J. Anal At Spectrom*, 1998, **13**, 463.

[48]P. P. Mahoney, S. J. Ray and G. M. Hieftje, *Appl. Spectrosc*, 1997, **51**, 16A.

[49]E. H. Evans and J. J. Giglio, *J. Anal At. Spectrom*, 1993, **8**, 1.

[50]S. D. Tanner and V. I. Baranov, *At. Spectrosc*, 1999, **20**, 45.

[51]M. A. Vaughan and G. Horlick, *Spectrochim. Acta, Part B,* 1990, **45**, 1289.

[52]E. Denoyer, K. Fredeen and J. Hager, *Anal. Chem*, 1991, **63**, 445A.

[53]J. Bowman, B. Fairman and T. Catterick, *J. Anal. At. Spectrom.*, 1997, **12**, 313.

[54]R. M. Olivas, C. R. Quetel and O. F. X. Donard, *J. Anal. At. Spectrom*, 1995, **10**, 865.

[55]J. Turner, S. J. Hill, E. H. Evans and B. Fairman, *J. Anal. At. Spectrom*, 1999, **14**, 121.

[56]J. P. Byrne, R. Mcintyre, M. E. Benyounes, D. C. Gregoire and C. L. Chakrabarti, *Can. J. Anal. Sci. Spectrosc*, 1997, **42**, 95.

[57]R. C. Hutton and A. N. Eaton, *J. Anal. At. Spectrom*, 1987, **2**, 595.

[58]T. van der Velde-Koerts and J. L. M. de Boer, *J. Anal. At. Spectrom.*, 1994, **9**, 1093.

[59]S. J. Hill, M. J. Ford and L. Ebdon, *J. Anal. At. Spectrom.*, 1992, **7**, 1157.

[60]C. E. Sieniawska, R. Mensikov and H. T. Delves, *J. Anal. At. Spectrom*, 1999, **14**, 109.

[61]E. H. Evans and L. Ebdon, *J. Anal. At. Spectrom.*, 1990, **5**, 425.

[62]S. D. Tanner, M. Paul, S. A. Beres and E. R. Denoyer, *At. Spectrosc*, 1995, **16**, 16.

[63]D. C. Gregoire, *Spectrochim. Acta, Part B*, 1987, **42**, 895.

[64]S. H. Tan and G. Horlick, *J. Anal. At. Spectrom*, 1987, **2**, 745.

[65]G. R. Gillson, D. J. Douglas, J. E. Fulford, K. Halligan and S. D. Tanner, *Anal. Chem*, 1988, **60**, 1472.

[66]J. Wang, E. H. Evans and J. A. Caruso, *J. Anal. At. Spectrom.*, 1991, **6**, 605.

CHAPTER FOUR

Meinhard Nebuliser CE-ICP-MS Interface

4.0 INTRODUCTION

In this Chapter, a preliminary evaluation of a CE-ICP-MS interface based on a glass concentric Meinhard nebuliser will be detailed.

4.1 EXPERIMENTAL

4.1.1 Reagents and Materials

Individual stock standard solutions of Ce and Ni were obtained from Sigma (Poole, UK). Borate buffers were prepared by dissolving the appropriate mass of di-sodium tetraborate (Sigma) in ultrapure (18.2 MΩ) Milli-Q water (Millipore, MA, USA). Buffer solutions were pH adjusted to 8.5 using Aristar HNO$_3$ (Sigma). Fused silica capillary (375 μm od, 100 μm id, 100 cm long) was purchased from Composite Metal Services, Worcester, UK. Capillaries were pre-conditioned using 0.5 M NaOH (Sigma) prior to their first use. A 10mM NH$_4$Cl solution (Sigma) spiked with 100 ng ml^{-1} Ce was used as the make-up flow.

4.1.2 Instrumentation

ICP-MS. A VG PlasmaQuad (PQI) inductively coupled plasma mass spectrometer (VG Elemental, Winsford, UK) was used. Data acquisition and interpretation was performed using Time Resolved Analysis (TRA) and

Masslynx software (VG Elemental). A summary of the ICP-MS operating

conditions is presented in Table 4.1.

Rf power	1350 W
Reflected power	0 W
Coolant gas flow	14.0 l min^{-1}
Auxiliary gas flow	0.8 l min^{-1}
Nebuliser gas flow	0.9 l min^{-1}
Sampler cone	Ni, 1.0 mm orifice
Skimmer cone	Ni, 0.7 mm orifice
Measurement mode	Peak jump (dwell time 10.24 ms)

Table 4 1. ICP-MS operating conditions

CE System. An in-house fabricated CE system, as previously described by

Sulaiman,[1] was used. The separation potential was produced by a Brandenburg

3807 high voltage power supply (Brandenburg, Surrey, UK) and an Iso-Tech

90 digital multimeter (RS Components, Corby, UK) was used for the

measurement of electrophoretic currents. For capillary rinsing and pre-

conditioning, a simple vacuum driven device was designed. A 100 ml Buchner

flask was fitted with a rubber bung into which a finger tight fitting (Omnifit,

Cambridge, UK) was placed. One end of the capillary was inserted through the

finger tight fitting and the other placed into the appropriate rinsing solution.

By connecting a vacuum pump to the Buchner flask, solution was drawn

through the capillary.

The CE system (excluding the high voltage power supply) was enclosed in a

perspex box which incorporated a safety light and auto shut off mechanism.

CE-ICP-MS Interface. The CE-ICP-MS interface was constructed using a Meinhard nebuliser (Meinhard, CA, USA), a 1/16 ″ PTFE T-piece (Omnifit, Cambridge, UK) and an U-shaped spray chamber. A schematic diagram of the interface is presented in Fig. 4.1. One end of the separation capillary was inserted through the T-piece and into a Pt-Ir tube [0.5 mm od, 0.4 mm id, 30 mm length, (Johnson Matthey, Reading, UK)]. The capillary was positioned so that it reached the end of the Pt-Ir tube, thereby minimising post capillary transport. The injection end of the capillary was placed in a buffer vial along with a Pt electrode. The Pt-Ir tube and capillary were then inserted directly into the nebuliser central tube. Silicone rubber tubing was used to ensure an air tight fit inside the central tube. Once inserted into the nebuliser, the capillary could be easily removed to allow rinsing or replacement.

Grounding of the capillary was achieved by the use of a coaxial sheath of electrolyte solution (make-up solution) which was pumped through the vertical arm of the T-piece using a Gilson Minipuls 3 peristaltic pump (Gilson Medical Electronic, Villiers-Le-Bel, France). The make-up flow was an important feature of the interface since it not only provided the electrical continuity but also satisfied the liquid flow requirements of the nebuliser. To complete the electrical circuit, a grounding lead from the power supply was soldered onto the Pt-Ir tube. The nebuliser was inserted into the spray chamber using a PTFE connector and the spray chamber was then connected to the ICP torch by means of a flexible Teflon tube. Samples were injected hydrostatically by elevating the sample vial to a height of 15 cm above the nebuliser level for 10 s.
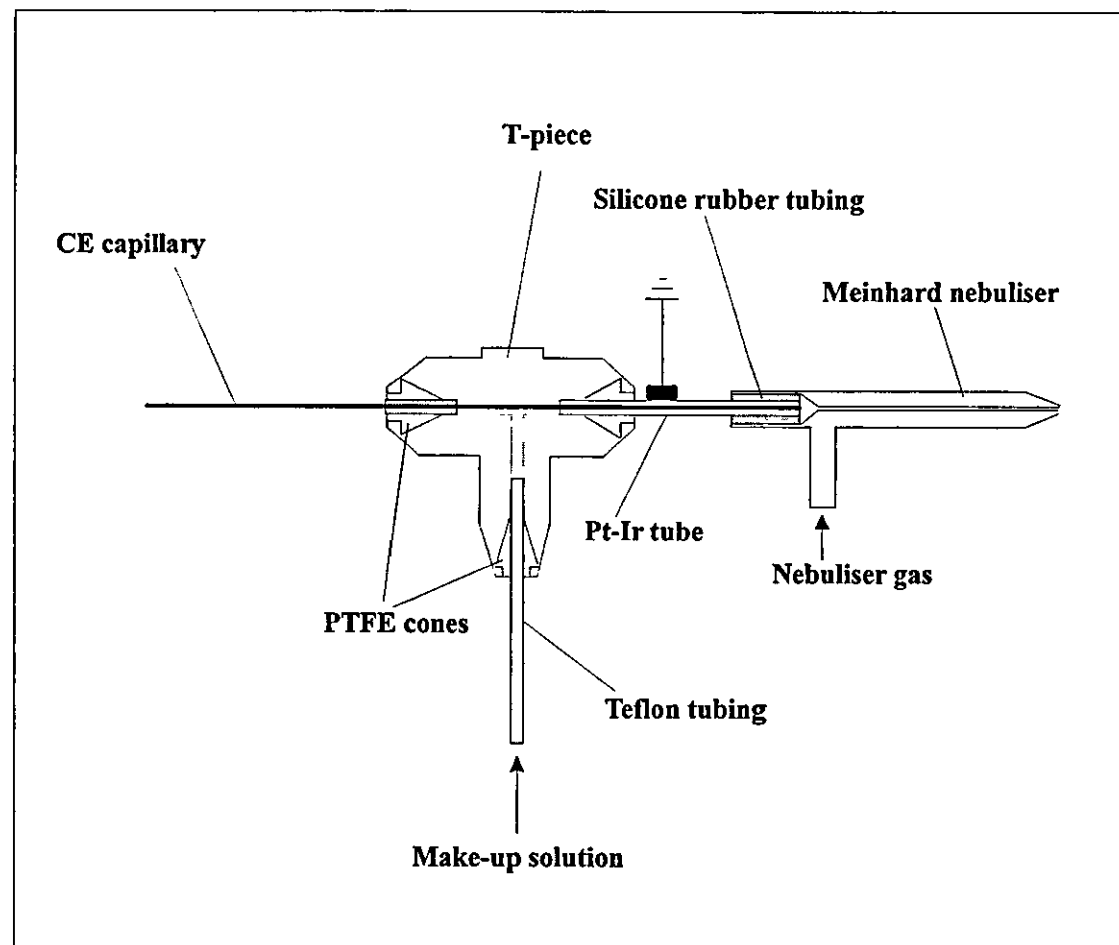
Figure 4.1. Schematic diagram of the Meinhard nebuliser CE-ICP-MS interface.

4.2 INTERFACE EVALUATION

A preliminary evaluation of the interface was undertaken by measurement of the solution flow rate within the separation capillary and its dependence upon the make-up flow rate. Solution flow rates in the capillary were measured by accurately weighing the mass of water, using a Mettler AE 240 balance (European Instruments, Oxford, UK), transferred from a pre-weighed vial over a 300 s time period. Measurements were repeated in triplicate and the mean flow rates calculated. The laminar flow induced in the capillary as a result of the nebuliser suction was also measured by injection of a Ni standard

4.2.1 Effect of Make-up Flow Rate on Capillary Flow Rate

The influence of make-up flow rate on the capillary flow rate was investigated by measuring solution flows through the capillary at various make-up flow rates between 0 and 100 μl min^{-1}. The separation voltage was zero during these measurements.

The make-up flow rate had a direct influence upon the magnitude of the solution flow through the capillary (Figure 4.2). Since the applied voltage was zero during these measurements, electroosmotic induced flow was eliminated and the flow through the capillary was entirely laminar flow induced by the nebuliser suction. At zero make-up flow, a laminar flow rate of ~ 4 μl min^{-1} was observed. As the make-up flow rate was increased, the laminar flow rate was reduced as the nebuliser demand was partially satisfied.

63
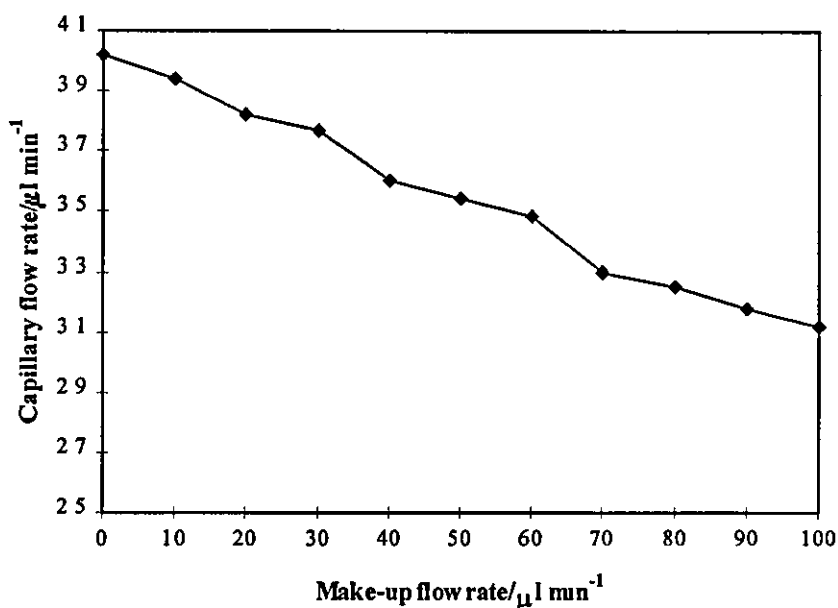
Figure 4.2. Capillary flow rate as a function of make-up flow rate.

4.2.2 Determination of Laminar Flow Rate

The laminar flow rate within the capillary was determined by injecting a Ni

standard (1 μg ml^{-1}) and measuring the migration time with and without an

applied voltage (+20 kV). A 20 mM borate buffer (pH 8.5) was used and the

make-up flow rate was set at 50 μl min^{-1}.

The migration time of the Ni^{2+} species was 181 s with an applied voltage of +20

kV, and 220 s in the absence of an applied voltage. The difference in migration

time was consistent with what was expected. In the absence of a voltage, the

analyte was transported through the capillary solely by the nebuliser suction.

However, upon the application of a voltage, the combined effect of the

electroosmotic flow, electrophoretic mobility and nebuliser suction resulted in

a shorter migration time.

When comparing the linear velocity of the laminar flow with the combined

laminar, electroosmotic and electrophoretic flow, it can be determined that

laminar flow accounted for 82 % of the analyte linear velocity (Fig. 4.3). The

parabolic velocity profile of laminar flow causes band broadening and

ultimately loss of resolution in CE. Thus, the 82 % laminar portion of the flow

velocity was clearly sufficient to completely degrade the resolution of a

separation.

It was demonstrated in Section 4.2.1 that increasing the make-up flow rate was

an effective method of reducing the nebuliser suction and therefore reducing

the laminar flow within the capillary. However, because the Meinhard

nebuliser is designed to operate at solution flow rates in the ml min^{-1} range, the

high make-up flow rate necessary to minimise the nebuliser suction would lead

to significant dilution of the sample. Hence, in order to maintain the inherent

resolution of CE, sensitivity must be compromised.

Migration time @ 20 kV = 181 s = 3.02 min

Migration time @ 0 kV = 220 s = 3.67 min

Linear velocity of laminar flow = $\dfrac{100 \text{ cm}}{3.67 \text{ min}}$ = $\underline{27.24 \text{ cm min}^{-1}}$

Laminar flow rate = $\pi r^2 l$ = $\pi(50 \times 10^{-6})^2(27.24 \times 10^{-2})$

$$= 2.14 \times 10^{-9} \text{ m}^3$$

$$= 2.14 \text{ } \mu l \text{ min}^{-1}$$

Combined laminar, electroosmotic and electrophoretic flow = $\dfrac{100 \text{cm}}{3.02 \text{ min}}$

$$= \underline{33.11 \text{ cm min}^{-1}}$$

Laminar flow accounts for $\left(\dfrac{27.24}{33.11}\right)$ x 100 = $\mathbf{82.3}$ % of the linear velocity

Figure 4.3. Calculation of the contribution of laminar flow to the analyte

linear velocity.

4.3 SUMMARY

The Meinhard nebuliser was not ideal for use in the CE-ICP-MS interface due

to its incompatibility with the low solution flow rates employed in CE.

Because of the high natural aspiration rate of the nebuliser, the laminar flow

induced in the separation capillary would be significant enough to completely

degrade resolution. The nebuliser suction and laminar flow could be

minimised by the use of the make-up flow, however, this was at the expense of

sensitivity. Clearly, a nebuliser designed to operate at low solution flow rates

is a fundamental requirement for CE-ICP-MS.

REFERENCES

1. A. B. Sulaiman, *PhD Thesis,* 1996, Loughborough University.

CHAPTER FIVE

Design and Optimisation of a Cyclonic Spray Chamber

5.0 INTRODUCTION

A spray chamber intended for use in CE-ICP-MS has demands placed upon it
that do not normally exist in conventional ICP-MS measurements. For
effective compatibility with CE, the spray chamber must produce minimal
broadening of sample peaks and, because of the small sample volumes
employed, should offer a high analyte transport efficiency. These demands are
most likely met by a low volume spray chamber offering rapid sample response
and washout characteristics.

In this Chapter, the design and optimisation of a rapid washout cyclonic spray
chamber will be detailed. The spray chamber was designed specifically for use
with a microconcentric nebuliser (MCN) and was optimised with respect to
response/washout characteristics and sample dispersion.

5.1 EXPERIMENTAL

A VG Plasma Quad PQ I ICP-MS instrument was used. Operating conditions,
unless otherwise stated, were as detailed in Chapter 4.

5.2 CYCLONIC SPRAY CHAMBER DESIGN

The spray chamber was fabricated from glass and had a general spherical shape
with a drain at the base and a horizontal mounting for the MCN on the side.

The internal volume of the spray chamber was 27 ml. A schematic diagram of the spray chamber is presented in Fig. 5.1.

The spray chamber design combines gravitational, centrifugal, turbulent and impact loss mechanisms to remove large droplets, increase analyte transport efficiency and reduce washout times. Sample aerosol from the nebuliser is directed horizontally into the chamber and intersects the chamber wall tangentially. This arrangement results in the sample aerosol experiencing a centrifugal force which serves to remove larger droplets from the polydisperse aerosol. In addition, the circulating action of the aerosol promotes aerosol re-entrainment which helps to minimise recirculation renebulisation. In recirculation renebulisation the aerosol strikes the walls of the spray chamber, liquid accumulates and is drawn back to the gas orifice where it may be re-entrained and renebulised.[1,2] This process can lead to band broadening and tailing and is therefore undesirable in a spray chamber intended for use in CE-ICP-MS. A dimple of 2.5 cm diameter was impressed into one side of the spray chamber and was designed to disrupt the circulating flow of aerosol, thereby generating turbulence and forcing larger droplets to collide with the dimple and with the outer wall of the chamber. The design of the dimple was similar to those incorporated into small vertical rotary spray chambers described by Wu and Hieftje[3] and Wu et al[4]
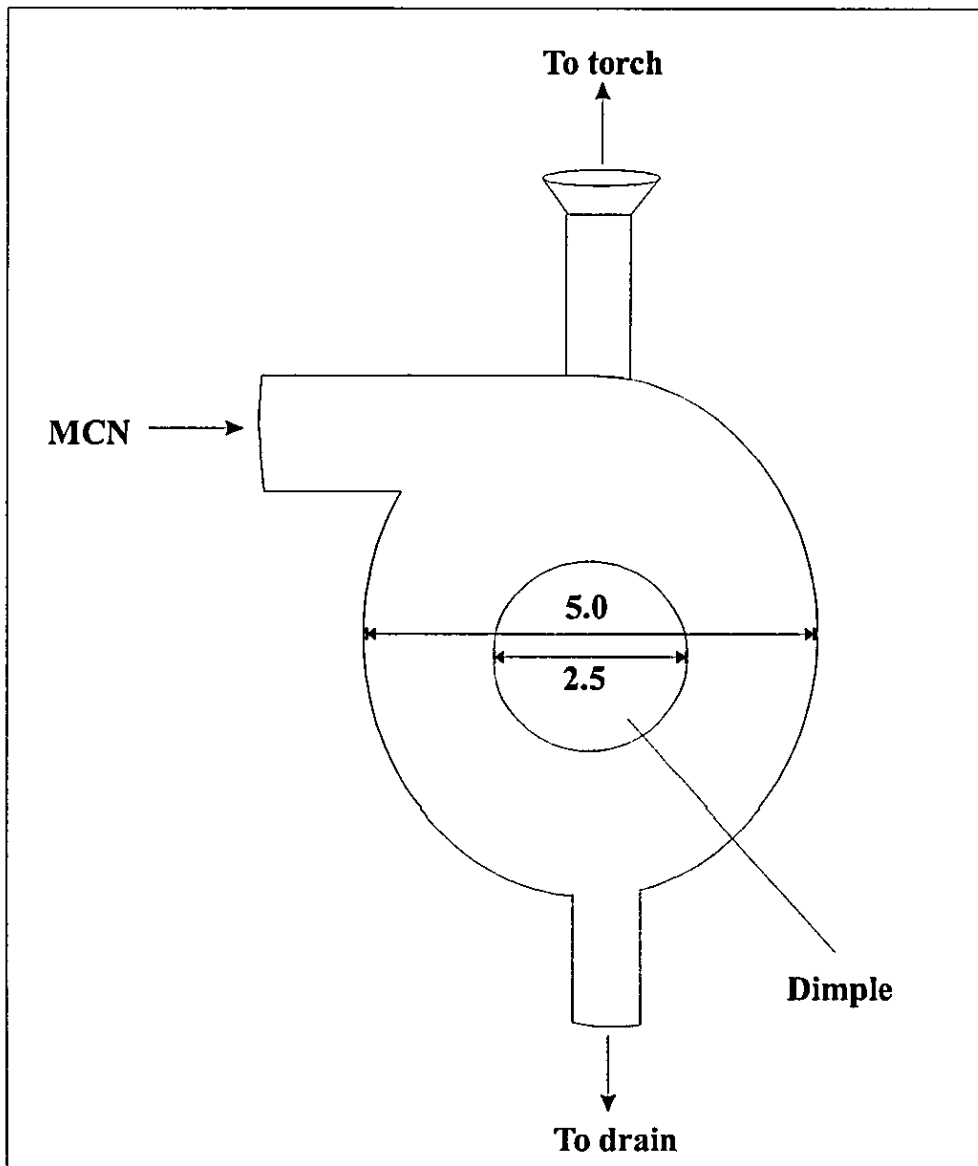
Figure 5.1. Schematic diagram of the cyclonic spray chamber. All units in

cm.

5.2.1 Spray Chamber Evaluation

The spray chamber was evaluated, and compared with a Scott-type double pass spray chamber, by measurement of sample response and washout times. The transient signals produced from flow injection (FI) sample introduction were measured in order to assess criteria important in CE, such as peak shape and dispersion. The effect of the position of the nebuliser within the spray chamber was also investigated.

5.2.1.1 SAMPLE RESPONSE AND WASHOUT TIMES

The sample response time was measured by pumping a test solution (In at 25 ng ml^{-1}) directly into the nebuliser using a peristaltic pump and monitoring the ^{115}In signal using TRA. The MCN was operated at a solution flow rate of 100 μl min^{-1} and a nebuliser gas flow of 0 9 l min^{-1}. The response time was defined as the time taken for the signal to equilibrate at its maximum value. Sample washout times were measured by replacing the test solution with a 1 % HNO$_3$ blank and monitoring the signal decay. Washout time was defined here as the period required for a signal to fall to 1 % of its initial value [1] Measurements were repeated in triplicate and the mean values calculated. In addition, the MCN was operated in self-aspiration mode and the response and washout times of the two spray chambers were measured.

The sample response and washout times for the cyclonic and Scott-type spray chambers are presented in Table 5.1.

Spray chamber	Response time/s	Washout time/s
Cyclonic[a]	115	105
Scott-type[a]	138	115
Cyclonic[b]	9	10
Scott-type[b]	11	42

[a] Peristaltic pump, [b] self-aspiration.

Table 5.1. Comparison of the response and washout times of the cyclonic

and Scott-type spray chambers.

The sample response and washout times of the two spray chambers, measured

using the peristaltic pump, were alarmingly long. The cyclonic spray chamber

provided a more rapid sample throughput than the Scott-type chamber, with

response and washout times 17 % and 9 % faster. However, in view of the

relatively small internal volume of the cyclonic spray chamber, the expected

improvement in washout time was not observed.

A theoretical washout time can be estimated from the residence time of a

particle in the spray chamber and from the volume of the chamber. If the

chamber functions as an ideal mixing volume, its washout time is

approximately three times the ratio of the volume of the chamber to the

nebuliser gas flow rate.[1,5] For the Scott-type and cyclonic spray chambers,

operated at a nebuliser gas flow rate of 0.9 l min^{-1}, theoretical washout times

were 40 s and 5.4 s, respectively.

By allowing the MCN to self-aspirate a significant improvement in sample

throughput rate was observed, with measured washout times much closer to the

estimated theoretical values. This observation indicated the presence of liquid phase dispersion in the peristaltic pump tubing.

When a solution is delivered at a low flow rate *via* a peristaltic pump liquid phase dispersion is prevalent as a result of the solution moving according to laminar flow where, the velocity is highest in the centre of the tubing and falls asymptotically to zero at the walls. In self-aspiration, when the sample tubing was transferred from the test solution to the blank, air was drawn into the tubing. An air segment will minimise dispersion by promoting a degree of turbulence within the flowing solution. Since turbulent flow is typified by a velocity profile approaching plug flow, dispersion does not prevail. In the case of the peristaltic pump, air was not introduced into the tubing because the pump was switched off when transferring from the test to the blank solution. Thus, the difference in response and washout times obtained using the peristaltic pump and self-aspiration were a result of liquid phase dispersion in the pump tubing.

In addition to liquid phase dispersion, a further factor influencing the long response and washout times of the cyclonic chamber was thought to be excessive aerosol recirculation. In an attempt to investigate possible aerosol recirculation and liquid phase dispersion effects, the following experiments were undertaken:

Recirculation. A glass bead (5.5 mm diameter) was placed inside the cyclonic

spray chamber and allowed to settle over the drain. The response and washout

times were then determined using the method described previously.

Dispersion. In an attempt to alleviate liquid phase dispersion, a segment of air

(approximately 6 cm long) was introduced into the pump tubing between the

sample and blank solutions. Response and washout times were then

determined. These measurements were then repeated with the glass bead

settled over the drain.

It was apparent that both aerosol recirculation and liquid phase dispersion were

contributing to the poor response and washout times of the cyclonic spray

chamber. The inclusion of the glass bead into the chamber had the effect of

stalling the recirculating flow of aerosol, and reduced the response and washout

times by 23 % and 28 %, respectively (Table 5.2). The most significant

improvement in response and washout times (94 % and 86 %, respectively) was

achieved by the introduction of an air segment into the pump tubing. This

clearly indicates the detrimental effect that laminar flow and liquid phase

dispersion had on response and washout times.

	Response time/s	Washout time/s
+ glass bead	88	76
+ air	7	12
+ glass bead, air	6	10

Table 5.2. Influence of recirculation and dispersion on the sample response and washout times of the cyclonic spray chamber.

5.2.1.2 FLOW INJECTION PEAK MEASUREMENTS

Transient signals were produced by FI sample introduction into the MCN/cyclonic spray chamber and MCN/Scott-type spray chamber combinations. Discrete aliquots of the test solution were introduced into the nebuliser/spray chamber combination using a Rheodyne FI valve (Rheodyne, California, USA) fitted with a 20 µl PTFE sampling loop. The carrier solution (1 % HNO_3) was delivered at 100 µl min^{-1} using a peristaltic pump. In order to minimise post valve dispersion, the FI valve was placed as close as possible to the nebuliser/spray chamber assembly by means of a Teflon connecting tube.

An example of the FI peaks produced using the two MCN/spray chamber combinations can be seen in Fig. 5.2. To provide a measure of the peak tailing and peak fronting, peak asymmetry values (As) were measured using the following equation:[6]
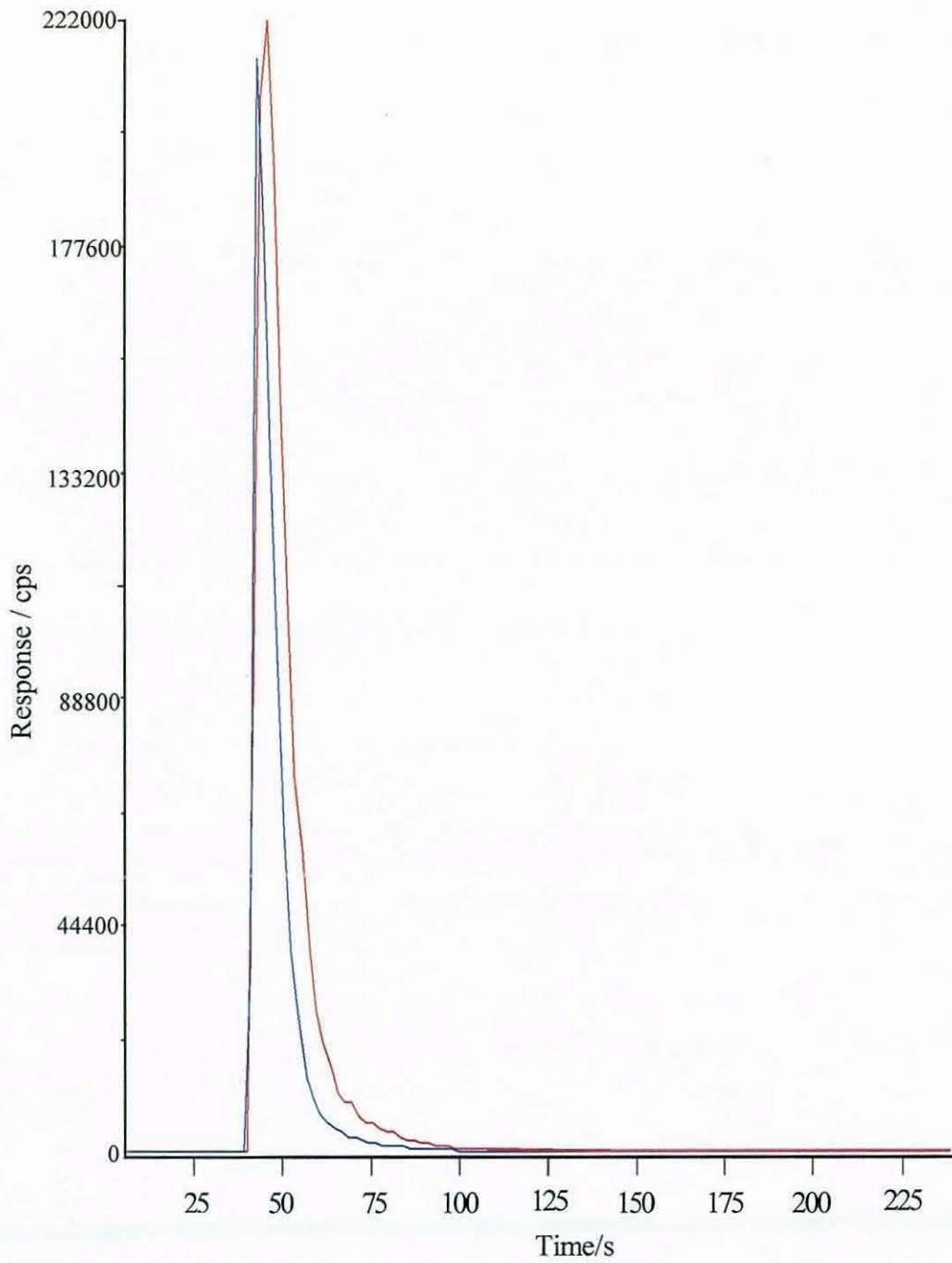
$$As = B/A \hspace{3cm} (Eqn. 5.1)$$

Figure 5.2. FI peaks produced using the Scott-type spray chamber (——) and

the cyclonic spray chamber (——).

where, at 10 % of the peak height, A represents the time between the peak maximum and leading edge of the peak, and B represents the time between the peak maximum and the tailing edge of the peak.

From the data complied in Table 5.3, it can be seen that the cyclonic spray chamber offered a reduction in band broadening compared with the Scott-type chamber. Peak widths at half peak height ($w_{1/2}$) were 5 s and 10 s for the cyclonic and Scott-type chambers, respectively. The increased peak width observed with the Scott-type chamber may be attributed to its larger dead volume. Peak tailing, represented by the B values, was more significant with the Scott-type spray chamber, and was likely to be a result of an increase in recirculation renebulisation. Undesirable echoes were not observed for either of the two spray chambers.

Spray chamber	$w_{1/2}$ /s	A/s	B/s	As
Cyclonic	5	4	12	3 0
Scott-type	10	7	17	2.4

Table 5.3. FI peak parameters obtained using the MCN/cyclonic spray chamber and the MCN/Scott-type spray chamber.

5.2.1.3 OPTIMISATION OF NEBULISER POSITION WITHIN THE SPRAY CHAMBER

To evaluate how the position of the nebuliser within the cyclonic spray chamber affected sensitivity and sample response/washout times, the MCN was placed as far forward as possible into the spray chamber so that distance from the nebuliser tip to the end of the MCN mounting was 18 mm. The ^{115}In signal and the sample response and washout times were then measured. Measurements were repeated with the MCN pulled back into its mounting so that the distance from the end of the mounting to the nebuliser tip was a) 14 mm and b) 10 mm.

The position of the nebuliser within the spray chamber had a significant effect upon the sensitivity and therefore analyte transport efficiency of the spray chamber. Pulling the nebuliser 8 mm back into its mounting resulted in a 41 % reduction in the observed sensitivity. However, this sensitivity loss was accompanied by a 2 s and 4 s improvement in the response and washout times, respectively.

Position of MCN /mm	^{115}In response/ x 10^5 counts s^{-1}	Response time/s	Washout time/s
18	2.7	6	12
14	1.9	4	12
10	1.6	4	8

Table 5.4. Influence of nebuliser position on signal response, response time and washout time.

5.3 MODIFIED CYCLONIC SPRAY CHAMBER

In view of the evaluation of the cyclonic spray chamber, a modified spray

chamber was designed and constructed. A schematic diagram and photograph

of the spray chamber are presented in Figs 5.3 and 5.4, respectively. The spray

chamber had an internal volume of 21 ml and was identical in design to the

original with the exception of a flow spoiler which was impressed into the side

of the chamber. The purpose of the flow spoiler was to mimic the effect of the

glass bead and stall the circulating flow of aerosol. A mini version of the

modified cyclonic spray chamber (internal volume 6.5 ml) and a spray chamber

with eight flow spoilers impressed around the body were also constructed.

5.3.1 Spray Chamber Evaluation

The response and washout times of the 21 ml and 6.5 ml cyclonic spray

chambers were measured, using the method described in Section 5 2.1.1. The

test solution used in this instance included Ce at 25 ng ml^{-1}. For comparative

purposes, measurements were repeated using a MCN/Scott-type spray chamber

and a cross-flow nebuliser/Scott-type chamber combination. The cross-flow

nebuliser was operated at 0.7 ml min^{-1}, the standard solution flow rate for

routine analysis.

The modified cyclonic spray chamber provided a rapid sample throughput, with

response and washout times of 6 s and 8 s, respectively (Table 5.5). Aerosol

recirculation was effectively minimised by the flow spoiler and a sample

To torch

MCN

5.0

2.5

Flow spoiler

Dimple

To drain

FRONT VIEW
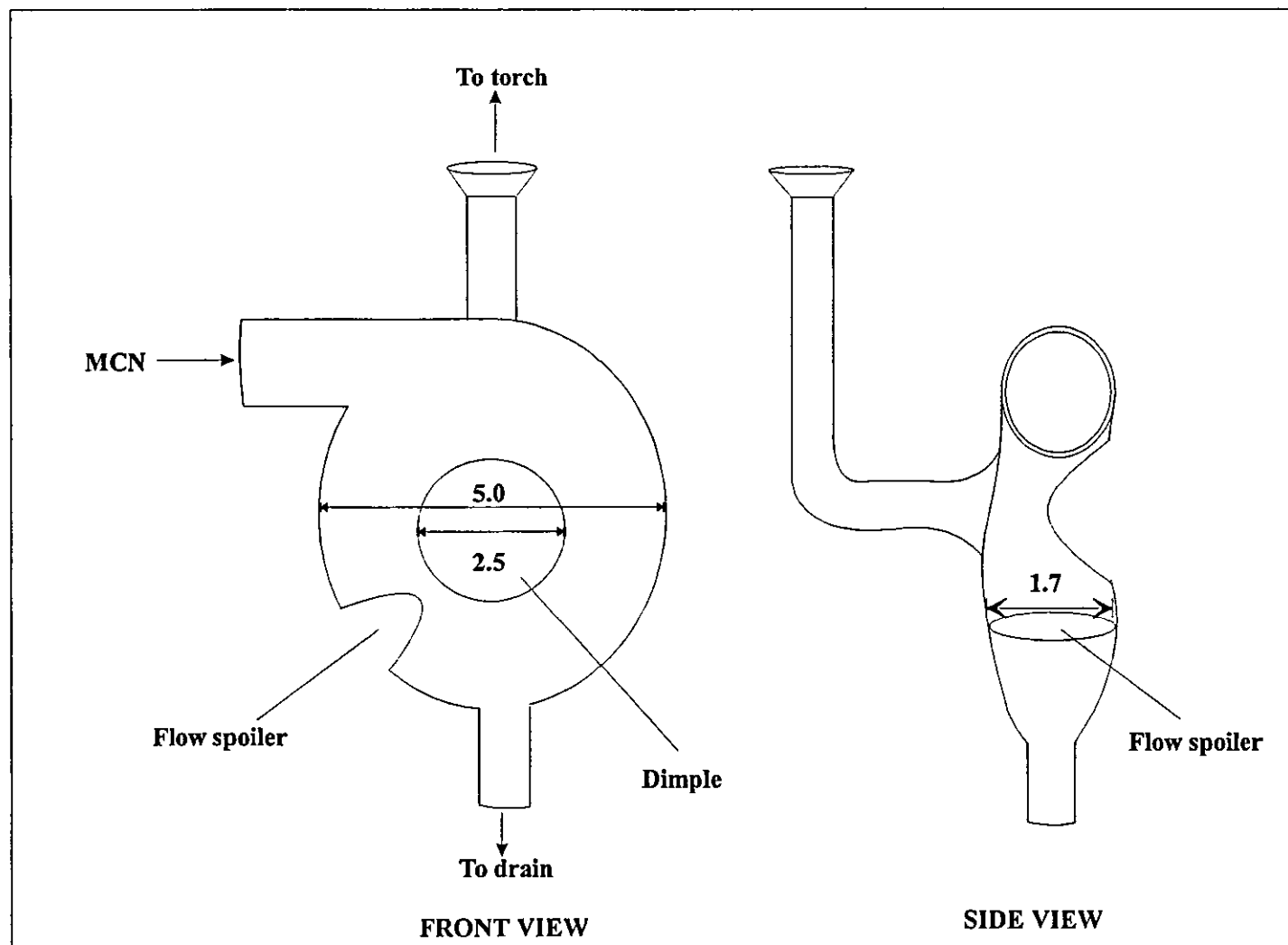
1.7

Flow spoiler

SIDE VIEW

Figure 5.3. Schematic diagram of the cyclonic spray chamber illustrating front and side views. All units in cm.

Figure 5.4. Photograph of the cyclonic spray chamber.

throughput 3.5 times faster than that provided by the Scott-type chamber was

achieved. The internal volume of the cyclonic spray chamber had no

significant effect on the response and washout times. With the 6.5 ml spray

chamber significant aerosol deposition was observed on the inner walls and was

reflected in the lower [115]In response.

Nebuliser/spray chamber	Response time/s	Washout time/s	[115]In response/ x 10^5 counts s^{-1}	CeO$^+$/Ce$^+$ (%)	Ce^{2+}/Ce$^+$ (%)
Cross-flow/Scott	13	25	2.4	0 9	0.8
MCN/Scott	15	28	1.6	0.7	0 6
MCN/cyclonic (21.0 ml)	6	8	1.8	0.7	0 6
MCN/cyclonic (6 5 ml)	6	8	1 3	0.6	0 6

Table 5.5. Comparison of the analytical characteristics of various

nebuliser/spray chamber combinations.

For the multi-flow spoiler chamber, the sample response and washout times

were similar to those obtained with the spray chamber incorporating one flow

spoiler.

5.4 SUMMARY

Rapid sample response and washout characteristics, and minimal sample

dispersion are clearly important in a spray chamber intended for CE-ICP-MS.

Liquid phase dispersion in the peristaltic pump tubing was identified as a

principal factor controlling the response and washout characteristics of the

cyclonic spray chamber. By eliminating liquid phase dispersion, with the introduction of an air segment, sample response and washout times were significantly improved. The cyclonic spray chamber, incorporating a dimple and flow spoiler, provided a rapid sample throughput approximately three times faster than that obtained using a Scott-type double pass spray chamber. Since response and washout times have a direct influence upon sample dispersion and therefore peak shape, the cyclonic spray chamber offers significant advantages over the Scott-type chamber for CE-ICP-MS.

REFERENCES

[1] B. L. Sharp, *J. Anal. At. Spectrom*, 1988, **3**, 939.

[2] J. A. Koropchak, S. Sadain and B. Szostek, *Spectrochim Acta,* 1996, **51B**, 1733.

[3] M. Wu and G. M. Hieftje, *Appl Spectrosc.,* 1992, **46**, 1912.

[4] M. Wu, Y. Madrid, J. A. Auxier and G. M. Hieftje, *Anal Chim. Acta,* 1994, **286**, 155.

[5] N. Z. Christchurch, *Can. J. Chem. Eng.,* 1985, **55**, 466.

[6] J. T. Landers, *Handbook of Capillary Electrophoresis,* 1997, CRC Press, New York.

CHAPTER SIX

Microconcentric Nebuliser CE-ICP-MS Interface

6.0 INTRODUCTION

This Chapter describes the design and characterisation of a CE-ICP-MS interface based on a commercial microconcentric nebuliser (MCN) and a cyclonic spray chamber. As discussed in Chapter 4, a key requirement of any CE-ICP-MS interface is a low flow nebuliser providing high analyte transport efficiency and small aerosol droplet sizes. The MCN offers a transport efficiency of up to 30% at solution flow rates of typically below 100 μl min^{-1}, and was preferred to other low flow nebulisers because of its simplicity and mechanical robustness (fabricated from PEEK, PTFE, fused silica). Furthermore, the MCN is relatively inexpensive when compared with, for example, the direct injection nebuliser (DIN) or the ultrasonic nebuliser (USN). The operating characteristics of the interface i.e., separation resolution, precision and limits of detection, will be investigated using the heavy metal binding protein, metallothionein (MT). Metallothionein is a low molecular mass (6000-7000 Da) cysteine-rich protein involved in the metabolism of heavy metals (Cd, Zn and Cu).[1-7] Polymorphism of metallothionein occurs during the evolution of a species and leads to two major isoforms, MTI and MTII, that are different in charge due to their amino acid composition.

.

6.1 EXPERIMENTAL

6.1.1 Reagents and Materials

Metallothioneins containing isoforms I and II (M7641, rabbit liver) and single isoform I (M5267) were purchased from Sigma. Metallothionein samples were prepared by dilution of the appropriate mass of standard with ultrapure (18.2 $M\Omega$) Milli-Q water. The electrophoresis buffer was 20 mM Tris (Sigma) adjusted to pH 7.8 with Aristar hydrochloric acid (FSA Laboratory Supplies, Loughborough, UK). A 10 mM NH_4NO_3 solution was used as the make-up flow. All solutions were vacuum degassed and filtered (through 0.45 μm) before use. 0.5 M NaOH was used to pre-condition the fused-silica capillary prior to the first use. For the UV detection work, 1 % mesityl oxide prepared by 1 % (v/v) dilution in 50 % methanol (Rathburn Chemicals, Walkerburn, UK) was used as an electroosmotic flow marker.

Individual stock standard solutions (atomic absorption grade) of Rb, Mn, Ba, Cd, Zn and In at 1000 μg ml^{-1} were obtained from Sigma. For the total metal determination in MT I, solutions containing Cd and Zn at 1000, 500, 250, 125 and 25 ng ml^{-1} were prepared by dilution of the 1000 μg ml^{-1} stock standard solutions in Milli-Q water. The ICP-MS instrument was tuned and optimised using a multi-element solution containing Be, Mg, Co, Ni, In, Ce, Pb, Bi and U at 25 ng ml^{-1} per metal, prepared by dilution of a stock standard solution [ICP-MS 100 solution (SPEX Industries, Edison, NJ, USA)] in 1% Aristar HNO_3.

6.1.2 Instrumentation

ICP-MS. A VG PlasmaQuad (PQ II Turbo Plus) inductively coupled plasma

mass spectrometer (VG Elemental, Winsford, UK) was used. Data acquisition

and interpretation was performed using Time Resolved Analysis (TRA) and

Masslynx software. The ICP-MS operating conditions are summarised in

Table 6.1.

Rf power	1350 W
Reflected power	0 W
Coolant gas flow	13.5 l min^{-1}
Auxiliary gas flow	1.45 l min^{-1}
Nebuliser gas flow	0.9 l min^{-1}
Sampler cone	Ni, 1.0 mm orifice
Skimmer cone	Ni, 0.7 mm orifice
Measurement mode	Peak jump (dwell time 10.24 ms)
Isotopes monitored	^{114}Cd, ^{111}Cd, ^{66}Zn, ^{64}Zn

Table 6.1. ICP-MS operating conditions.

CE System. Separations were performed using a Prince Technologies Crystal

310 CE system (Prince Technologies, Sunderland, UK). The CE system had a

double piston arrangement that allowed both positive and negative pressures to

be applied to the inlet vial. A 4225 variable UV/VIS detector (Thermo

Separation Products, Hemel Hempstead, UK) was used for on-capillary UV

detection. A fused-silica capillary (total length 77 cm, 60 cm to window) was

used and an absorbing wavelength of 200 nm was monitored. Samples were

injected hydrostatically and the capillary was rinsed with buffer for 2 mins

between each run. Electropherograms were recorded using a Dell OptiPlex Gs

computer and ProGC software (Thermo Unicam, Cambridge, UK). Data was

acquired at a sampling rate of 10 Hz.

CE-ICP-MS Interface. The interface incorporated a commercial MCN

(CETAC Technologies, Cheshire, UK), the T-piece assembly as described in

Chapter 4, and a small cyclonic spray chamber (as detailed in Chapter 5). A

schematic diagram and photograph of the interface are presented in Fig. 6.1 and

6.2, respectively. The separation capillary was passed through a hole in the

side of the CE system and was inserted into the T-piece assembly. The Pt-Ir

tube and capillary were connected directly into the back of the MCN using a

standard nut and ferrule. The capillary was sheathed, up to the point of

entering the T-piece, using Teflon tubing (0.03 in id, 0.063 in od). The purpose

of the capillary sheath was to prevent drifts in the capillary temperature (caused

by fluctuations in the laboratory temperature) which may affect the migration

time reproducibilty. The Pt-Ir tube was connected to the ground electrode of

the CE system using a grounding lead and a crocodile-type clip. The grounding

lead could be easily removed from the Pt-Ir tube thus allowing greater

flexibility than the solder connection employed in the previous interface.

6.2 INTERFACE CHARACTERISATION

6.2.1 Nebuliser Natural Aspiration Rate

The natural aspiration rate of three MCN's was measured as a function of

nebuliser gas flow rate. A 10 cm long piece of Teflon tubing was connected to

the nebuliser and the mass of water transferred from a pre-weighed vessel over
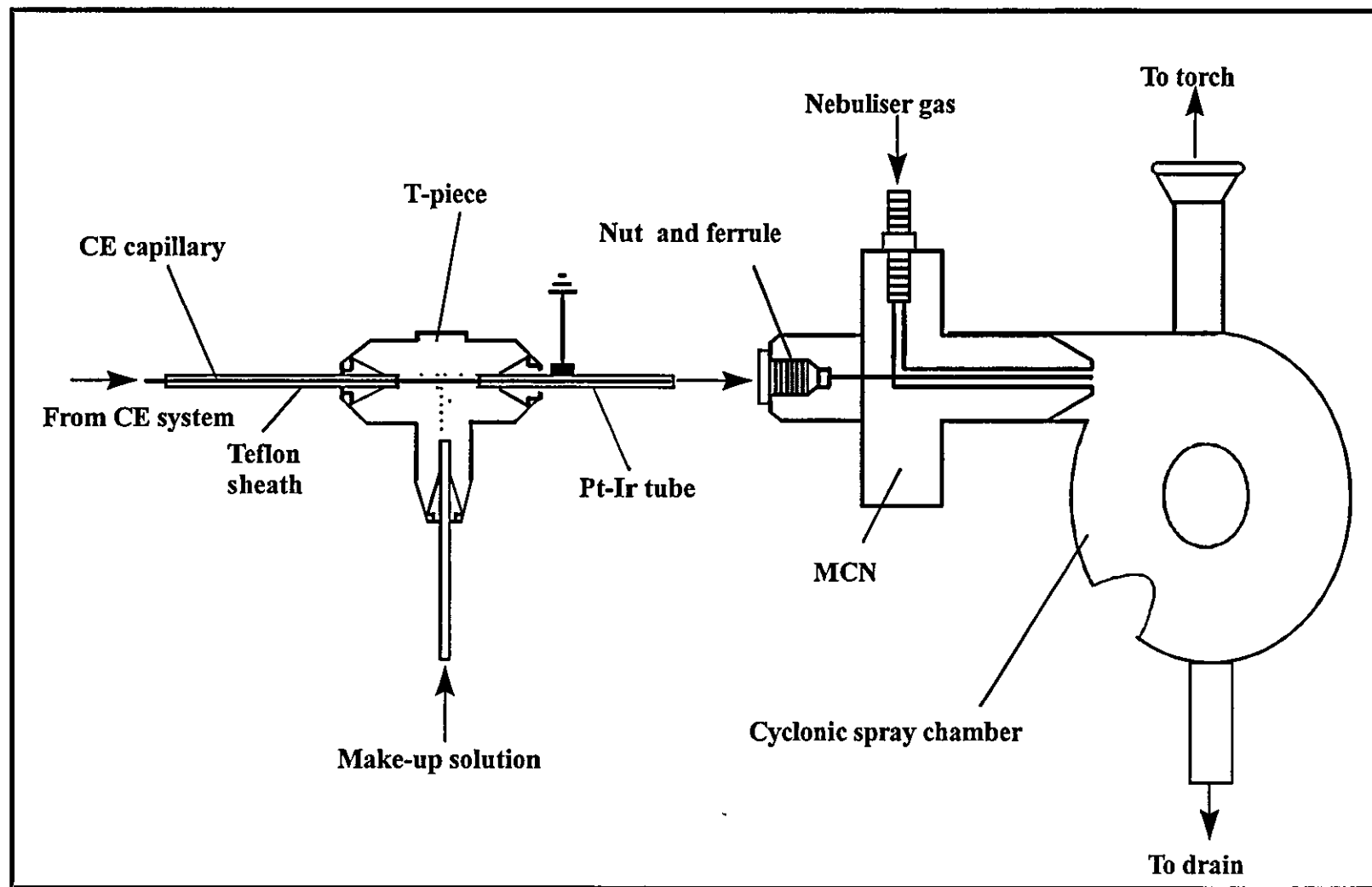
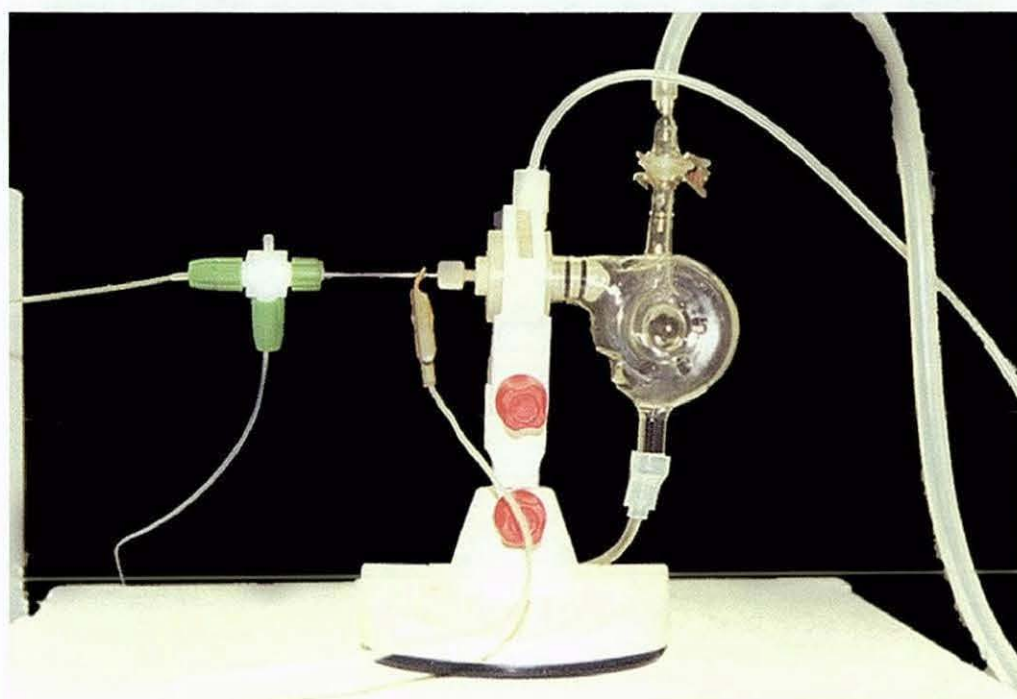*Figure 6.1. Schematic diagram of the MCN CE-ICP-MS interface.*

Figure 6.2. Photograph of the MCN CE-ICP-MS interface.

a 3 mins period was measured. It was necessary to ensure that the nebuliser

and water vessel were on the same level to prevent hydrodynamic resistance

restricting the uptake of water. All measurements were repeated in triplicate

and mean values calculated.

The natural aspiration rate of each MCN increased with increasing nebuliser

gas flow rate (Table 6.2). As the velocity of the nebuliser gas was increased,

the partial vacuum generated at the back of the MCN increased and

consequently the natural aspiration rate was enhanced. It is interesting to note

that although the three nebulisers were of identical design their natural

aspiration rates varied.

Nebuliser gas flow rate/l min^{-1}	MCN 1 natural aspiration rate/μl min^{-1}	MCN 2 natural aspiration rate/μl min^{-1}	MCN 3 natural aspiration rate/μl min^{-1}
1.0	163	248	164
0.9	125	215	153
0.8	103	184	143
0.7	69	159	135

Table 6.2. Natural aspiration rate as a function of nebuliser gas flow rate for

three MCN's.

6.2.2 Test Separation

To ensure the interface was operating effectively before characterisation with

metallothionein, a test separation was undertaken. Three inorganic cations (Rb,

Ba and Mn each at 10 μg ml^{-1}) were separated using a 5 mM 4-aminopyridine

buffer (pH 5.8) and an applied voltage of +15 kV (Fig. 6.3). Repeat separations

of the inorganic cations highlighted a problem with the MCN ceasing to self-

aspirate. After five repeat injections no sample peaks were detected and the

solution flow through the capillary was identified as being towards the inlet

vial. The central capillary of the MCN had blocked and consequently a back

pressure developed which caused the flow to be reversed in the separation

capillary. The MCN was unblocked by reverse flushing with 1 % HNO_3

however, after several repeat injections the MCN ceased to self-aspirate again.

The nebuliser was investigated over several days and a random loss of

nebuliser suction due to blockage of the nebuliser was observed. The two other

MCN's were investigated and also demonstrated a similar problem.

As a result of the problems experienced with the MCN a new MCN, identical

in design to the previous ones, but with an all-silica central capillary, was

employed. According to the manufacturers, the all-silica central capillary is

less susceptible to blockage compared with the polyimide coated capillary of

the old design MCN. The remainder of the work detailed in this Chapter was

undertaken using the all-silica MCN.

6.2.3 Pump Selection

As described in Chapter 4, grounding of the capillary was achieved by the use

of a coaxial sheath of make-up solution which was pumped through the vertical

arm of the T-piece. Initially, a peristaltic pump was used to deliver the make-

up solution. However, previous authors[8] have reported undesirable pulsing
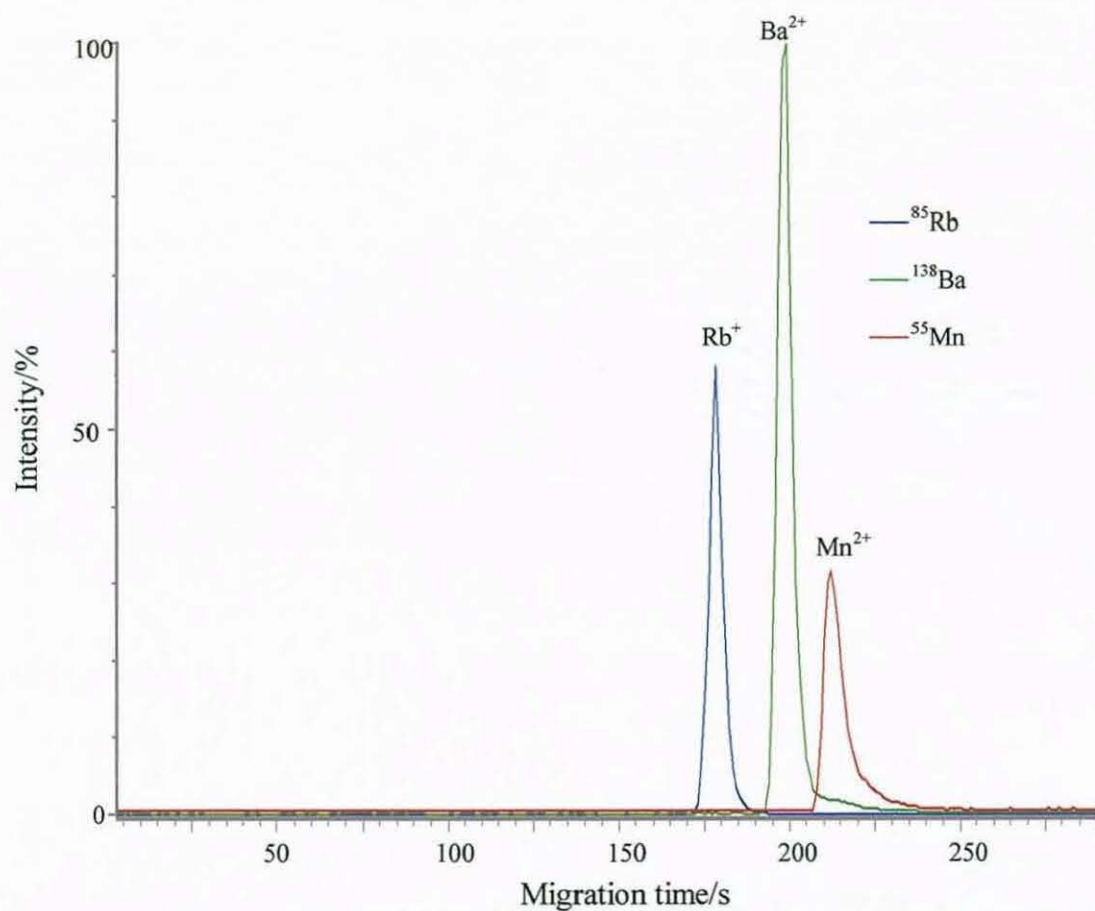
Figure 6.3. CE-ICP-MS electropherogram of an aqueous standard containing Rb, Ba and Mn (each at 10 μg ml⁻¹). Conditions: 15 kV; 5 mM 4-aminopyridine buffer (pH 5.8); fused-silica capillary, 50 μm id, 70 cm length; sample injection, 80 mbar for 12 s; 60 μl min⁻¹ make-up flow rate (10 mM NH₄NO₃).

effects generated by peristaltic pumps employed at low flow rates in CE-ICP-MS systems. To assess the suitability of the peristaltic pump for use in the CE-ICP-MS interface, make-up solution spiked with In (at 50 ng ml^{-1}) was pumped into the MCN at a flow rate of 20 μl min^{-1} and the ^{115}In signal was monitored using TRA. To help minimise possible pulsing, microbore pump tubing (0.19 mm bore) and higher pump rotation rates were employed. A microbore HPLC pump (Dionex GP40 Microbore Gradient Pump, Dionex, Camberley, UK) and self-aspiration were also assessed as possible methods for delivering the make-up solution.

The ^{115}In signals obtained using the peristaltic pump, HPLC pump and self aspiration are presented in Fig. 6.4. Undesirable pulsing effects were not observed using the peristaltic pump and the signal was stable. Self-aspiration also provided a stable signal but was not preferred because it was practically difficult to adopt. Calibration of the self-aspiration flow rate could only be carried out by varying the hydrostatic head on the solution. The signal obtained using the HPLC pump was the most unstable of the three. During operation, the back pressure of the HPLC pump fluctuated significantly which would indicate that the pump was struggling to maintain the desired low flow rate.
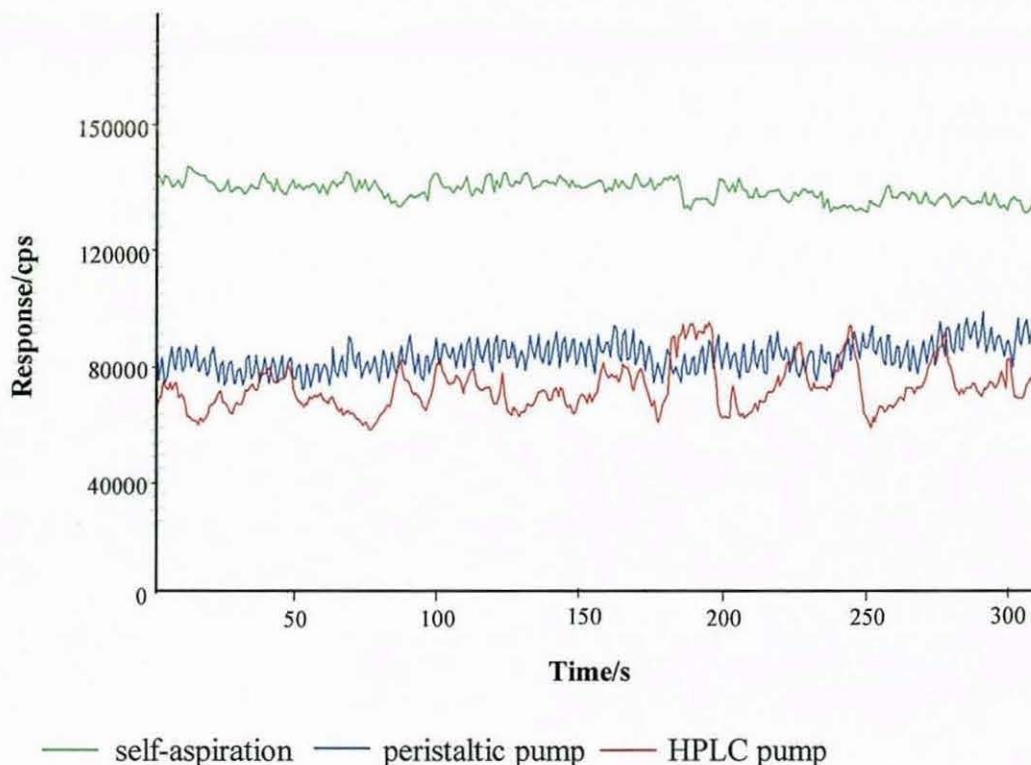
Figure 6.4. Comparison of the ^{115}In traces obtained using a peristaltic pump, HPLC pump and self-aspiration.

6.2.4 Separation Resolution

One of the principal characteristics of a CE-ICP-MS interface must be the ability

to transport separated sample components to the plasma without compromising

the electrophoretic resolution. To assess whether the interface adversely

affected resolution, individual isoforms of metallothionein were separated and

detected on-capillary using a UV detector. This separation was then repeated

using CE-ICP-MS and the corresponding separation resolutions were

compared. Separation resolution (Rs) was calculated using the following

equation[9]:

$$Rs = \frac{1}{4}\left(N^{\frac{1}{2}} \frac{\Delta t}{\bar{t}}\right)$$ (Eqn. 6.1)

where N is the efficiency, Δt is the difference in migration time (s) and $\bar{t}$ is the

mean migration time (s).

6.2.4.1 ON-CAPILLARY UV DETECTION

Isoforms of metallothionein were separated at pH 7.8 using a 20 mM Tris

buffer and an applied voltage of +25 kV. 1 % mesityl oxide was employed as

an electroosmotic flow marker. The UV detected electropherogram obtained is

illustrated in Fig. 6.5. The two predominant peaks were identified as the two

major isoforms of metallothionein, MT I and MT II. Four smaller peaks were

also observed in the electropherogram, but the identity of these was unknown.

It was probable, however, that these peaks were unknown isoforms of

metallothionein. It has been reported that rabbit liver metallothionein may

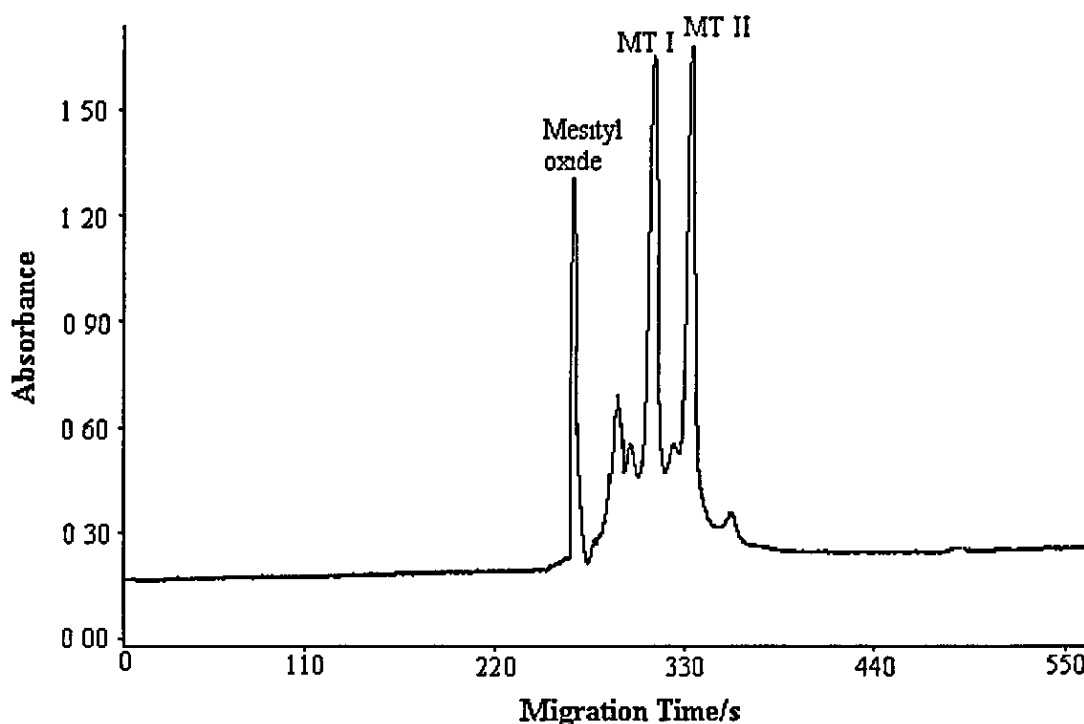consist of up to six individual isoforms, although only MT I and MT II have

been identified.[3]

Figure 6.5. UV detected electropherogram of rabbit liver metallothionein

(1000 µg ml⁻¹). Conditions: UV wavelength 200 nm; 25 kV; 20 mM Tris

buffer (pH 7.8); fused silica capillary 50 µm i.d., 77 cm total length, 60 cm to

window; sample injection 80 mbar for 12 s (19 nl); neutral marker 1 %

mesityl oxide.

6.2.4.2 ICP-MS DETECTION

For CE-ICP-MS, it was necessary to optimise the make-up flow rate in order to

minimise the nebuliser suction and resolve the metallothionein isoforms.

Suction from the self-aspirating nebuliser will have a detrimental effect upon

resolution by inducing laminar flow within the separation capillary. This

suction effect can be offset by pumping a sufficient flow of make-up solution to

satisfy the demand of the nebuliser.[10] The make-up flow was also employed

during sample injection to prevent air bubbles and excess of sample being

loaded into the capillary as a result of the nebuliser suction. The make-up flow

rate was increased (to the natural aspiration rate of the MCN) after the buffer

rinse and was resumed to the experimental rate immediately upon application

of the voltage. In previous interfaces,[10,11] the nebuliser gas flow has been turned

off during sample injection to prevent such problems. However, this method

may reduce the overall precision of the system because of the time taken in

resuming the gas flow to its original value. The nebuliser gas flow rate must be

increased slowly to prevent possible extinction of the plasma, consequently the

probability of associated irreproducibilities may be enhanced.

To determine the optimum make-up flow rate, isoforms of rabbit liver

metallothionein were separated by CE-ICP-MS using make-up flow rates

between 10 and 100 μl min^{-1}. Electrophoretic conditions as described in

Section 6.2.4.1 were employed. The total integrated peak area (^{114}Cd) and

resolution of MT I and MT II were measured for each make-up flow rate. A

graph representing the total peak area and resolution as a function of make-up

flow rate is presented in Fig. 6.6.

At the lowest make-up flow rate, 10 μl min^{-1}, inadequate compensation for the

nebuliser suction was achieved and consequently MT I and MT II were

completely unresolved (Fig. 6.7). As the make-up flow rate was increased,

resolution of the two isoforms improved as the nebuliser suction, and laminar

flow, were reduced. However, in order to improve resolution, sensitivity was

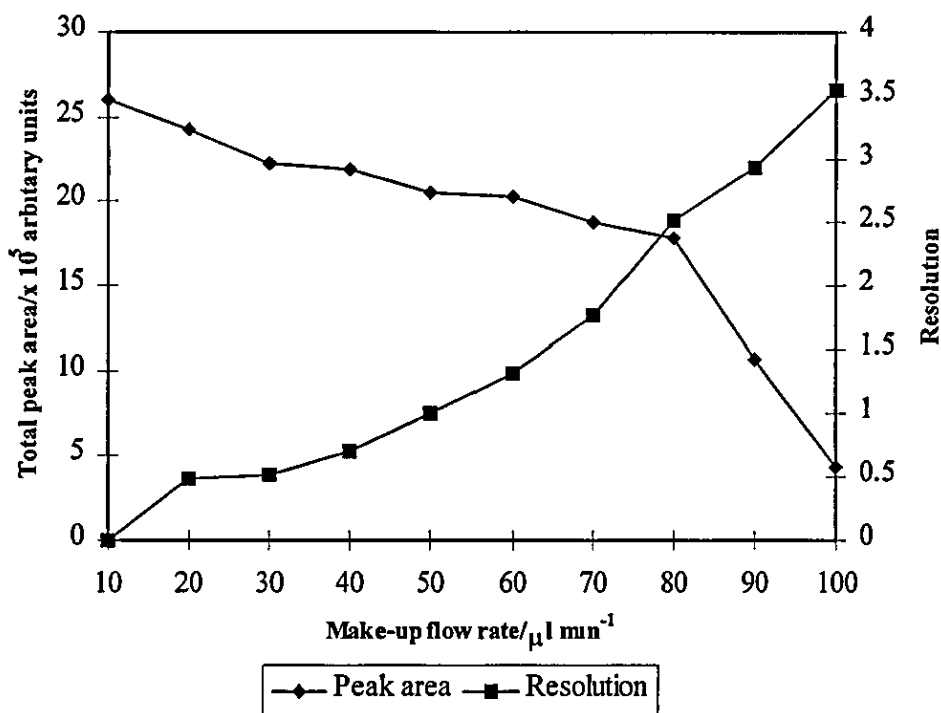compromised as a result of sample dilution by the make-up flow.

Figure 6.6. Graph representing the resolution and total peak area of MT I

and MT II as a function of make-up flow rate.

With an injected sample volume of 19 nl and an analyte peak width of 7 s, the

dilution resulting from a 100 µl min⁻¹ make-up flow was a factor of 614. It was

therefore necessary to select a make-up flow rate that offered a compromise

between resolution and sensitivity. From Fig. 6.6, it can be determined that a

flow rate of 80 µl min⁻¹ provided the optimum resolution (Rs = 2.52) and

sensitivity. The ^{114}Cd CE-ICP-MS electropherogram of rabbit liver

metallothionein obtained at 80 µl min⁻¹ make-up flow rate is illustrated in Fig.

6.8.
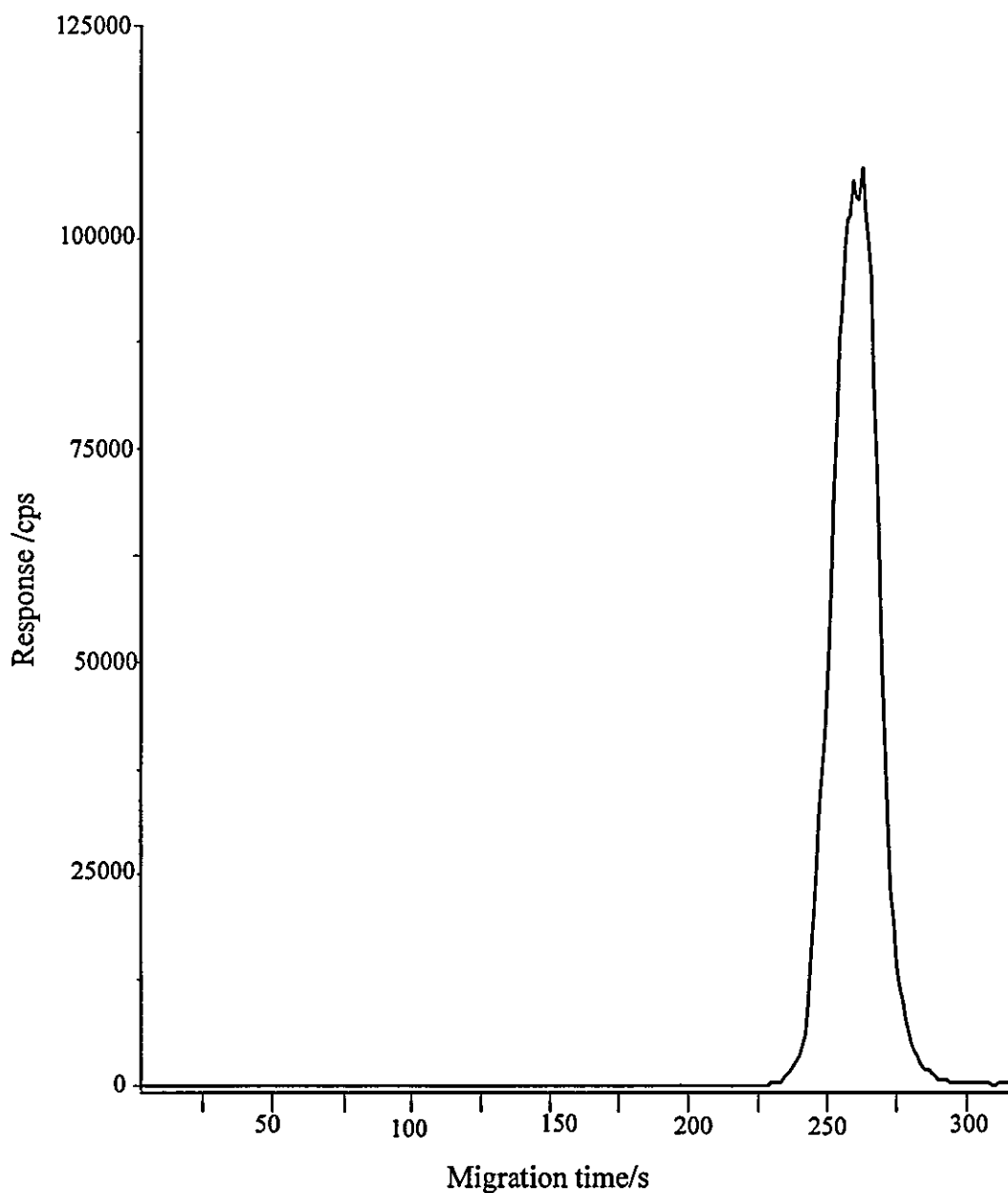
Figure 6.7. ^{114}*Cd CE-ICP-MS electropherogram of rabbit liver*

metallothionein (1000 µg ml^{-1}). Conditions: 25 kV; 20 mM Tris buffer (pH

7.8); fused-silica capillary, 50 µm id, 77 cm length; sample injection, 80 mbar

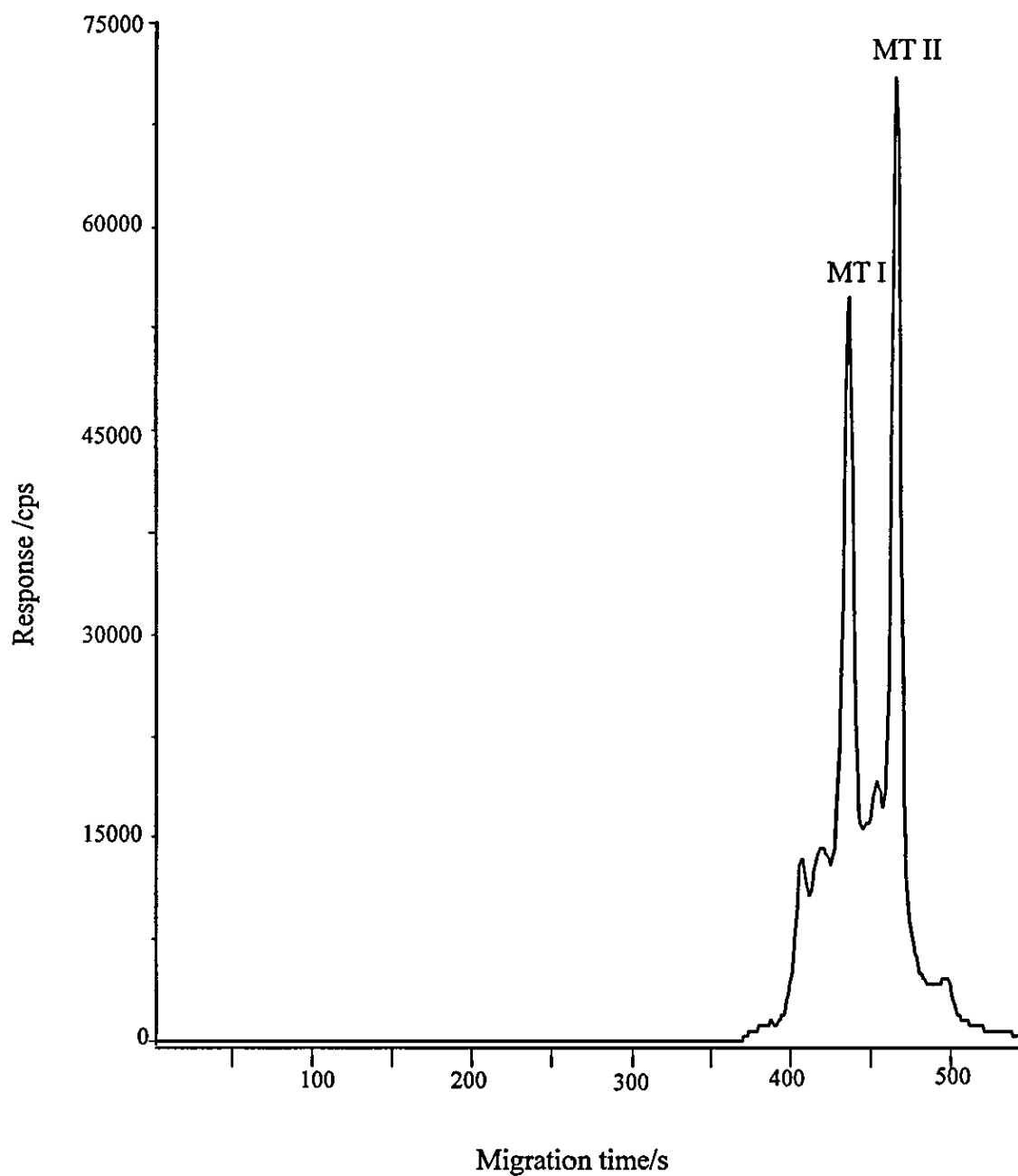*for 12 s (19 nl); 10 µl min^{-1} make-up flow rate (10 mM NH$_4$NO$_3$).*

Figure 6.8. ${}^{114}Cd$ CE-ICP-MS electropherogram of rabbit liver

metallothionein (1000 μl ml^{-1}). Conditions as in Fig. 6.6 except that the

make-up flow rate was 80 μl min^{-1}.

By utilising an optimised make-up flow to counterbalance nebuliser suction, a good separation of the two metallothionein isoforms was achieved. However, as a result of the compromised sensitivity, an alternative method for minimising nebuliser suction without the use of a high make-up flow rate was sought. In a previous concentric nebuliser interface,[10] a negative pressure was applied to the inlet vial as a counterbalancing force opposing the nebuliser suction and an improvement in separation resolution was reported. By using a negative pressure to counterbalance nebuliser suction, a low make-up flow rate can be employed therefore minimising sample dilution.

The effect of employing a negative pressure to counterbalance nebuliser suction can be seen in Fig. 6.9. This electropherogram was obtained using a make-up flow rate of 10 μl min^{-1} and an applied buffer reservoir pressure of -130 mbar. At 10 μl min^{-1} suction from the MCN was prominent, however the negative pressure applied to the buffer vial was sufficient to counterbalance this suction and the result was resolution of the two isoforms (Rs = 3). The migration times and resolution values listed in Table 6.3 demonstrate the effect of employing a negative pressure. The presence of residual nebuliser suction at a make-up flow rate of 80 μl min^{-1} was indicated by the shorter migration times. Resolution, under negative pressure conditions, was improved compared with that achieved using a high make-up flow rate. This was accompanied by a two fold increase in sensitivity associated with reducing the make-up flow rate to 10 μl min^{-1}. The sensitivity enhancement, however, was not as significant as would be expected from an 8 fold reduction in sample dilution. This may be an
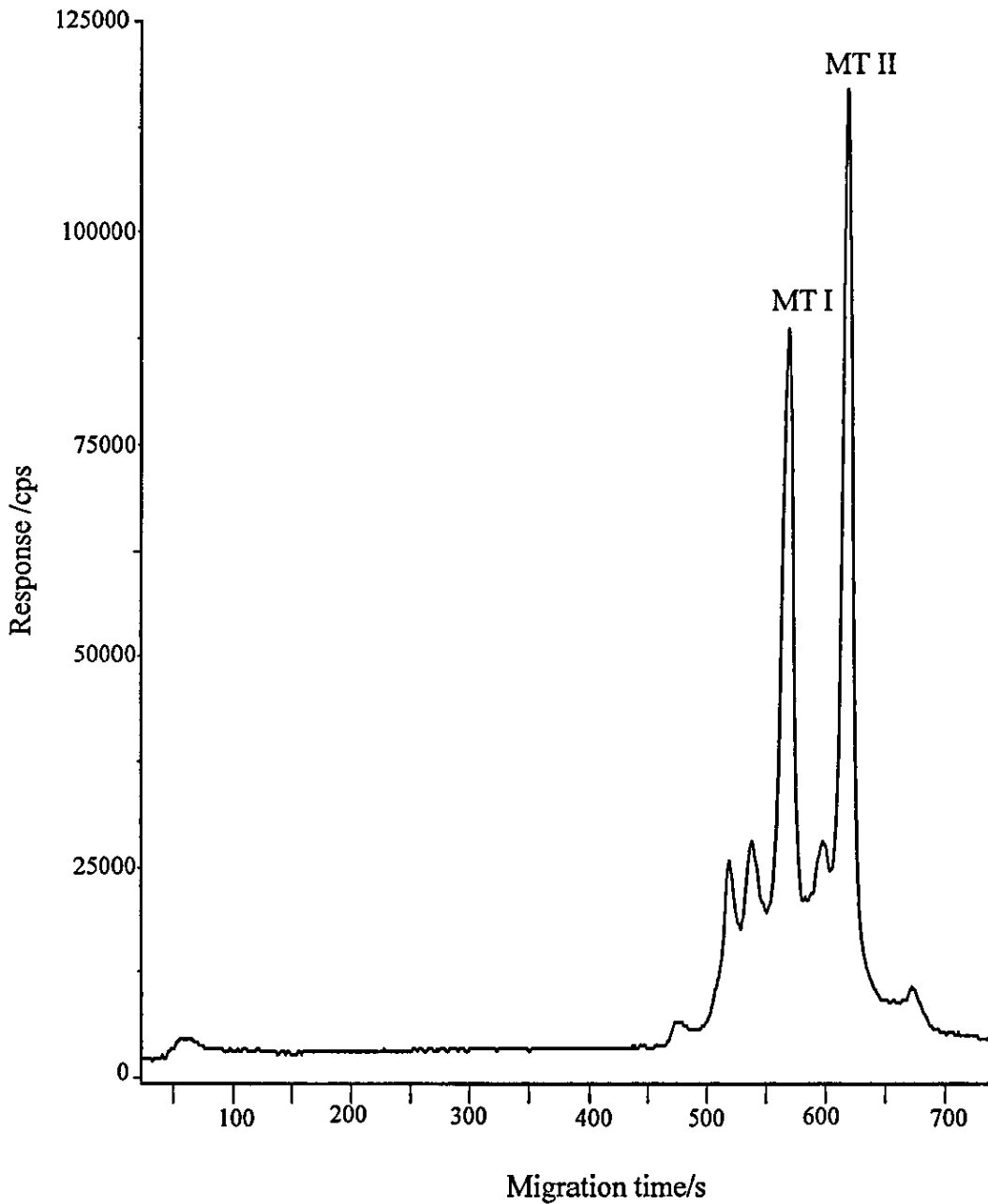
Figure 6.9. ^{114}Cd CE-ICP-MS electropherogram of rabbit liver

metallothionein (1000 μl ml^{-1}). Conditions as in Fig. 6.6 except that an

applied pressure of –130 mbar was used.

indication that the MCN was beginning to display marginal performance at such low solution flow rates.

Make up flow rate/ µl min⁻¹	Applied negative pressure /mbar	Migration time/s MT I	MT II	Resolution
80[a]	0	438	468	2.52
10[a]	-130	568	619	3.00
0[b]	0	313	333	2 45

[a]ICP-MS detection. [b] UV detection.

Table 6.3. Comparison of the resolution obtained using CE-ICP-MS and

CE-UV.

Compared with the resolution obtained using on-capillary UV detection, CE-ICP-MS offered an improvement. This improvement, however, was to some extent due to the difference in effective capillary length. For UV detection, the distance to the detection window was 60 cm whereas in CE-ICP-MS the solutes travelled the whole capillary length (77 cm) before reaching the detector. Separation resolution is directly related to capillary length, although a maximum length limit exists above which resolution deteriorates due to molecular diffusion.

6.2.5 Precision

The precision of the CE-ICP-MS system was assessed by measurement of the migration time, peak area and peak height repeatabilities of MT I and MT II. With ten consecutive injections of metallothionein (1000 µg ml⁻¹) RSD's were between 8 and 15 % (Table 6.4).

	MT I RSD/%	MT II RSD/%
Migration time	8	9
Peak area	15	13
Peak height	11	12

Table 6.4. Migration time, peak area and peak height precision (% RSD).

One area that requires improvement in CE is that of precision. Fluctuations in the migration times of solutes is one of the major causes of imprecision in CE,[12] with RSD's up to 5 %. It was not surprising that with CE-ICP-MS the precision was worse that that of conventional CE. Imprecision in CE can be caused by a number of factors, including variations in the EOF, sample adsorption on to capillary walls and buffer depletion. However, the major cause of imprecision in the CE-ICP-MS system was thought to be the irreproducibility of the nebuliser suction. Variations in the magnitude of the nebuliser suction were observed from day to day and during each day's use, and were caused by (1) the partial or complete blockage of the nebuliser capillary as a result of buffer salt crystallisation, and (2) the presence of air bubbles in the back of the nebuliser. The nebuliser suction had the greatest influence on the precision of the system because it not only affected the migration time, but also the sample volume injected (and hence the peak area and peak height). During sample injection the make-up flow rate was increased to the natural aspiration rate of the MCN to prevent suction on the capillary. If, for example, the nebuliser suction reduced, the make-up flow rate would then

exceed the natural aspiration rate and cause a back pressure to develop. The back pressure opposes the injection pressure and consequently a smaller sample volume will be loaded into the capillary.

In order to obtain reproducible results with CE, workers have suggested the use of internal standards and also the quotation of electrophoretic mobility rather than migration time as a measure of an analytes electrophoretic properties. With the further complication of transporting analytes to the off-capillary detector, such measures are particularly appropriate in CE-ICP-MS.

6.2.6 Detection Limits

CE-ICP-MS detection limits for the isotopes ^{114}Cd, ^{111}Cd, ^{66}Zn and ^{64}Zn were determined, under negative pressure conditions, using rabbit liver MT I. The ICP-MS peak areas were integrated using Masslynx and calibrated as a function of MT I concentration. MT I concentration detection limits were determined from 3 times the blank signal. The signal linearity for the four isotopes was measured over the concentration range of 1000 - 62.5 µg ml^{-1} MT I. Signals were linear with correlation coefficients of 0.9996, 0.9994, 0.9998 and 0.9998 for ^{114}Cd, ^{111}Cd, ^{66}Zn and ^{64}Zn respectively. Calibration curves for Cd and Zn are presented in Appendix I.

To determine the concentration detection limits of metals bound to MT I, it was necessary to quantify the total metal content in MT I. A 1000 µg ml^{-1} solution of MT I was diluted with Milli-Q water to 5 µg ml^{-1} and the metal

concentration in this sample was measured against an aqueous standard

calibration (1000-25 ng ml^{-1} Cd and Zn). The standards and MT I sample were

analysed by flow injection-ICP-MS using a 20 μl loop and the standard ICP-

MS configuration i.e., cross-flow nebuliser and Scott-type spray chamber. 1 %

HNO$_3$ was used as the carrier solution. Calibration graphs for Cd and Zn are

presented in Appendix I. The percentage by mass of metallothionein was 7.28,

7.20, 0.68 and 0.66 % for ^{114}Cd, ^{111}Cd, ^{66}Zn and ^{64}Zn, respectively.

The CE-ICP-MS concentration detection limits of MT I, the concentration

detection limits of the metals bound to MT I and the absolute metal detection

limits, based on a 19 nl injection volume, are presented in Table 6 5.

	^{114}Cd	^{111}Cd	^{66}Zn	^{64}Zn
MT I concentration LOD/μg ml^{-1} solution	1.52	2.52	68.74	71.97
Metal concentration LOD/ μg g^{-1} MT	0.11	0.18	0.47	0.48
Absolute metal LOD/fg	2.09	3.42	8.93	9.12

Table 6.5. CE-ICP-MS detection limits.

6.3 SUMMARY

The combination of a MCN and small cyclonic spray chamber provided a

simple, easily assembled CE-ICP-MS interface. Nebuliser suction was

identified as the principal factor controlling electrophoretic resolution in the

CE-ICP-MS system. To maintain resolution, the nebuliser suction was

counterbalanced by either an optimised make-up flow or by the application of a

negative pressure. The negative pressure method was preferred since it did not

significantly compromise sensitivity. The analytical value of the CE-ICP-MS

system was significantly limited by its poor precision which was attributed

principally to the irreproducibility of the nebuliser suction.

REFERENCES

[1]V. Virtanen, G. Bordin and A.-R. Roriquez, *J. Chromatogr. A,* 1996, **734,** 391.

[2]K. Takatera, N. Osaki, H. Yamaguchi and T. Watanabe, *Anal, Sci ,* 1994, **10,** 907.

[3]M. P. Richards and J. H. Beattie, *J Chromatogr B,* 1995, **669,** 27.

[4]C. B. Knudsen and J. H. Beattie, *J. Chromatogr. A,* 1997, **792,** 463.

[5]E. Torres, A. Cid, P. Fidalgo and J. Abalde, *J. Chromatogr. A,* 1997, **775,** 339.

[6]J. H. Beattie and M. P. Richards, *J. Chromatogr. A,* 1995, **700,** 95.

[7]H. Chassaigne and R. Lobinski, *J. Chromatogr. A,* 1998, **829,** 127.

[8]K. L. Sutton, C. B'Hymer and J. A. Caruso. *J. Anal At Spectrom.,* 1998, **13,** 885.

[9]P. D. Grossman and J. C. Colburn, *Capillary Electrophoresis· Theory and Practice,* 1992, Academic Press, San Diego.

[10]J. A. Kinzer, J. W. Olesik and S. V. Olesik, *Anal Chem ,* 1996, **68,** 3250.

[11]Q. Lu, S. M. Bird and R. M. Barnes, *Anal. Chem ,* 1995, **67,** 2949.

[12]J. Yang. S. Bose and D. S. Hage, *J. Chromatogr. A,* 1996, **735,** 209.

CHAPTER SEVEN

MicroMist Nebuliser CE-ICP-MS Interface

7.0 INTRODUCTION

In view of the poor repeatability demonstrated by the MCN-CE-ICP-MS

system, a new interface was designed incorporating a microconcentric

MicroMist nebuliser (Glass Expansion, Australia). The MicroMist nebuliser

was fabricated from glass and consequently may not exhibit the problems

demonstrated by the MCN i.e., it may be less susceptible to blocking by

crystallisation of buffer salt and any air bubbles present in the back of the

nebuliser will be visually detected. To compare the performance characteristics

of the two interfaces, the MicroMist interface was evaluated in the same

manner as the MCN interface using rabbit liver metallothionein.

7.1 EXPERIMENTAL

Reagents and instrumentation as detailed in Chapter 6 were employed.

$Co(Gly)_3$ obtained from The Royal Veterinary and Agricultural University,

Copenhagen was used as an electroosmotic flow marker.

CE-ICP-MS Interface. The interface was very similar in design to the MCN

interface, incorporating a MicroMist nebuliser and the original T-piece and

cyclonic spray chamber. A schematic diagram and photograph of the interface

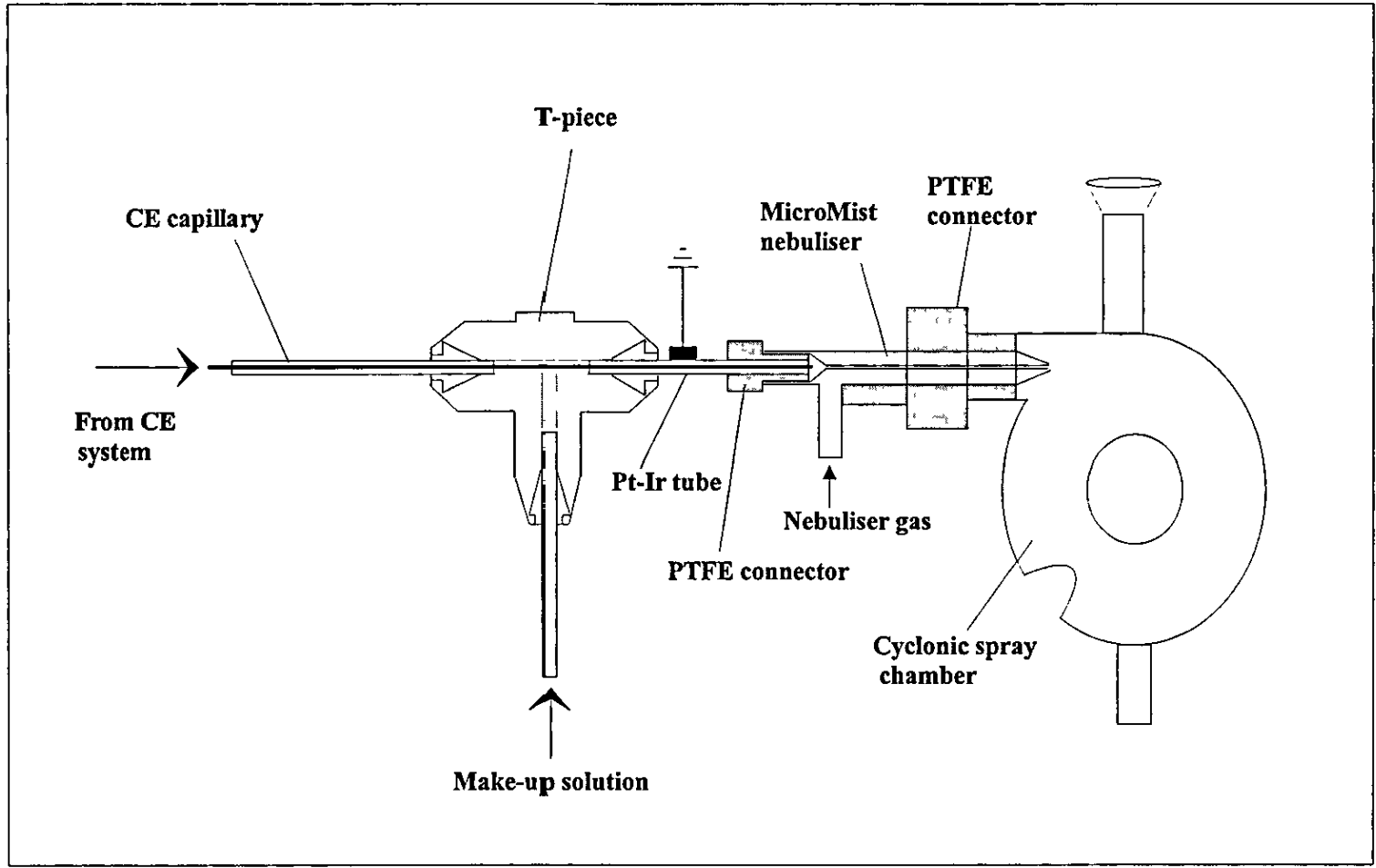are presented in Figs. 7.1 and 7.2, respectively.

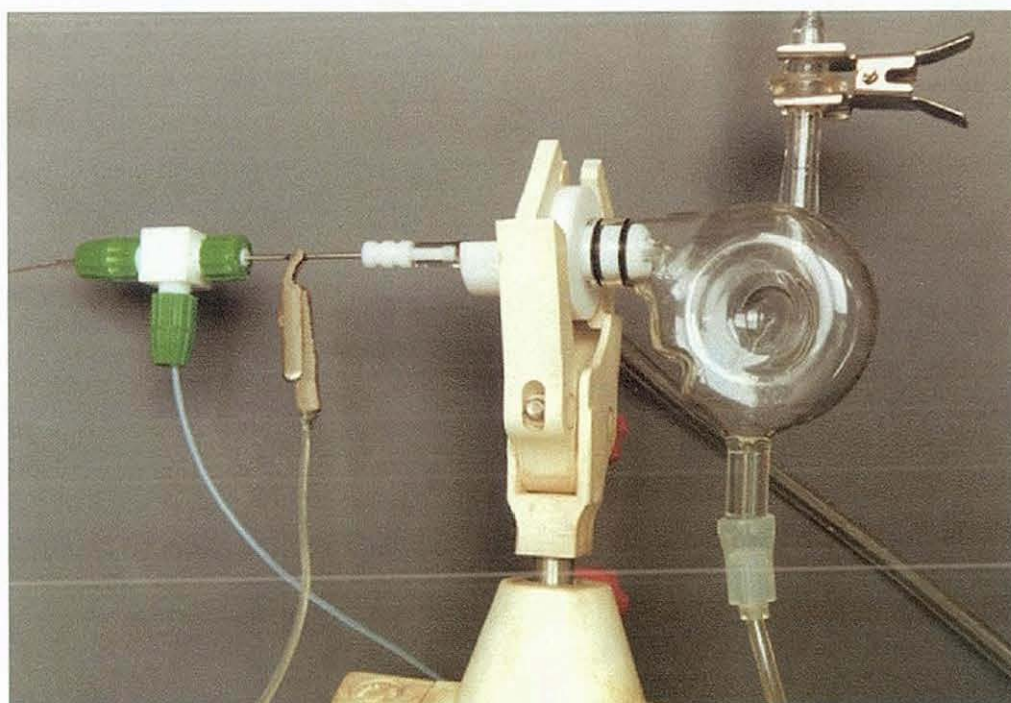*Figure 7.1. Schematic diagram of the MicroMist nebuliser CE-ICP-MS interface.*

Figure 7.2. Photograph of the MicroMist nebuliser CE-ICP-MS interface.

The Pt-Ir tube and separation capillary were connected directly into the central

tube of the MicroMist nebuliser using a 'push-in' type PTFE connector. The

position of the capillary within the central tube was variable over a distance of

4 mm inside the central tube. The nebuliser was inserted into a machined

PTFE connector which was then connected into the cyclonic spray chamber.

7.2 INTERFACE CHARACTERISATION

7.2.1 Nebuliser Evaluation

Prior to use in the interface, the operating characteristics of the MicroMist

nebuliser were evaluated. The nebuliser gas flow rate was optimised for

maximum sensitivity and the natural aspiration rate of the nebuliser was

measured as a function of nebuliser gas flow rate. A 25 ng ml^{-1} In solution was

introduced into the nebuliser at 50 μl min^{-1} and the ^{115}In signal was measured as

a function of nebuliser gas flow rate. The ICP-MS ion lenses were re-tuned at

each gas flow rate for optimum sensitivity. To measure the natural aspiration

rate of the nebuliser, a self-aspiration tube was connected to the nebuliser and

the mass of water transferred from a pre-weighed vessel (over a 3 mins time

period) was measured   All measurements were repeated in triplicate.

The natural aspiration rate of the nebuliser was found to decrease as the

nebuliser gas flow rate was increased (Fig. 7.3). This was an unusual property

of the nebuliser and was in contrast to the MCN (and other concentric

nebulisers) which demonstrate the opposite effect. The behaviour of the

MicroMist nebuliser may be explained by considering the geometry of the

nebuliser; the central tube was recessed with respect to the nebuliser tip. By increasing the nebuliser gas flow, the pressure of the stagnated gas beyond the recessed tip may increase, thus leading to a reduction in the natural aspiration rate. The optimum nebuliser gas flow rate i.e., that providing the maximum [115]In response was 0.75 l min^{-1} (Fig. 7.4).
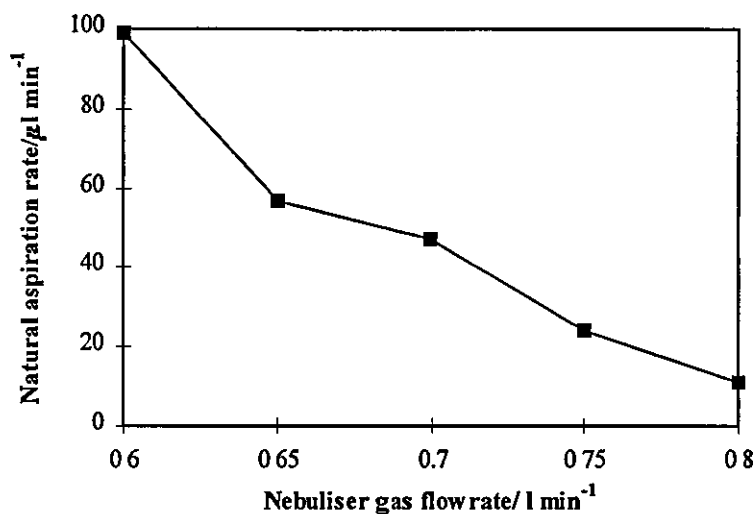

Figure 7.3. Natural aspiration rate of the MicroMist nebuliser as a function of nebuliser gas flow rate.
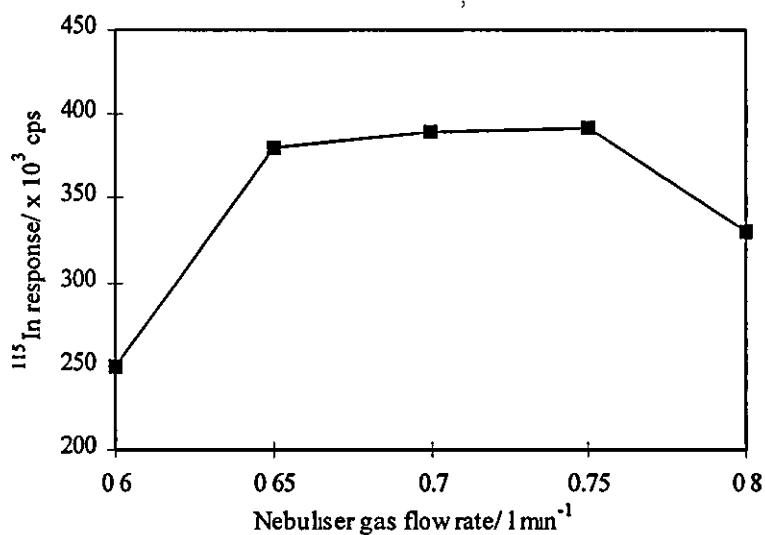

Figure 7.4. [115]In response as a function of nebuliser gas flow rate.

7.2.2 Optimisation of Capillary Position

To investigate the influence of the capillary position on signal intensity and

migration time (i e , nebuliser suction), rabbit liver metallothionein separations

were performed with the capillary positioned at 0, 1, 2, 3 and 4 mm inside the

central nebuliser tube. Electrophoretic conditions as detailed in Chapter 6 and

a make-up flow rate of 10 µl min⁻¹ were employed. The migration time and

peak height of MT II were measured at each capillary position and are

presented graphically in Figure 7.5.

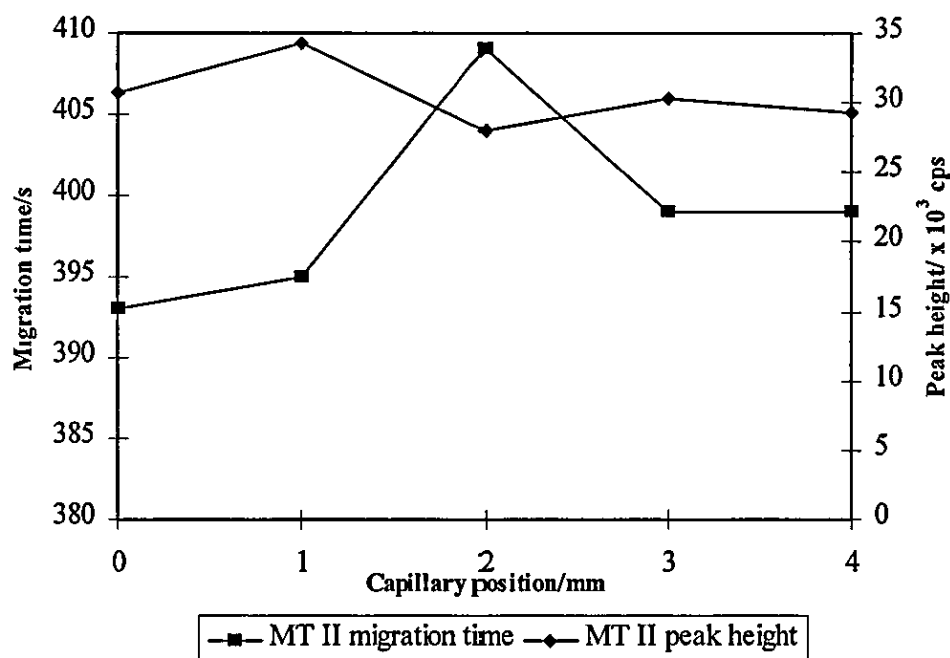*Figure 7.5. Influence of capillary position on MT II migration time and*

peak height (for ^{114}Cd).

There was no obvious correlation between the position of the CE capillary and

the migration time and peak height. This was a very favourable feature of the

interface since it was not necessary to precisely position the capillary each time

the interface was connected, therefore leading to a more reproducible system.

For other concentric nebuliser CE-ICP-MS interfaces[1-4] the opposite

observation has been reported, where the signal intensity and migration time

were sensitive to the precise capillary position.

7.2.3 Separation Resolution

As was the case with the MCN, suction from the self aspirating MicroMist

nebuliser had a detrimental affect upon the resolution of MT I and MT II.

However, because the natural aspiration rate of the MicroMist nebuliser was

lower than the MCN (typically by 50 %), the laminar flow induced in the

capillary was less and consequently, at a make-up flow rate of 10 μl min^{-1},

resolution of the two isoforms was achieved (Fig. 7.6 a). This was in contrast

to the MCN interface where at a make-up flow rate of 10 μl min^{-1} complete loss

in resolution of the two isoforms was observed. By using a negative pressure

to counterbalance the nebuliser suction, an improvement in the resolution was

observed (Fig 7.6 b). The effect of the nebuliser suction can also be observed

in the faster migration times when no negative pressure was employed.

7.2.4 Precision

The precision of the CE-ICP-MS system was determined by measurement of

the migration time, peak area and peak height repeatabilities for 10 consecutive

injections of metallothionein (1000 μg ml^{-1}). To correct for solute migration

time variations caused by shifts in the electroosmotic flow and nebuliser

suction, an internal standard (electroosmotic flow marker) was employed.

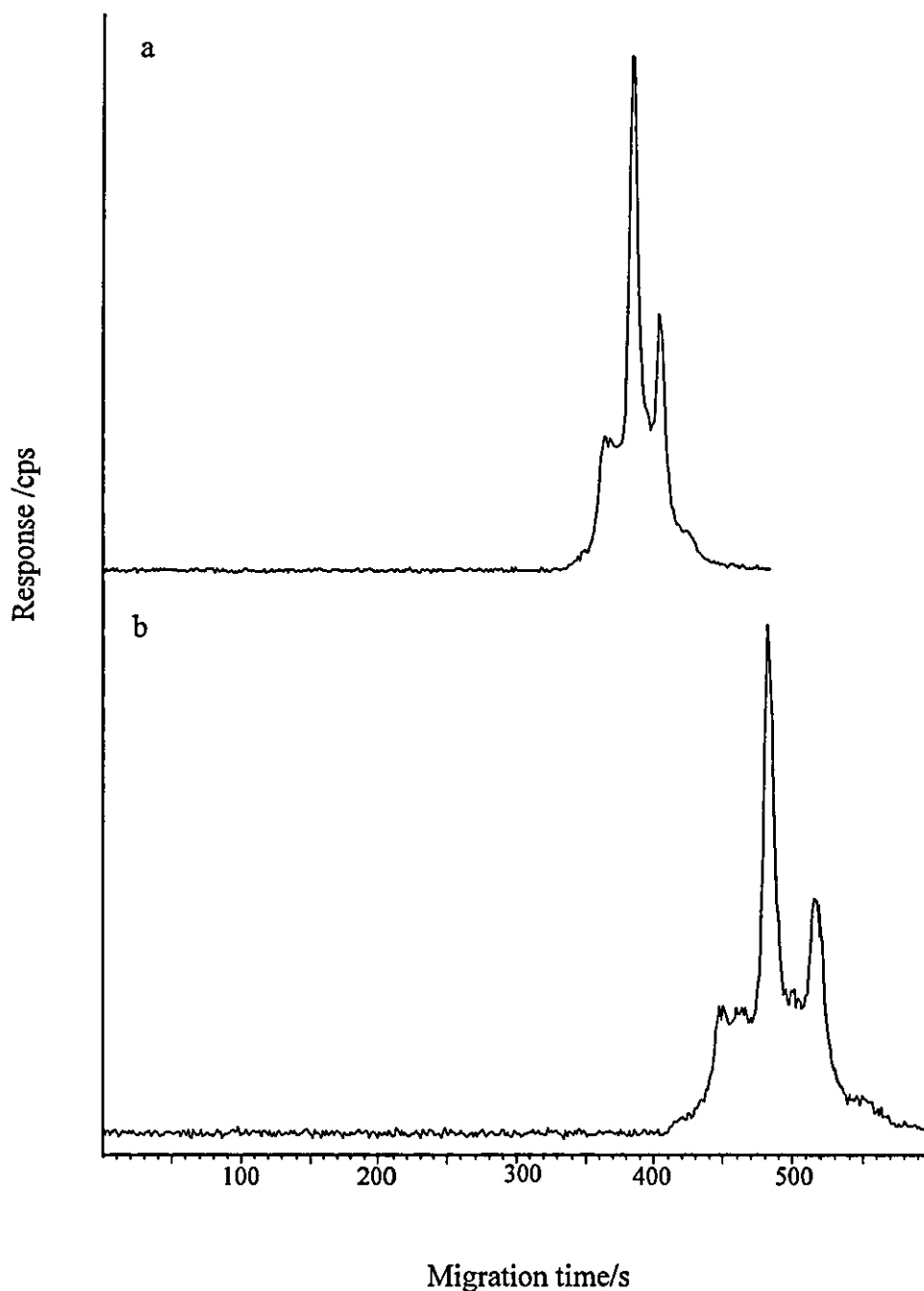*Figure 7.6.* ¹¹⁴*Cd electropherograms of rabbit liver metallothionein (1000 μg ml^{-1}) illustrating the effect of negative pressure on resolution. a; 10 μl min^{-1} make-up flow rate, b; 10 μl min^{-1} make-up flow rate, -50 mbar applied pressure.*

Relative migration times (R_t) were calculated using the following equation:[5]

$$R_t = \frac{t_{net}}{t_{eo}}$$
(Eqn. 7.1)

where, t_{net} is the net migration time of the solute and t_{eo} is the migration time of

the electroosmotic flow marker.

A summary of the migration time, peak area and peak height RSD's are

presented in Table 7.1. RSD's were below 4.3% and were significantly

improved (by up to 85 %) compared with the MCN interface. This

improvement can be attributed solely to the reproducible nature of the

MicroMist nebuliser suction. By using an internal standard to correct for shifts

in migration times, the migration time precision was reduced to 0.5 %.

	MT I RSD/%	MT II RSD/%
Peak height	4.3	4.2
Peak area	2.3	2.9
Migration time	1.9	1.9
Relative migration time	0.5	0.4

Table 7.1. Precision data for the MicroMist nebuliser CE-ICP-MS system.

7.2.5 Detection Limits

CE-ICP-MS detection limits were determined using rabbit liver MT I, as

described in Chapter 6. Zn was not detected in the MT I standard and

consequently only ^{114}Cd and ^{111}Cd detection limits were determined. Signals

were linear (over the concentration range of 1000 - 62.5 μg ml^{-1} MT I) with

correlation coefficients of 0.9997 and 0.9994 for ^{114}Cd and ^{111}Cd respectively.

Calibration curves for ^{114}Cd and ^{111}Cd are presented in Appendix I. A summary

of the CE-ICP-MS detection limits is provided in Table 7.2. The absolute

metal detection limits were higher (by approx. a factor of 2) than those obtained

using the MCN interface.

	^{114}Cd	^{111}Cd
MT I concentration LOD/μg ml^{-1} solution	6.91	7.88
Metal concentration LOD/ μg g^{-1} MT	0.50	0.57
Absolute metal LOD/fg	4.77	5.44

Table 7.2. CE-ICP-MS detection limits.

7.3 SUMMARY

A comparison of the MicroMist and MCN interfaces showed the MicroMist

interface to be superior in terms of precision. The RSD's measured for the

MicroMist interface were up to 85 % lower than those obtained with the MCN

interface. This improvement was attributed solely to the reproducible nature of

the MicroMist nebuliser suction. Migration time drifts were corrected by the

use of an electroosmotic flow marker and resulted in a migration time RSD of

0.5 %. The detection limits achieved using the MicroMist interface were

higher, by approximately a factor of 2, than those obtained using the MCN.

This may be a result of a difference in the droplet size distribution of the

primary aerosols generated by the two nebulisers.

REFERENCES

[1] Q. Lu, S. M. Bird and R. M. Barnes, *Anal. Chem.,* 1995, **67**, 2949.

[2] B. Michalke and P. Schramel, *Fresenius' J. Anal Chem ,* 1997, **357**, 594.

[3] S. Lustig, B. Michalke, W. Beck and P. Schramel, *Fresenius' J. Anal Chem ,* 1998, **360**, 18.

[4] M. Van Holderbeke, Y. Zhao, F. Vanhaecke, L. Moens, R. Dams and P. Sandra, *J. Anal. At. Spectrom ,* 1999, **14**, 229.

[5] J. Yang, S. Bose and D. S. Hage, *J Chromatogr. A,* 1996, **735**, 209.

CHAPTER EIGHT

The Speciation of Selenium In Yeast

8.0 INTRODUCTION

Selenium is an essential element for biological systems known both as a

nutrient and as a potential toxicant. The tolerance range between beneficial and

toxic concentrations is very narrow, and both an excessive and insufficient

intake of selenium can have serious health implications. Selenium toxicity,

selenosis, can lead to skin lesions, hair loss and abnormalities of the nervous

system, whilst selenium deficiency has been linked with heart disease, arthritis

and infertility.[1] Selenium also has a suggested role in the prevention of

cancers[2,3] due to its incorporation in the human enzyme glutathione peroxidase

which inhibits the oxidative role of peroxides and hydroperoxides.

The nutritional bioavailability, toxicity and cancer preventive activity of

selenium have been shown to be highly species dependent.[4-7] Selenium in the

form of selenomethionine is less efficacious than selenite in preventing cancer

because selenite is more easily metabolised to methyl selenol, the form of

selenium active against cancer.[4] In contrast, the bioavailability of

selenomethionine is greater than that of selenite. Human studies have shown

selenomethionine to have an apparent absorption of > 90 %[7] whilst the

absorption of selenite was in the range of 30 % to 60 %.[8,9]

Due to the nutritional and cancer preventive benefits, selenium enriched yeast

is widely used as a source of selenium in nutritional supplements.

Clark *et al.*[2] reported that the consumption of yeast derived selenium nutritional supplements was associated with statistically significant reductions in total cancer mortality and cancer incidence. This finding has led to much interest in the speciation of selenium in selenium enriched yeasts. Gilon *et al.*[10] and Olivas *et al.*[11] reported the presence of three different forms of selenium in yeast; inorganic selenium, selenocystine and selenomethionine. In the work by Bird *et al.*[12,13] more than twenty selenium species, including selenocystine, selenomethionine and methylselenocysteine, were reported to be present in selenium enriched yeast. To date, the majority of studies have focused on the use of HPLC-ICP-MS methods for the speciation of selenium in yeast, with particular reference to ion pair and ion exchange chromatography. Although CE methods have been developed to separate organic and inorganic selenium species,[14-17] as yet the technique has not been applied directly to yeast samples.

In this Chapter, the development of a CE-ICP-MS method for the speciation of selenium in selenium enriched yeast and selenium nutritional supplements will be detailed.

8.1 EXPERIMENTAL

8.1.1 Reagents and Samples

Sodium selenite, sodium selenate, seleno-DL-methionine and seleno-DL-cystine were purchased from Sigma. Standard solutions of the four selenium species were prepared by dilution of the appropriate mass of standard in Milli-Q water. A 100 ng ml^{-1} selenium solution was used for tuning the ICP-MS and

was prepared by dilution of a 1000 $\mu g\ ml^{-1}$ stock standard solution (Sigma) in 1

% HNO_3. Sodium carbonate [Na_2CO_3 (Sigma)] was used as the electrophoresis

buffer and was prepared by dissolution in Milli-Q water. The make-up flow

solution was 5 mM NH_4NO_3 and $Co(gly)_3$ was used as the EOF marker. The

extraction enzyme, protease XIV, was purchased from Sigma. A certified

reference material, DOLT-2, was purchased from Promochem (Welwyn Garden

City, UK).

Four different samples were analysed: Sample A was an industrially produced

selenium enriched yeast (1948 $\mu g\ g^{-1}$ Se); sample B was a commercially

available yeast based selenium supplement (333 $\mu g\ g^{-1}$ Se); sample C was a

commercially available non-yeast based selenium supplement (400 $\mu g\ g^{-1}$ Se);

sample D was a ^{77}Se isotopically enriched yeast produced at the Institute of

Food Research, Norwich.

8.1.2 Instrumentation

ICP-MS. For the speciation analysis, a VG PlasmaQuad (PQ I) ICP-MS

instrument was used. For the total selenium determinations, a Perkin Elmer

Sciex Elan 6000 (Perkin Elmer, Beaconsfield, UK) ICP-MS instrument fitted

with a cross flow nebuliser and double pass spray chamber was employed.

Typical operating conditions for the two ICP-MS instruments are provided in

Table 8.1.

	VG PQ I	PE Elan 6000
Rf power/W	Optimised	1350
Reflected power/W	0	0
Coolant gas flow/ $1\,\mathrm{min}^{-1}$	13.5	14.0
Auxiliary gas flow/ $1\,\mathrm{min}^{-1}$	0.8	0.8
Nebuliser gas flow/ $1\,\mathrm{min}^{-1}$	Optimised	0.8
Measurement mode	Peak jump (dwell time 10.24 ms)	Peak jump (dwell time 100 ms)
Isotopes monitored	^{59}Co, ^{76}Se, ^{77}Se, ^{78}Se, ^{82}Se	^{74}Se, ^{76}Se, ^{77}Se, ^{78}Se, ^{82}Se

Table 8.1. ICP-MS operating conditions.

CE System. Separations were performed using the Prince Technologies Crystal

310 CE system as described in Chapter 6.

CE-ICP-MS Interface. The MicroMist nebuliser interface as detailed in

Chapter 7 was employed.

Microwave. Total selenium concentration in the yeast samples was determined

by ICP-MS following acid digestion in a closed vessel Perkin Elmer Multiwave

microwave (Perkin Elmer, Beaconsfield, UK).

8.2 RESULTS AND DISCUSSION

8.2.1 Optimisation of Rf Power and Nebuliser Gas flow Rate

The Rf forward power and nebuliser gas flow rate were optimised in order to attain the maximum sensitivity for selenium. A 100 ng ml^{-1} selenium solution was introduced into the MicroMist nebuliser at 10 µl min^{-1}, and the ^{82}Se response was measured as a function of forward power and nebuliser gas flow rate. The selenium solution was delivered using a peristaltic pump and the ICP-MS ion lenses were re-tuned each time the power or nebuliser gas flow rate was changed.

As the nebuliser gas flow was increased from 0.6 to 0.7 l min^{-1} the selenium ion intensity increased (Fig. 8.1). Beyond a nebuliser gas flow rate of 0.7 l min^{-1} the selenium ion intensity decreased, thus yielding an optimum nebuliser gas flow rate of 0.7 l min^{-1}. Increasing the Rf forward power from 1350 to 1500 W, at 0.7 l min^{-1} nebuliser gas flow rate, resulted in a 16 % enhancement of the selenium signal. At other nebuliser gas flow rates a marginal increase in the selenium ion intensity was achieved by increasing the Rf power. Therefore, a forward power of 1500 W and nebuliser gas flow rate of 0.7 l min^{-1} were selected to provide the optimum selenium sensitivity.
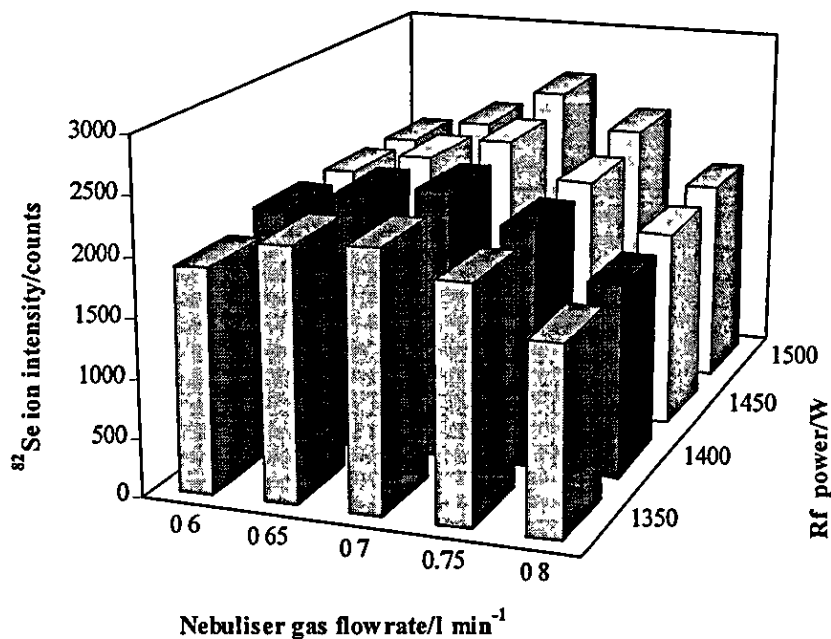
Figure 8.1. ^{82}Se ion intensity as a function of Rf forward power and

nebuliser gas flow rate.

8.2.2 CE-ICP-MS Separation of Selenium Species

A CE-ICP-MS method was developed for the separation of two organic

[selenomethionine (SeMet), selenocystine (SeCys)] and two inorganic (sodium

selenate, sodium selenite) selenium species. As a result of the high upper pKa

values of SeMet, SeCys and selenite, and the strongly acidic nature of selenate

(Table 8.2), electrophoretic conditions were selected to ensure the selenium

species were in their anionic forms and a strong EOF was generated. A strong

EOF was necessary in order to overcome the natural electrophoretic mobility of

the anions towards the anode and to transport the anions towards the nebuliser

(cathode). To maximise the EOF a high voltage, high pH and low ionic

strength buffer were employed.

Compound	Structure	pKa
Sodium selenite (Se^{IV})	ONa | Se——ONa || O	2 60, 8.30
Sodium selenate (Se^{VI})	ONa | O=Se——ONa || O	<1, 2.00
Selenocystine (SeCys)	(Se——CH$_2$——CH——CO$_2$H)$_2$ | NH$_2$	2.10, 8.91
Selenomethionine (SeMet)	CH$_3$—Se—CH$_2$—CH$_2$—CH—CO$_2$H | NH$_2$	2.28, 9.21

Table 8.2. Structure and pKa values for selenious compounds of interest.

Separation of the four selenium species (each at 50 μg ml^{-1} Se) was carried out

using a 10 mM Na_2CO_3 buffer (pH 11) and an applied voltage of +30 kV (Fig.

8.2). Mobility orders were determined by injections of the individual selenium

species with the EOF marker (Table 8.3). The electrophoretic and

electroosmotic mobilities were calculated using the following equations:

$$\mu_{net} = \mu + \mu_{eo} \qquad \text{(Eqn. 8.1)}$$

$$\mu_{eo} = \frac{l\,L}{V\,t} \qquad \text{(Eqn. 8.2)}$$

$$\mu_{net} = \frac{l\,L}{V\,t} \qquad \text{(Eqn. 8.3)}$$

where, μ_{net} is the net mobility of the species, μ is the actual mobility of the

species, μ_{eo} is the mobility of the EOF marker, l is the effective capillary length,

L is the total capillary length, V is the applied voltage and t is the migration

time.

	EOF t_m/s	μ_{eo}/x 10^{-4} cm^{2}V^{-1}s^{-1}	t_m/s	μ/x 10^{-4} cm^{2}V^{-1}s^{-1}	R_t
Peak 1	171	9.55	227	-2.35	1.32
Peak 2	171	9.55	279	-3.70	1.63
Peak 3	171	9.55	413	-5 60	2.42
Peak 4	171	9.55	543	-6.55	3.18
SeMet	172	9.50	227	-2.30	1.32
SeCys	172	9.50	278	-3.62	1.62
Selenite	170	9.61	407	-5 60	2.39
Selenate	173	9.44	555	-6.50	3.21

Table 8.3. Migration times, mobilities, and relative migration times of the

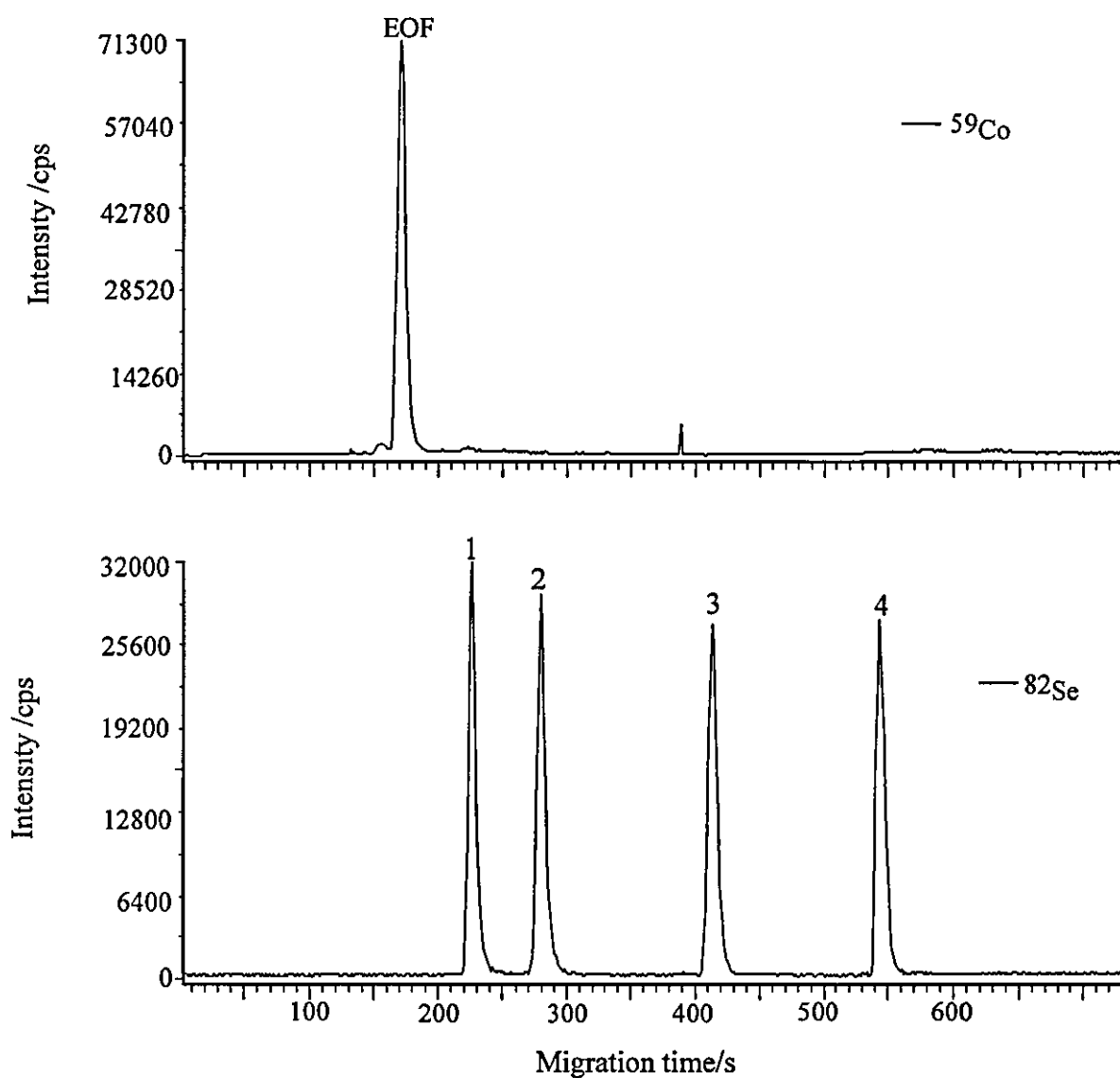*EOF marker and selenium species in the mixed and individual standards.*

Figure 8.2. CE-ICP-MS electropherograms for the separation of SeMet,

SeCys, selenite and selenate (each at approx. 50 μg ml^{-1} Se). Conditions: 30

kV; 10 mM Na$_2$CO$_3$ buffer (pH 11); fused-silica capillary, 50 μm id, 375 μm

od, 70 cm length; sample injection, 100 mbar for 6 s (13 nl); EOF marker Co

(gly)$_3$ (approx. 1 μg ml^{-1} Co); 5 mM NH$_4$NO$_3$ make-up solution @ 10 μl min^{-1}.

Resolution of the four selenium species was achieved in the absence of a negative pressure without the need for further optimisation of electrophoretic conditions. An efficiency of 2.0×10^4 theoretical plates (for selenate) was achieved The fact that a negative pressure was not required indicated that the laminar flow induced by the MicroMist nebuliser suction was minimal. In fact, laminar flow (determined by injection of the EOF marker in the absence of an applied voltage) was found to account for approximately 17 % of the solutes linear velocity (Fig. 8.3).

Migration time @ 30 kV = 165 s = 2.75 min

Migration time @ 0 kV = 967 s = 16.12 min

Linear velocity of laminar flow $= \dfrac{70 \text{ cm}}{16.12 \text{ min}} = 4.3 \text{ cm min}^{-1}$

Laminar flow rate $= \pi r^2 l = \pi(25 \times 10^{-6})^2(4.3 \times 10^{-2})$

$$= 8.44 \times 10^{-11} \text{ m}^3$$

$$= 0.08 \text{ } \mu l \text{ min}^{-1}$$

Combined laminar and electroosmotic flow $= \dfrac{70 \text{ cm}}{2\ 75 \text{ min}} = 25.5 \text{ cm min}^{-1}$

Combined laminar and electroosmotic flow rate $= \pi(25 \times 10^{-6})(25.5 \times 10^{-2})$

$$= 0.5 \text{ } \mu l \text{ min}^{-1}$$

Laminar flow accounts for $\left(\dfrac{4.3}{25.5}\right) \times 100 = 16.9 \text{ %}$ of the linear velocity

---

Figure 8.3. Calculation of the contribution of laminar flow to the analyte linear velocity.

8.2.2.1 IONIC STRENGTH MEDIATED STACKING

In order to enhance sensitivity, on-capillary ionic strength mediated stacking was employed. In this method, stacking occurs when the conductivity of the sample is significantly lower (at least 10 fold) than that of the run buffer. According to Ohms Law, upon the application of a voltage a proportionally greater electric field will develop across the sample plug causing ions to migrate faster. When the ions reach the boundary between the sample plug and run buffer the field strength decreases and the ions begin to migrate with a slower mobility. This process continues until all the sample ions have reached the boundary and are concentrated into a narrow band. At this point, the field becomes homogeneous in the band and normal electrophoresis begins.

To measure the sensitivity enhancement achievable using stacking, a standard containing four selenium species was prepared in 10 mM Na_2CO_3 and a second equivalent standard was prepared in water. The two standards were analysed in triplicate by CE-ICP-MS and the corresponding ^{82}Se peak areas were integrated. A sensitivity enhancement of a factor of three was obtained by preparing the standard in water.

8.2.2.2 PRECISION

Migration time, relative migration time and peak area repeatability was measured for 10 consecutive injections of the mixed selenium standard (50 µg ml^{-1} Se for each species). RSD's were less than 6 3 % and 1 6 % for the peak area and migration time, respectively (Table 8.4).

	Co(gly)$_3$	SeMet	SeCys	Selenite	Selenate
Migration time	1.2	1.2	1.2	1.6	1.1
Relative migration time	-	0 5	0.5	1.0	1.0
Peak area	6.0	6.3	5.9	6.0	5.9

Table 8.4. Migration time, relative migration time and peak area RSD's (%).

Selenium peak areas were measured for the isotope ^{82}Se.

8.2.3 Sensitivity Enhancement Using Ethanol

The accurate and sensitive determination of selenium by ICP-MS is problematic owing to the formation of polyatomic ions in the plasma (Table 8 5) and to the high first ionisation energy of selenium (9.75 eV) which, in an argon plasma, yields only a 33 % ionisation.[18] A number of approaches have been developed to reduce the presence of spectroscopic interferences and to enhance the selenium sensitivity in ICP-MS. Such approaches include, modification of the sample introduction mode,[11,19,20] the addition of molecular gases such as nitrogen[21,22] and methane,[23] and the addition of organic solvents such as ethanol,[24] methanol,[11,12,25] propan-2-ol[26] and butanol-1-ol.[27,28]

Isotope	Abundance/%	Spectroscopic interferent
^{74}Se	0.9	^{38}Ar^{36}Ar, ^{74}Ge
^{76}Se	9.4	^{40}Ar^{36}Ar, ^{38}Ar$_2$, ^{76}Ge
^{77}Se	7.6	^{40}Ar^{37}Cl
^{78}Se	23.8	^{40}Ar^{38}Ar, ^{78}Kr
^{80}Se	49.6	^{40}Ar$_2$
^{82}Se	8.7	^{40}Ar$_2$H$_2$, ^{82}Kr, ^{40}Ar^{42}Ca, ^{81}BrH

Table 8.5. ICP-MS spectroscopic interferences on selenium.

To investigate how the addition of ethanol affected the selenium sensitivity in the CE-ICP-MS system, separation of the selenium standards was undertaken using 5 mM NH_4NO_3 make-up solution which was prepared in a) water, b) 1% v/v ethanol, c) 5 % v/v ethanol and d) 10 % v/v ethanol. Separations using the four make-up solutions were carried out in triplicate and the corresponding peak areas integrated. A graph representing [82]Se and [59]Co peak areas as a function of ethanol concentration can be seen in Fig. 8.4.
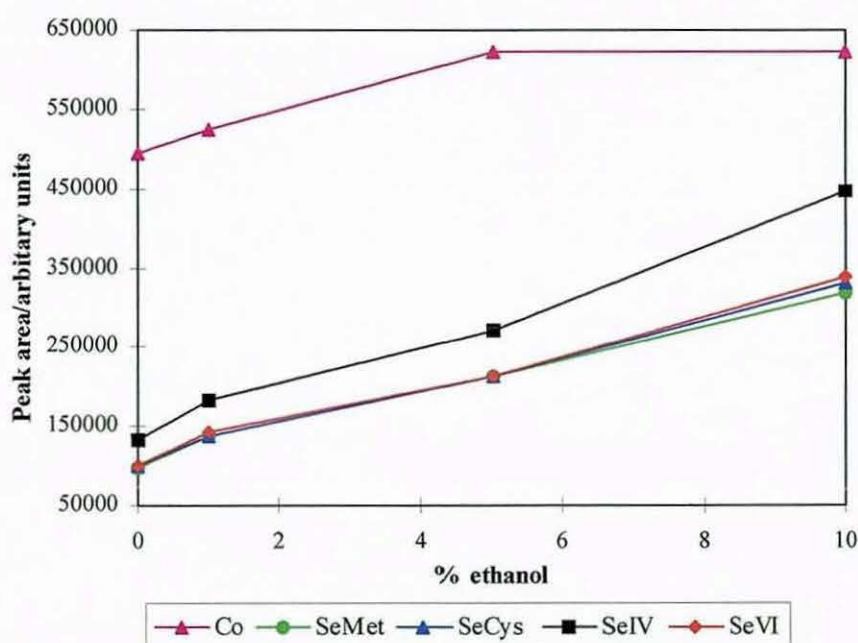
Figure 8.4. Sensitivity enhancement in the presence of increasing concentrations of ethanol.

Increasing the ethanol concentration in the make-up flow had the effect of enhancing both the selenium and cobalt signals. With the addition of 10 % ethanol, an enhancement factor of 3.3 and 1.3 for selenium and cobalt, respectively was observed. The fact that the enhancement factor for the two

elements was significantly different indicated that a number of processes may be contributing to the increase in sensitivity. The first process may be directly related to the formation of droplets and desolvation in the plasma. The presence of ethanol will change the physicochemical properties of the solution, reducing the viscosity and surface tension thus leading to an overall smaller droplet size distribution. Finer droplets will yield an increase in the sample transport efficiency and lower the desolvation effects required in the plasma.

A second factor may relate more specifically to the ionisation mechanisms occurring in the plasma. The introduction of carbon containing solvents into the plasma will result in an increase in the population of C^+ and/or carbon containing polyatomic ions. Since carbon has a higher ionisation potential (11.26 eV) than Se, the degree of ionisation of poorly ionised analytes will be improved as a result of electron transfer to carbon and carbon containing polyatomic ions. The ionisation enhancement factor will be less significant for those analytes with lower ionisation energies.[11,25]

A third factor may be associated with a change in the geometry of the plasma which may ultimately lead to an optimisation of the ion extraction efficiency. Vanhaecke *et al.*[29] reported that when a solvent is introduced into a plasma, the plasma contracts causing a spatial shift of the zone of maximum M^+ density and modification of the sampling depth.

8.2.4 Detection Limits

Calibration standards containing SeMet, SeCys, selenite and selenate at selenium concentrations of 50, 25, 12.5, 6.25 and 3.125 μg ml^{-1} were prepared in water and analysed in triplicate. Calibration graphs were obtained from ^{82}Se peak areas and were linear in the concentration range studied. Calibration graphs are presented in Appendix I. Detection limits were calculated from three times the blank signal and are presented in Table 8.6.

	SeMet	SeCys	Selenite	Selenate
LOD/ng ml^{-1}	355	349	284	293
Absolute LOD/pg	4.6	4 5	3.7	3.8

Table 8.6. CE-ICP-MS detection limits for SeMet, SeCys, selenite and selenate.

8.2.5 Sample Preparation

In order to obtain accurate speciation information, it is essential that the endogenous selenium species present in the yeast are extracted without modification of their chemical form. Previous studies of selenium speciation in yeast have utilised acid hydrolysis,[10] hot water[10,12,13,30,31] and proteolytic enzyme[10,12,13,30,31] extraction methods, with the enzyme method providing the greatest extraction efficiency. In this work, samples were extracted using a non-specific enzyme, protease XIV, which is capable of breaking down the peptide bonds of any protein and reverting it to the amino acid components.

Samples were ground using a pestle and mortar, 0.25 g was weighed into a 15

ml centrifuge tube and protease was added followed by 2.5 ml of 18 MΩ water.

To evaluate how the mass of enzyme and temperature affected the extraction

efficiency, extractions were undertaken using three different masses of protease

(12.5 mg, 25 mg and 50 mg) and two extraction temperatures (room

temperature and 37 °C). Samples were shaken in the dark at room temperature

(using a Gallenkamp wrist action shaker) for 24 hrs. Those samples being

extracted at 37 °C were placed in a shaking water bath (Grant OLS 200) at 110

strokes min^{-1} for 24 hrs. The solutions were centrifuged for 30 mins using an

IEC Centra centrifuge running at 8000 rev min^{-1}. Supernatants were then

removed and filtered through a 0.45 μm Millex-HV filter. Because of the

limited availability of sample D only one extraction (25 mg protease, room

temperature) was undertaken.

8.2.6 Total Selenium Determination and Extraction Efficiency

Total selenium concentrations in the unextracted and extracted samples was

determined by ICP-MS following closed vessel acid digestion. For the

unextracted samples, 0.1 g was weighed into a 50 ml high pressure Quartz

vessel and 5 ml of concentrated HNO_3 was added. The sample was then

subjected to 45 min digestion program of elevated temperature and pressure.

Following digestion, the samples were quantitatively transferred into test tubes

and the volume was made up to 10 ml using 18 MΩ water. An aliquot (1 ml)

of the digest was then added to 4 ml of a 1 % HNO_3 diluent containing 12.5 ng

ml^{-1} Rh internal standard before analysis by direct measurement ICP-MS. In

the case of sample A, a greater dilution was necessary because of its high selenium concentration thus, 0.25 ml of digest was added to 4 ml diluent and 0.75 ml concentrated HNO_3. Four concentrated HNO_3 blanks and one blank spiked with 25 µg selenium (to give a final spike concentration of 500 ng ml^{-1}) were digested in the same manner as the samples. For quality control purposes a certified reference material (CRM), DOLT-2 (Se concentration $6.06 \pm 0\,49$ µg ml^{-1}) was analysed in triplicate. DOLT-2 is a fish-based CRM and was selected because of its high selenium concentration. It is good practice to select a CRM with a similar matrix to the samples being analysed, however, a yeast based CRM was not available.

For the extracted samples both the supernatant and remaining solid pellet were analysed for total selenium concentration. An aliquot (1.0 ml for samples B,C and D, 0 25 ml for sample A) of the supernatant was digested in the manner described previously. For the pellets, 1.0 g was digested. All samples were digested and analysed in duplicate.

Stock calibration standards at selenium concentrations of 10 µg ml^{-1}, 3 µg ml^{-1}, 1 µg ml^{-1}, 300 ng ml^{-1}, 100 ng ml^{-1}, 30 ng ml^{-1} and 10 ng ml^{-1} were prepared in 50 % HNO_3. Working calibration standards were prepared by five fold dilution of the stock standards in the measurement diluent to give final selenium concentrations of 2000, 600, 200, 60, 20, 6 and 2 ng ml^{-1}. Selenium was quantified using ^{82}Se.

The total selenium concentration in the four samples, the selenium

concentration in the supernatants and the selenium concentration in the pellets

are presented in Tables 8.7, 8.8 and 8.9, respectively. All results were blank

and recovery corrected. For the reference material, a selenium concentration of

7.07 ± 0.08 µg g^{-1} was obtained and was within the accepted ± 20 % NAMAS

criteria.

Sample	Se concentration/µg g^{-1}
A	2092.7
B	401.3
C	444.8
D	160.6

Table 8.7. Total selenium concentrations in samples A, B, C and D.

Extraction conditions	A	B	C	D
12.5 mg protease, RT	170.5	35.8	43.0	-
12.5 mg protease, 37 °C	162.0	35.3	42.6	-
25 mg protease, RT	180.6	31.6	43.0	10.3
25 mg protease, 37 °C	165.1	29.7	46.2	-
50 mg protease, RT	170.0	37.0	40.3	-
50 mg protease, 37 °C	168.9	33.5	43.4	-

Table 8.8. Selenium concentration(µg ml^{-1}) in the supernatants.

Extraction conditions	A	B	C	D
12.5 mg protease, RT	257.7	49.4	30.5	-
12.5 mg protease, 37 °C	340.9	45.5	29.1	-
25 mg protease, RT	277.7	39.3	31.3	36.2
25 mg protease, 37 °C	391.8	41.7	31.4	-
50 mg protease, RT	303.2	44.0	26.1	-
50 mg protease, 37 °C	449.1	48.3	23.1	-

Table 8.9. Selenium concentration ($\mu g\ g^{-1}$) in the pellets.

Extraction efficiencies were found to be > 74 % (Table 8.10), with yields for sample A in the range of 77 % - 86 %, sample B in the range of 74 % - 92 % and sample C in the range of 91 % - 104 %. For sample D, a lower extraction efficiency of 64 % was obtained. The mass of protease used in the extraction had no apparent effect upon the yield of selenium extracted. At the elevated temperature of 37 °C, a marginally lower extraction yield was observed for samples A and B. However, for sample C this was not observed.

Extraction conditions	A	B	C	D
12.5 mg protease, RT	81.5	89.0	96.7	-
12.5 mg protease, 37 °C	77.4	88.0	95.8	-
25 mg protease, RT	86.3	78.7	96.7	64.1
25 mg protease, 37 °C	78.9	74.0	103.9	-
50 mg protease, RT	81.2	92.2	90.6	-
50 mg protease, 37 °C	80.7	83.5	97.6	-

Table 8.10. Extraction efficiencies (%).

8.2.7 Speciation Analysis

Supernatants were analysed directly without dilution using the CE-ICP-MS

method detailed in Section 8.2.2. Identification of selenium species was carried

out by comparison of the migration and relative migration times with standards,

and by spiking experiments.

SAMPLE A

The ^{82}Se CE-ICP-MS electropherogram for sample A is presented in Fig. 8.5.

One predominant selenium species with a migration time of 261 s ($R_t = 1.33$)

was present in the sample, in addition to three smaller unresolved peaks. The

chemical form of the major selenium species in the yeast was identified as

selenomethionine. A semi-quantitative measure of the selenomethionine

concentration in the sample was determined by CE-ICP-MS using standard

addition. The sample was spiked with selenomethionine (at 50 µg ml^{-1} Se) and

the spiked and unspiked samples were analysed in triplicate. The concentration

of selenomethionine was found to be 155 µg ml^{-1}.

SAMPLE B

For sample B, one selenium peak with a migration time of 614 s ($R_t = 3.04$)

was present in the electropherogram (Fig. 8.6). The relative migration time of

the peak was lower than that obtained for a selenate standard ($R_t = 3.18$),

however spiking experiments indicated that the chemical form of the selenium

present in sample B was likely to be selenate. A semi-quantitative measure of
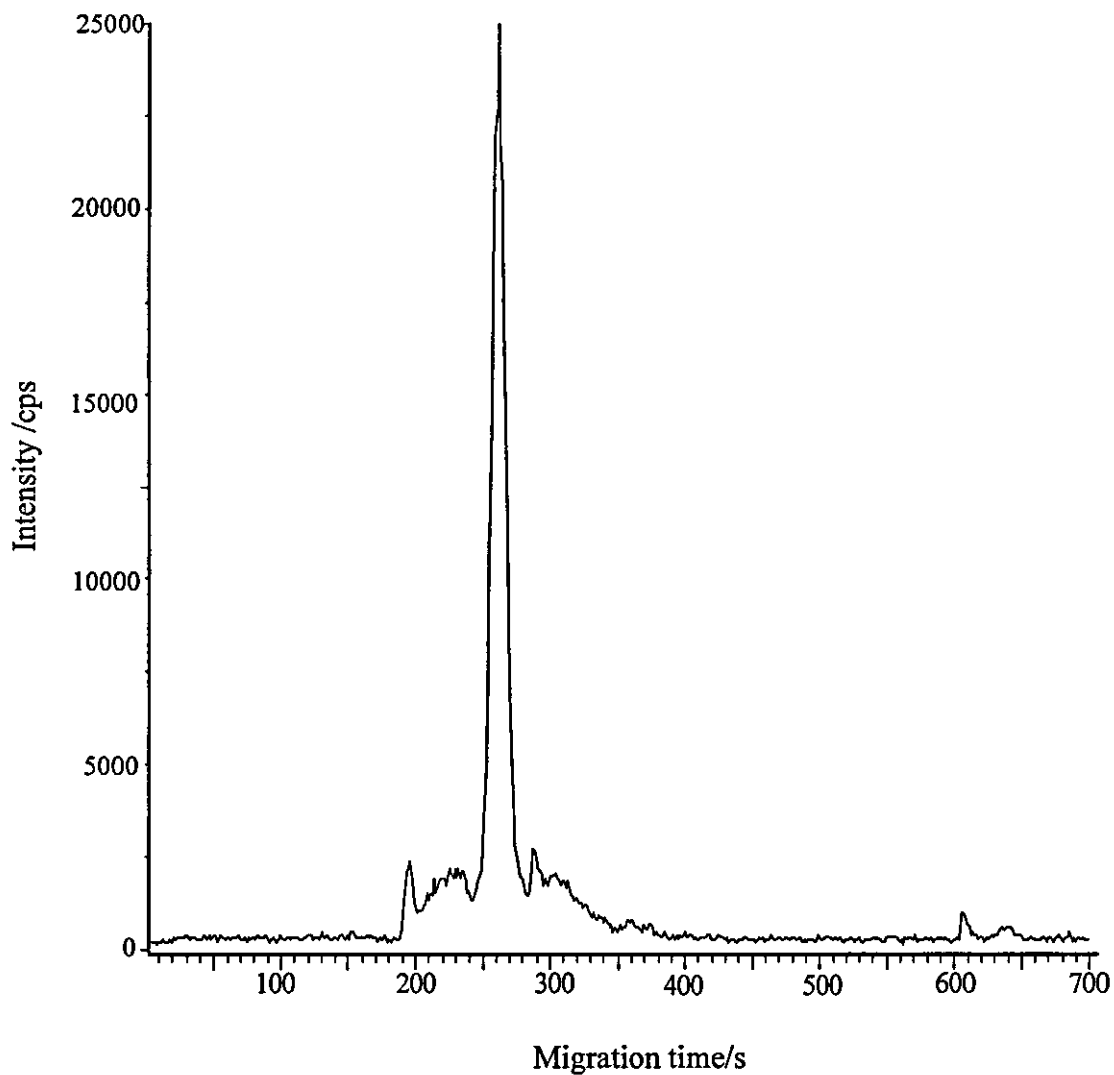
Figure 8.5. ^{82}*Se CE-ICP-MS electropherogram of sample A, EOF = 196 s.*

Conditions as Fig. 8.2 except 5 mM NH$_4$NO$_3$ prepared in 10 % ethanol used
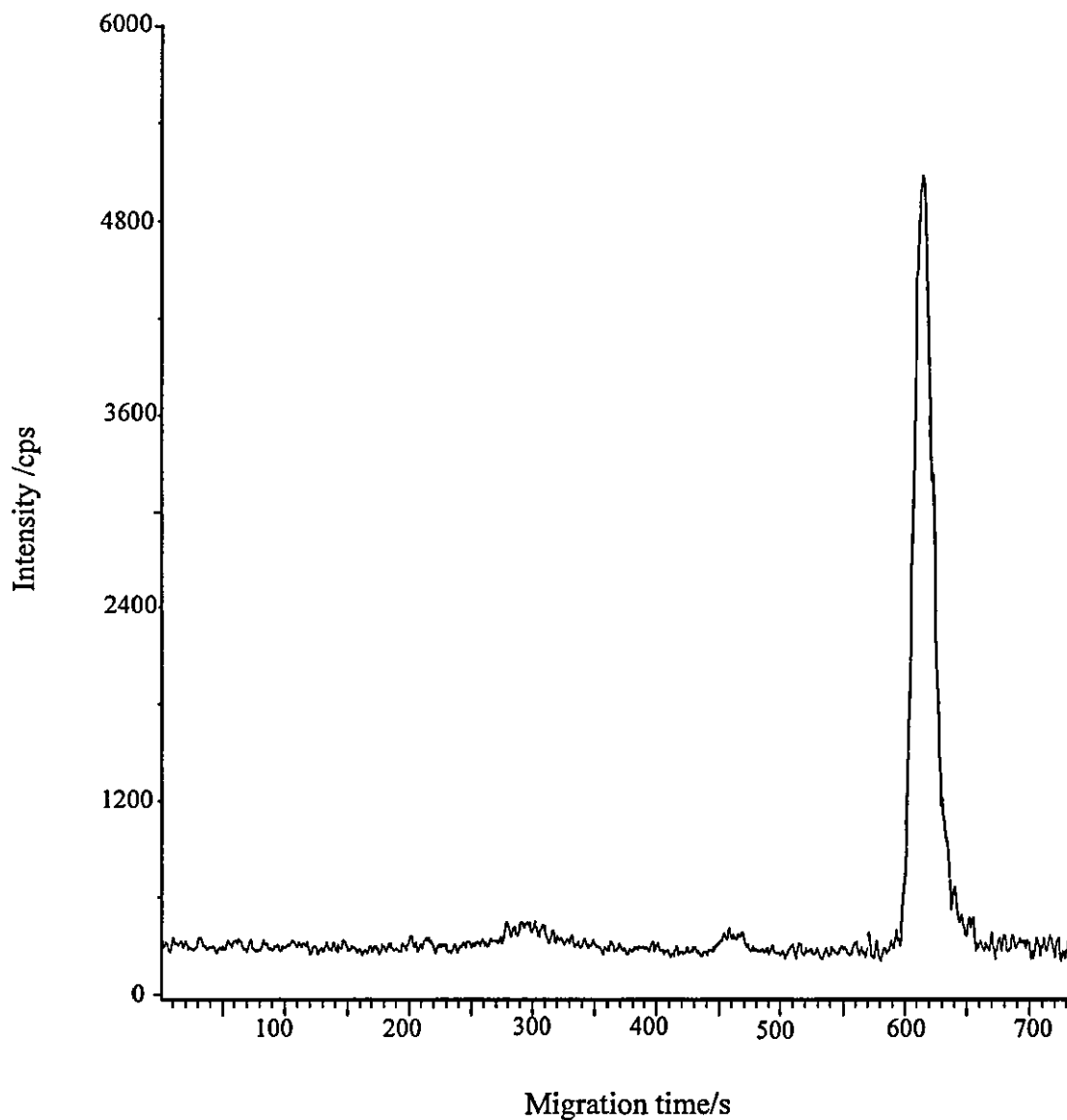
at the make-up flow.

Figure 8.6. ^{82}Se CE-ICP-MS electropherogram of sample B, EOF = 201 s.

Conditions as Fig. 8.5.

the selenium concentration in the sample was determined using standard addition. The sample was spiked with selenate (50 μg ml^{-1} as Se) and the spiked and unspiked samples were analysed in triplicate. The concentration of selenate was calculated to be 28.8 μg ml^{-1}. This was approximately 20 % lower than the total selenium concentration determined by ICP-MS.

SAMPLE C

One selenium peak with a migration time of 618 s (R_t = 2.99) was present in the electropherogram for sample C (Fig. 8.7). As was observed with sample B, the relative migration time of the peak was lower than that observed for a selenate standard. However, spiking experiments indicated that the chemical form of selenium in the sample was selenate. This was inconsistent with the suppliers specification which stated that the sample was selenomethionine. By means of standard addition, the selenium concentration in the sample was determined to be 44.9 μg ml^{-1}. This was equivalent to a recovery of 104.4 %.

SAMPLE D

For sample D, the electropherogram was less easy to interpret and contained either one broad tailing peak or possibly a number of unresolved peaks (Fig. 8.8). The migration time of the major peak was 210 s and was equivalent to the EOF marker, thus indicating the presence of a neutral species. However, spiking of the sample with selenomethionine (50 μg ml^{-1} Se) highlighted an abnormality where by the selenomethionine spike also migrated with a mobility
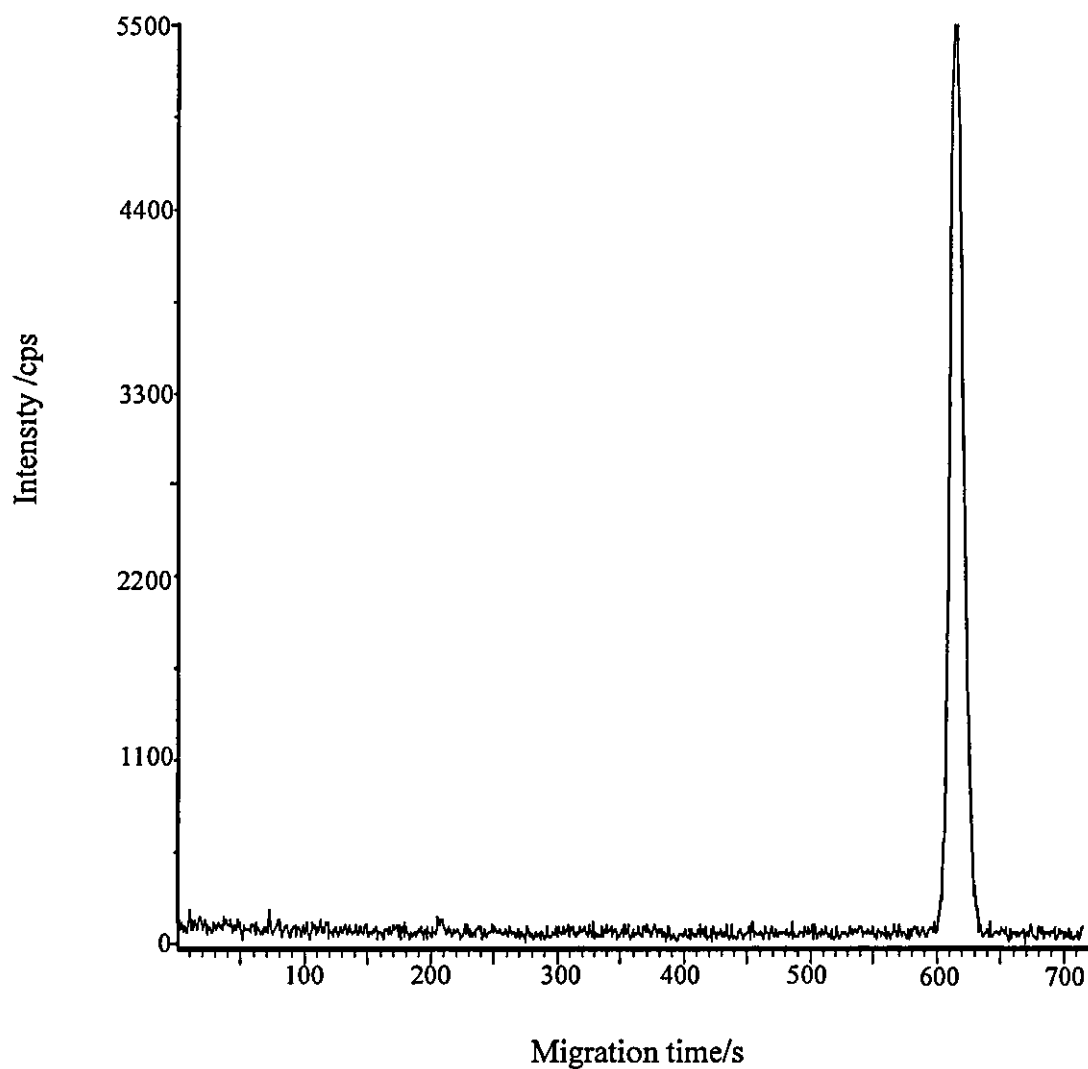
143

Figure 8.7. ^{82}Se CE-ICP-MS electropherogram of sample C, EOF = 207 s.

Conditions as Fig. 8.5.

equal to the EOF (Fig. 8.9). At pH 11 selenomethionine was anionic, therefore electrophoretic separation was not occurring and the injected analytes were co-migrating with the EOF. Following analysis of the spiked sample D, a standard containing four selenium species was analysed. Relative migration times were normal, thus indicating that the system was operating correctly and that the observed co-migration was specific to sample D.

The fact that SeMet migrated with a mobility equal to the EOF was apparently due to the sample matrix and may indicate the presence of a colloid. It may be the case that during the extraction procedure the sample formed a colloid which, due to its overall neutral charge status, would migrate with the EOF. When SeMet was added to the sample it may interact with the colloid and therefore co-migrate. In an attempt to identify the possible presence of a colloid two approaches were taken. Firstly, the sample was ultrasonicated in a sonic bath and secondly the sample was rinsed repeatedly in water, freeze dried and then extracted. During the manufacture of the sample it was washed several times in saline solution thus leaving the sample with a relatively high salt concentration. A high salt concentration may promote the formation of a colloid or adduct so the sample was washed in an attempt to remove the salt.

Both ultrasonicating and washing the sample had no effect upon the co-migration with the EOF. The washed and unwashed extracts were also diluted in 0.5 %, 1.0 % and 5 % (v/v) ethanol in an attempt to disrupt any colloidal
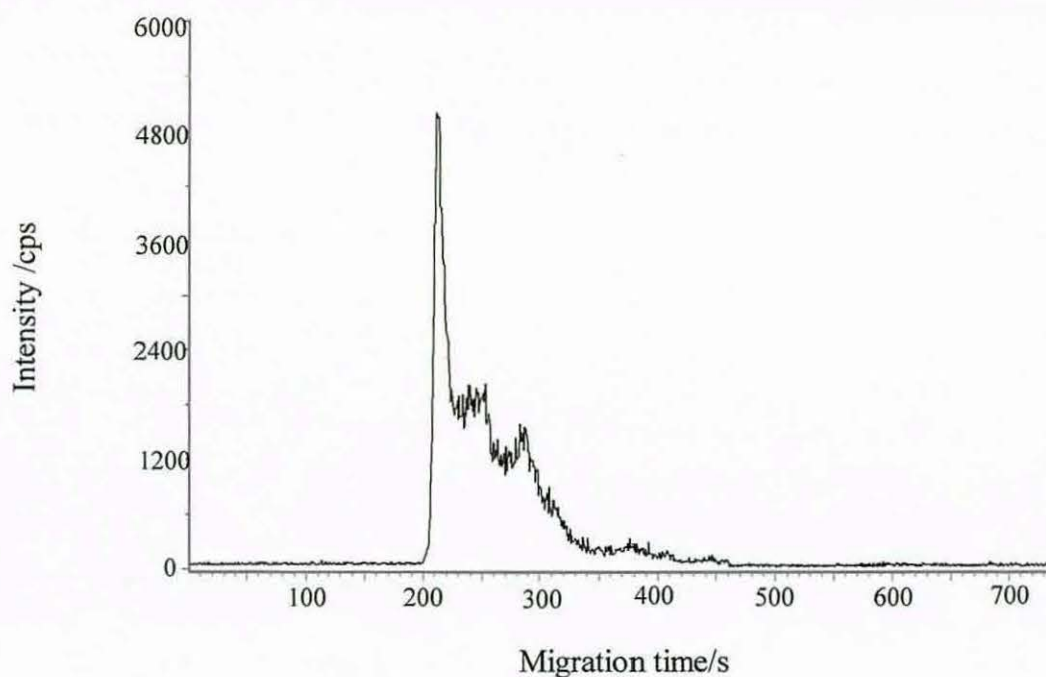
Figure 8.8. ***^{77}Se CE-ICP-MS electropherogram of sample D, EOF = 210 s.***

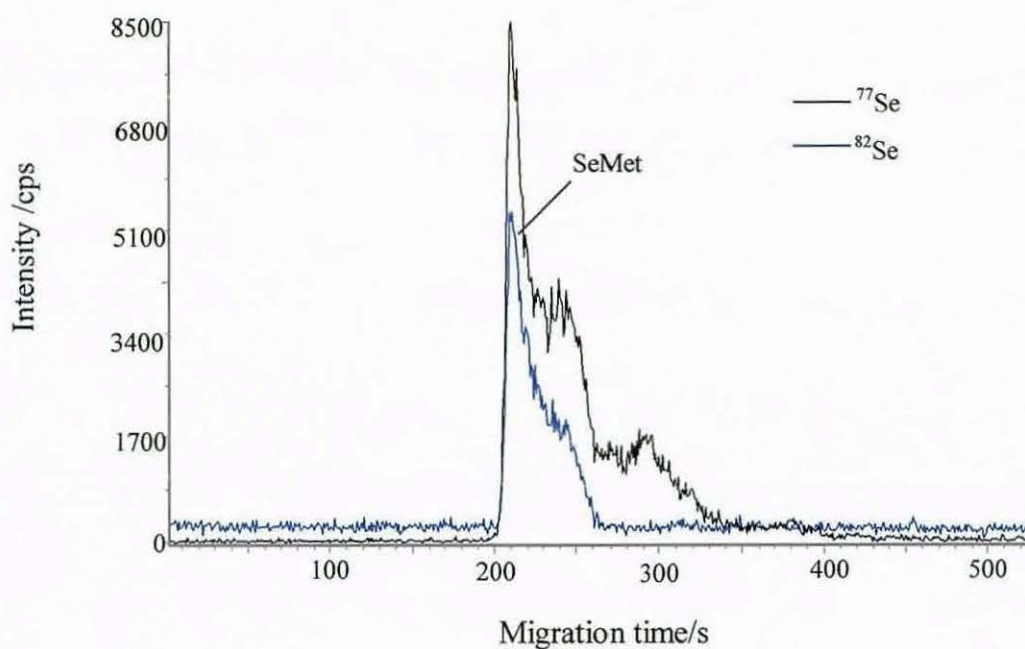***Conditions as Fig. 8.5.***

Figure 8.9. ***CE-ICP-MS electropherogram of sample D spiked with SeMet***

(50 µg ml^{-1} Se), EOF = 210 s. Conditions as Fig. 8.5.

species present. However, no difference was observed in the electropherograms of the alcoholic extracts. The sample was also spiked individually with SeCys, selenite and selenate (each at 50 µg ml^{-1} Se). In contrast to the SeMet spike, the SeCys, selenite and selenate spikes did not migrate with the EOF, however their relative migration times were different to the relative migration times of standards (Table 8.11). For the two organic species, their migration time was reduced in the presence of sample D, whilst for the inorganic species an increase in migration time was observed.

SAMPLE	EOF/s	SeMet R_t	SeCys R_t	Selenite R_t	Selenate R_t
Standard	171	1.32	1.63	2.42	3.18
D + SeMet	210	1.00	-	-	-
D + SeCys	208	-	1.38	-	-
D + Selenite	209	-	-	2.73	-
D + Selenate	207	-	-	-	3.37

Table 8.11. A comparison of the relative migration times of standards added to sample D and relative migration times of standards in aqueous solutions.

8.3 SUMMARY

The CE-ICP-MS method developed provided an efficient, reproducible separation of selenomethionine, selenocystine, selenite and selenate. As a result of the generally poor sensitivity of ICP-MS for selenium, sensitivity enhancement was achieved by the addition of 10 % (v/v) ethanol to the make-up solution and by on-capillary sample stacking. The samples were extracted using a proteolytic enzyme extraction method that provided high extraction

yields of > 74 %. The chemical form of selenium present in the samples was identified by comparison of migration times with standards and by spiking experiments. In sample A, the major selenium containing species was selenomethionine, sample B was inorganic selenate and sample C was also inorganic selenate. For sample C, the speciation was inconsistent with the suppliers specification which stated that the sample was selenomethionine. The speciation of sample D was not undertaken because of difficulties with a matrix effect that caused a shift in the migration time of spiked standards. It was apparent that the standards were interacting to varying degrees with the sample matrix and their mobilities were thus being affected.

REFERENCES

[1]L. H. Foster and S. Sumar, *Crit. Rev Food Sci Nutr.*, 1997, **37**, 211.

[2]L. C. Clark, G. F. Combs, B. W. Turnbull, E. H. Slate, D. K. Chalker, J. Chow, L. S. Davis, R. A. Glover, G. F. Graham, E. G. Gross, A. Krongrad, J. L. Lesher, H. K. Park, B. B. Sanders, C. L. Smith, J. R. Taylor, *J. Am. Med. Assoc*, 1996, **276**, 1957.

[3]T. C. Stadtman, *J. Biol. Chem.*, 1991, **266**, 257.

[4]C. Ip, C. Hayes, R. M. Bidnick and H. E. Ganther, *Cancer Res*, 1991, **51**, 595.

[5]S. J. Fairweather-Tait, *Eur. J. Clin. Nutr.*, 1997, **51**, S20.

[6]W. C. Willet and M J. Stampfer, *J. Am. Coll Toxicol.*, 1986, **5**, 29.

[7]C. A. Swanson, B. H. Patterson, O. A. Levander, C. Veillon, P. R. Taylor, K. Helzlsouer, P. A. McAdam and L A. Zech, *Am J. Clin Nutr.*, 1991, **54**, 917.

[8]P. B. Moser-Veillon, A. R. Mangels, K. Y. Patterson and C. Veillon, *Analyst,* 1992, **117**, 559.

[9]C. D. Thomson and M. F. Robinson, *Am. J. Clin. Nutr.*, 1986, **44**, 659.

[10]A. Gilon, M. Astruc and M. Potin-Gautier, *Appl Organomet. Chem*, 1995, **9**, 623.

[11]R. M. Olivas, C. R. Quetel and O. F. X. Donard, *J. Anal At. Spectrom.*, 1995, **10**, *865.*

[12]S. M. Bird, P. C. Uden, J. F. Tyson, E. Block and E. Denoyer, *J Anal. At Spectrom*, 1997, **12**, 785.

[13]S. M. Bird, H. Ge, P. C. Uden, J. F. Tyson, E. Block and E. Denoyer, *J. Chromatogr A,* 1997, **789**, 349.

[14]M. Albert, C. Demesmay and J. L. Rocca, *Fresenius' J Anal Chem,* 1995, **351,** 426.

[15]B. Michalke and P. Schramel, *Electrophoresis,* 1998, **19**, 270.

[16]B. Michalke and P. Schramel, *J. Chromatogr. A,* 1998, **807**, 71.

[17]B. Michalke, P. Schramel and A. Kettrup, *Fresenius' J. Anal. Chem.,* 1999, **363**, 456.

[18]K. E. Jarvis, A. L. Gray and R. S. Houk, *Handbook of Inductively Coupled Plasma Mass Spectrometry,* Blackie and Sons, Glasgow, 1992.

[19]J. Bowman, B. Fairman and T. Catterick, *J. Anal. At. Spectrom.,* 1997, **12**, 313.

[20]M. A. Quijano, A. M. Gutierrez, M. Perez Conde and C. Camara, *J. Anal At. Spectrom,* 1995, **10**, 871.

[21]T. van der Velde-Koerts and J. L. M de Boer, *J. Anal At Spectrom,* 1994, **9**, 1093.

[22]J. Turner, S. J. Hill, E. H. Evans and B. Fairman, *J. Anal At. Spectrom,* 1999, **14**, 121.

[23]S. J. Hill, M. J. Ford and L. Ebdon, *J. Anal. At. Spectrom.,* 1992, **7**, 1157.

[24]J. Goossens, F. Vanhacke, L. Moens and R. Dams, *Anal Chim. Acta,* 1993, **280**, 137.

[25]E. H. Larsen and S. Sturup, *J. Anal. At. Spectrom.,* 1994, **9**, 1099.

[26]E. H. Evans and L. Ebdon, *J. Anal. At. Spectrom,* 1990, **5**, 425.

[27]H. T. Delves and C. Sieniawska, *J Anal. At. Spectrom.,* 1997, **12**, 387.

[28]C. E. Sieniawska, R. Mensikov and H. T. Delves, *J Anal. At. Spectrom*,

1999, **14**, 109.

[29]F. Vanhaecke, R. Dams and C. Vandecasteele, *J. Anal. At. Spectrom*,

1993, **8**, 433.

[30]J. Zheng, W. Goessler and W. Kosmu, *Trace Elem. Electrol*, 1998, **15**, 70.

[31]C. Casiot, J. Szpunar, R. Lobinski and M. Potin-Gautier, *J Anal At*

Spectrom, 1999, **36**, 645.

CHAPTER NINE

The Speciation of Selenium in Yeast By HPLC-ICP-MS

9.0 INTRODUCTION

The direct coupling of high performance liquid chromatography (HPLC) with

ICP-MS is an established approach to elemental speciation. The technique,

with particular reference to ion exchange and ion pair mechanisms, has been

used in a number of studies for the speciation of selenium in selenium enriched

yeast.[1-6] In this Chapter, an anion exchange HPLC-ICP-MS method will be

used for the speciation of selenium in selenium enriched yeasts. The four

samples analysed by CE-ICP-MS in Chapter 8 were analysed by the HPLC

method and the results from the two techniques compared.

9.1 EXPERIMENTAL

9.1.1 Reagents

Selenium standards and samples, as detailed in Chapter 8, were used.

Standards were prepared by dissolution in the mobile phase. The mobile phase

was 5mM salicylate (pH 8.5) prepared in the following manner; 0.3453 g

salicylic acid (Sigma) was dissolved in 5.0 ml methanol and 0.4003 g of

sodium salicylate (Sigma) and 950 ml Milli-Q water were added. The pH was

adjusted to 8.5 by drop-wise addition of 5 % Tris and the volume was then

made up to 1000 ml using Milli-Q water. The mobile phase was vacuum

degassed prior to use.

9.1.2 Instrumentation

ICP-MS. The PQ1 ICP-MS fitted with a cross-flow nebuliser and Scott-type double pass spray chamber was employed. The instrument was operated using the conditions detailed in Chapter 8, with the exception of the nebuliser gas flow rate which was 0.8 l min^{-1}.

HPLC. The HPLC system was a Dionex DX500 (Dionex, Camberley, UK) comprising of a GP40 gradient pump and ASM autosampler. A 120 mm x 4.6 mm id Polysphere IC An-2 anion exchange column (Merck) preceded by a guard column (25 x 4.6 mm) of the same packing was used. The Rheodyne 9010 six-port injection valve (Rheodyne, CA, USA) was fitted with a 50 μl PEEK sample loop. Isocratic separation was achieved using a 5 mM salicylate mobile phase (pH 8.5) delivered at a flow rate of 0.75 ml min^{-1}. The column outlet of the HPLC was connected directly to the nebuliser *via* a Teflon tube (0.5 mm id).

9.2 RESULTS AND DISCUSSION

9.2.1 Separation of Selenium Species

Anion exchange separation of selenomethionine, selenocystine, sodium selenite and sodium selenate was carried out using a method adapted from Crews *et al.*[7] Anion exchange was the selected mode of chromatography because it utilises the pH dependent anionic character of the four species and allows the use of an aqueous mobile phase (organic mobile phases employed in reverse phase HPLC can cause instability in the plasma). The separation mechanism in anion

exchange is governed by the ionisation of species. Separation occurs as a result of the interaction of anions with quaternary ammonium sites bound to the polymeric stationary phase.

The HPLC-ICP-MS chromatogram for the separation of the four selenium species (at selenium concentrations of approximately 18 μg ml^{-1}) can be seen in Fig. 9.1. The retention order of the species was determined by injections of the individual standards and can be explained by considering the pKa's of the species. At pH 8.5, selenate is in the form of SeO$_4^{2-}$ and thus has the strongest ionic interaction with the quaternary ammonium ions and elutes last. Selenite exists as SeO$_3^-$ and therefore elutes later than the two organic species, SeCys and SeMet, which exist in equilibrium between the zwitterionic and anionic forms. SeMet elutes before SeCys because its anionic form possesses one negative charge localised to the carboxylate group [CH$_3$SeCH$_2$CH(NH$_2$)COO$^-$] whilst the anionic form of SeCys has two negative charges [$^-$OOC(NH$_2$)CHCH$_2$SeSeCH$_2$CH(NH$_2$)COO$^-$]. The retention factors (k) of the two organic species indicated weak interactions with the stationary phase (Table 9.1). The void volume of the column was measured by passing a solution of LiCl (10 ng ml^{-1}) through the column at different flow rates. The void volume was found to be 1.50 $\pm$ 0.02 ml (Table 9.2).

Column recoveries were determined by post-column injections of the mixed selenium standard. Recoveries between 78 and 92 % were obtained (Table 9.1).
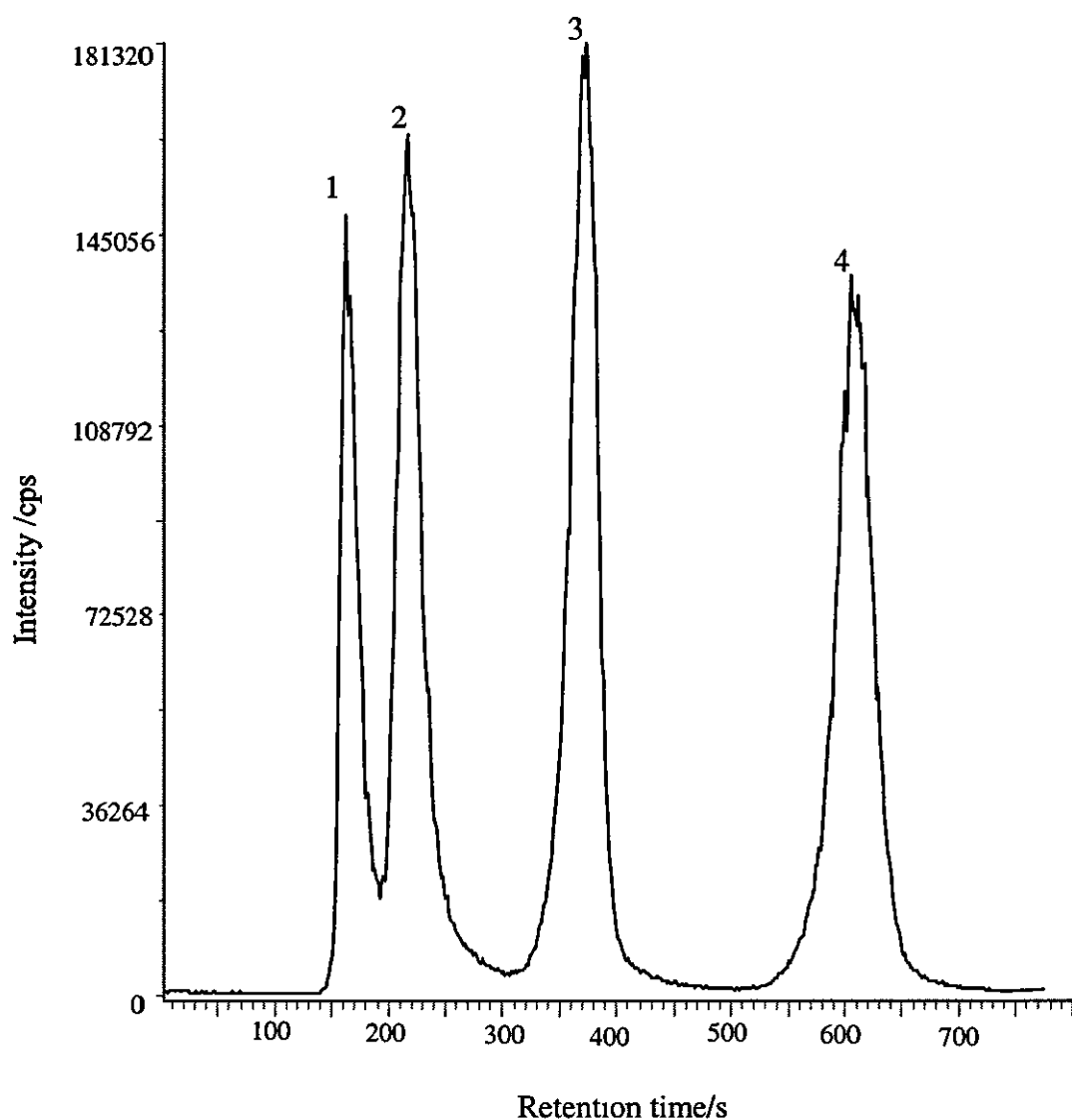
Figure 9.1. ^{82}Se HPLC-ICP-MS chromatogram of selenium standards (each at ~18 µg ml^{-1} Se). 1 - SeMet (t_r = 162 s), 2 - SeCys (t_r = 217 s), 3 - selenite (t_r = 373 s), 4 - selenate (t_r = 606). Chromatographic conditions; 120 mm x 4.6 mm id Polysphere IC An-2 anion exchange column, 5 mM salicylate mobile phase (pH 8.5), 0.75 ml min^{-1} flow rate, 50µl injection.

	SeMet	SeCys	Selenite	Selenate
Retention time/s	162	217	373	606
Retention factor	0.35	0.81	2.11	4.05
Efficiency/theoretical plates	363	417	1140	1486
Column recovery/%	88	78	92	92

Table 9.1.   Retention time, retention factor, efficiency and column recovery

for the four selenium standards.

Flow rate/ml min^{-1}	t_0/s	Void volume/ml
1.0	91	1.52
0.75	120	1.50
0.5	179	1.49

Table 9.2.   Void volume of the column calculated at three different flow rates.

9.2.1.1 PRECISION

The precision of the system was assessed by measurement of the retention time, peak height and peak area repeatability. For 10 consecutive injections of the mixed selenium standard (18 μg ml^{-1} Se for each species) RSD's were less than 8 % (Table 9.3).

	SeMet	SeCys	Selenite	Selenate
Retention time	0.4	0.9	0.4	0.9
Peak height	4.5	6.6	5.3	5.2
Peak area	4.8	8.0	3.4	3.4

Table 9.3. Precision data for the HPLC-ICP-MS system (% RSD).

9.2.2 Speciation Analysis

For the speciation, samples were prepared by enzyme extraction as detailed in
Chapter 8. Since the level of enzyme and the extraction temperature had no
apparent affect upon the extraction efficiency, at least at those conditions
investigated, 12.5 mg protease and room temperature were employed.
Supernatants were analysed following dilution (1 + 1) with the mobile phase.

SAMPLE A

For sample A, two unresolved selenium peaks with retention times of 126 s and
145 s were observed in the chromatogram (Fig. 9.2). The retention times of the
two peaks did not equate with the retention times of any of the four standards
analysed. The sample was spiked with SeCys, SeMet, selenite and selenate
(each at ~ 18 μg ml^{-1} Se) and the chromatogram of the spiked sample can be
seen in Figure 9.3. Whilst selenate was observed in the chromatogram at a
retention time of 600 s, the three other spiked standards were not apparent at
the retention times expected. In addition to the selenate peak, one split peak at
143 s and one broad peak eluting between 200 and 400 s were observed.
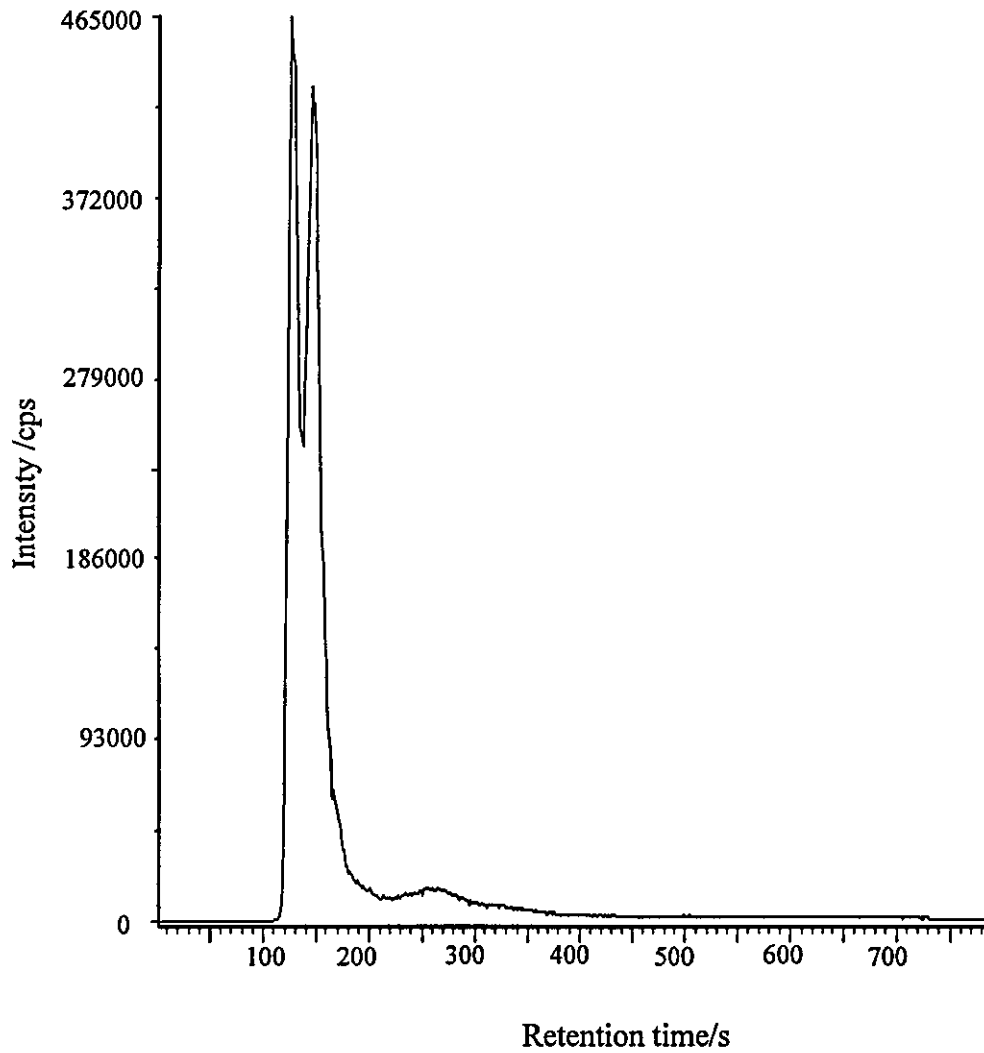
Figure 9.2 ^{82}Se HPLC-ICP-MS chromatogram of sample A.

Chromatographic conditions as Fig. 9.1.
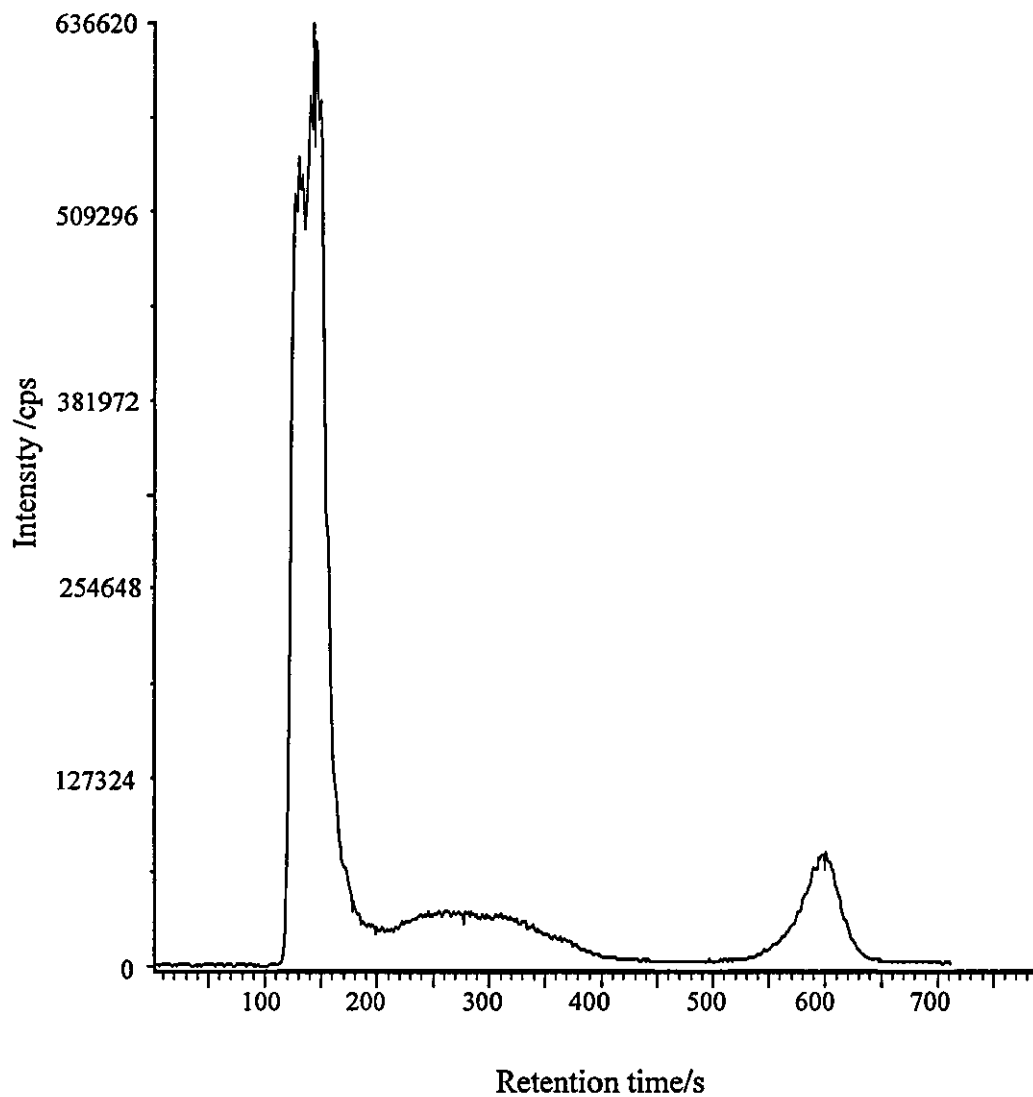
Figure 9.3. ^{82}Se HPLC-ICP-MS chromatogram of sample A spiked with

SeMet, SeCys, selenite and selenate (each at ~18 µg ml^{-1} Se).

Chromatographic conditions as Fig. 9.1.

To identify if the sample matrix was affecting the elution of the spiked

standards, sample A was diluted (1 + 3) in mobile phase and then spiked with

the four standards. In the resulting chromatogram (Fig. 9.4 chromatogram A)

the selenate peak (t_r = 598 s) was observed in addition to two new peaks at

retention times of 154 s and 350 s. Further dilutions of the sample were carried

out and the diluted samples were spiked with the four standards. The effect of

diluting the sample matrix can be seen in the chromatograms in Fig. 9.4. At the

dilution (1 + 3), peaks at retention times of 154 s and 350 s, plus the selenate

peak were observed. As the dilution factor of the sample matrix was increased,

a new peak at 212 s (presumably SeCys) became more apparent, the intensity

of the selenate peak and the peak at 350 s (presumably selenite) remained

unchanged, and the peak at 154 s (SeMet) reduced in intensity. At the highest

dilution (1 + 15), the four spiked standards were clearly visible although

resolution of SeMet and SeCys was poor.

A possible explanation for these observations may be that the sample matrix

was preferentially binding to the active sites on the column, thus in the more

concentrated sample the standards had little interaction with the column and

were not resolved. Because selenate had such a high affinity for the quaternary

ammonium ions its elution was not affected by the sample matrix. In anion

exchange a competitive affinity for the active sites occurs and therefore as the

sample matrix was diluted the interaction of the standards with the column

increased. It may be the case that the sample had a high salt concentration

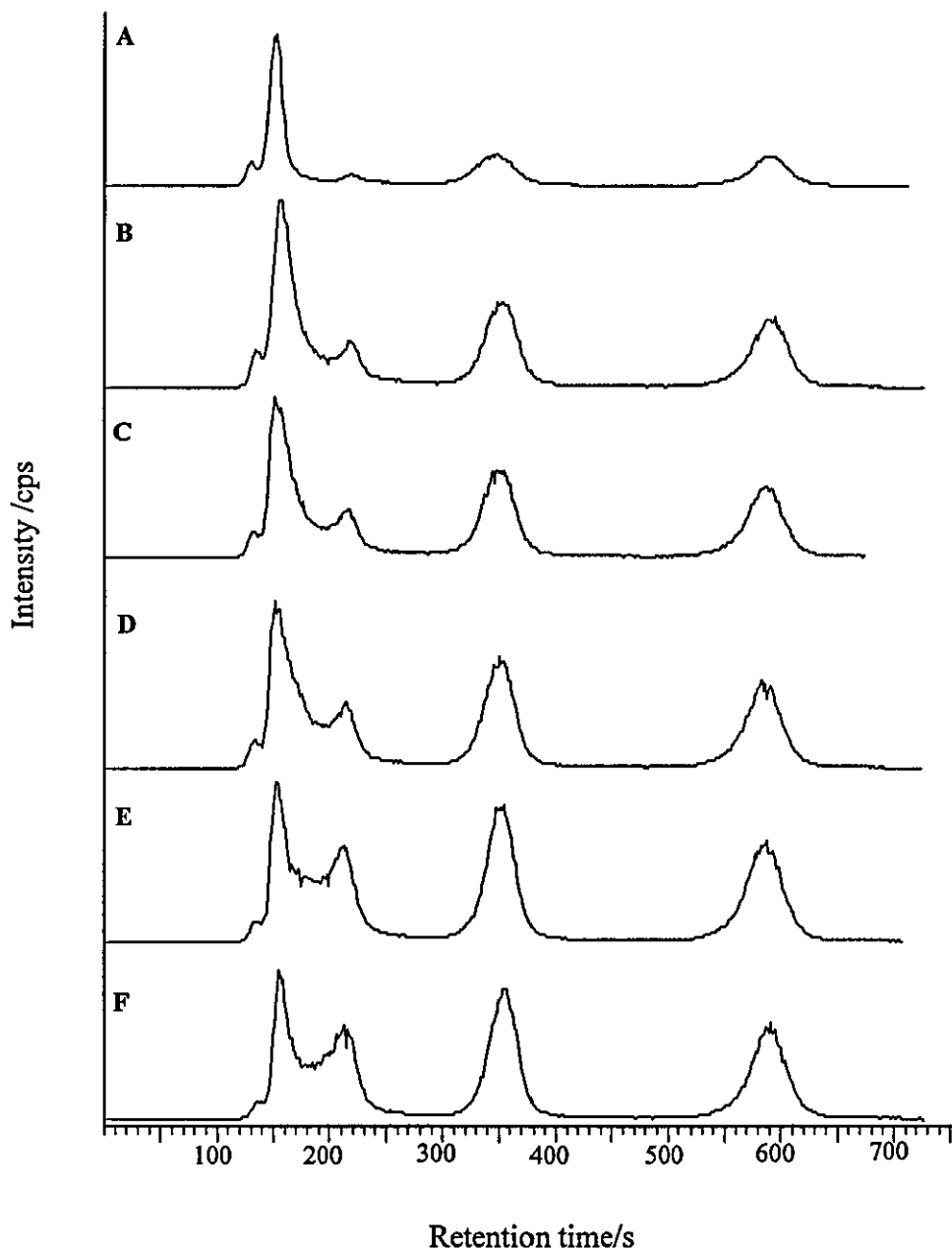which preferentially bound to the active sites.

Figure 9.4. ^{82}Se HPLC-ICP-MS chromatograms of diluted sample A spiked

with SeMet, SeCys, selenite and selenate (each at ~18 μg ml^{-1} Se). A - (1 + 3)

dilution, B - (1 + 5) dilution, C - (1 + 7) dilution, D - (1 + 9) dilution, E - (1 +

13) dilution, F - (1 + 15) dilution. Chromatographic conditions as Fig. 9.1.

In order to identify the selenium species present in sample A, without the
interfering effect of the matrix, the sample was diluted (1 + 15). Two selenium
peaks with retention times of 136 s and 156 s were observed. In comparison
with the undiluted sample, the retention times of the two peaks had shifted
slightly. Comparison with the retention times of the spiked sample would
indicate that the peak at 156 s was SeMet, however the identity of the other
peak was unknown.

SAMPLE B

Sample B was analysed initially in its undiluted form and one selenium peak
with a retention time of 600 s was observed (Fig. 9.5). However, spiking of the
sample with the four standards highlighted the same matrix effect observed for
sample A. Therefore, sample B was diluted (1 + 15) and re-analysed. The
diluted sample was then spiked with the four standards and the major selenium
species in the sample, according to the retention time, was selenate. This was
in agreement with the speciation carried out using CE-ICP-MS.

SAMPLE C

Analysis of sample C showed one selenium peak with a retention time of 609 s
(Fig. 9.6). Spiking of the sample indicated the chemical form of selenium in
the sample to be selenate. Again, this was consistent with the speciation
information obtained using CE-ICP-MS. It is interesting to note that sample C
was analysed directly without the need for further dilution and no matrix effect
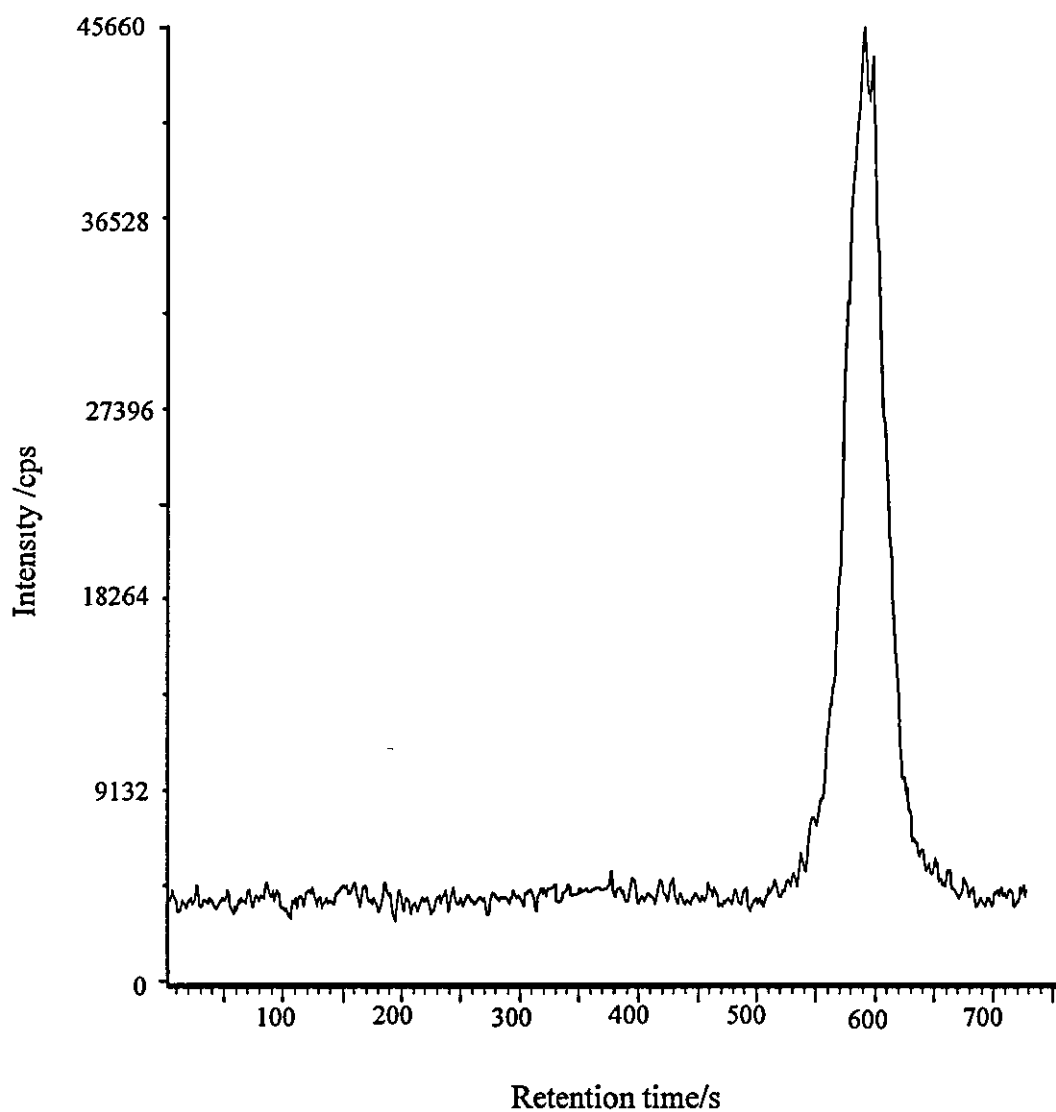
Figure 9.5. ⁸²Se HPLC-ICP-MS chromatogram of sample B.

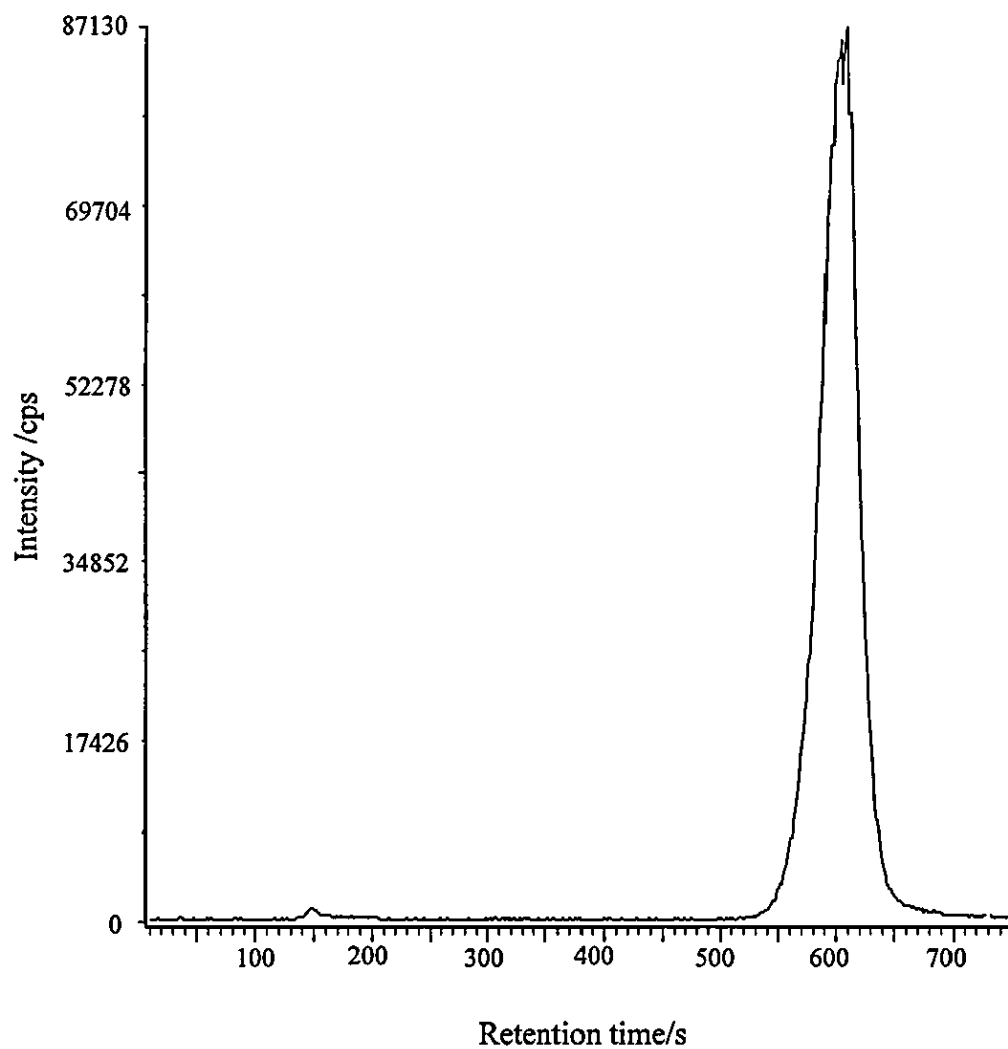*Chromatographic conditions as Fig. 9.1.*

Figure 9.6. ^{82}Se HPLC-ICP-MS chromatogram of sample C.

Chromatographic conditions as Fig. 9.1.

was observed. Since sample C was a non-yeast based supplement it would

further confirm that the matrix effect was due to the yeast itself.

SAMPLE D

The matrix effect was also apparent in the analysis of sample D, therefore the

sample was analysed at a dilution of (1 + 15). The chromatogram for sample D

(Fig. 9.7) showed one selenium peak at a retention time of 156 s and one

smaller peak with a retention time of 273 s. Spiking experiments indicated that

the major selenium containing species in the sample was SeMet, with the

identity of the peak at 273 s unknown. The behaviour of sample D in the

chromatographic system was no different to that of samples A and B and

therefore an insight into why sample D could not be analysed by CE was not

obtained.

9.3 SUMMARY

SeMet, SeCys, selenite and selenate were separated on the basis of their pH

dependent anionic character using anion exchange HPLC. The efficiency of

the separation was poor due to significant band broadening and baseline

resolution of SeMet and SeCys was not achieved. The chromatographic

conditions were not fully optimised and therefore the efficiency and resolution

could have been improved. The speciation of samples A, B and D proved to be

problematic due to an apparent matrix effect. Analysis of the samples, diluted

(1 +1) in mobile phase, was not possible because the sample matrix

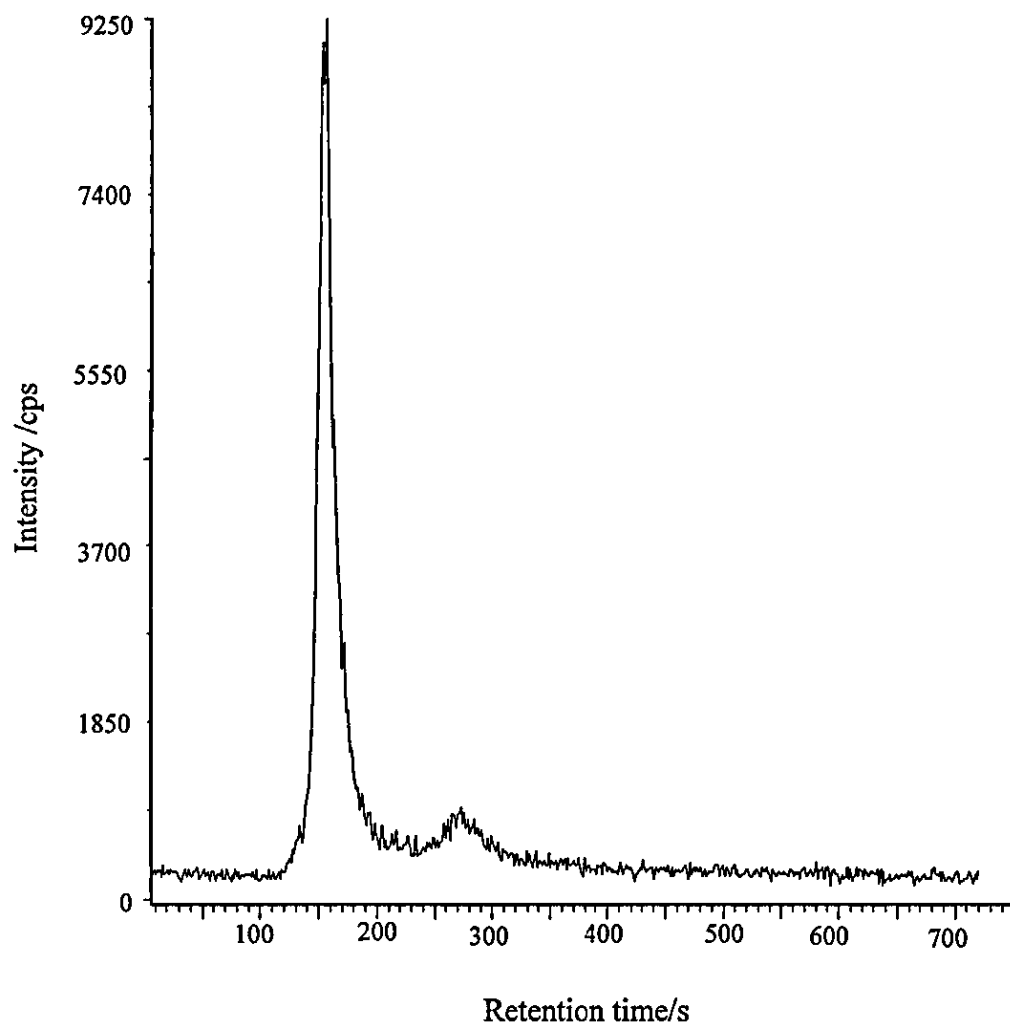preferentially bound to the active sites on the column and thus prevented

Figure 9.7. ^{77}*Se HPLC-ICP-MS chromatogram of sample D.*

Chromatographic conditions as Fig. 9.1.

retention of the analytes. By diluting the sample matrix retention of spiked

standards could be achieved. The matrix effect was not apparent in the analysis

of sample C, a non-yeast based selenium supplement. This further indicated

that the matrix effect was indeed due to the yeast itself. Speciation was

undertaken on samples diluted (1 + 15) in the mobile phase. SeMet and one

unidentified selenium species were present in sample A, inorganic selenate was

the chemical form of selenium in samples B and C, and for sample D SeMet

was the major selenium containing species.

REFERENCES

[1]A. Gilon, M. Astruc and M. Potin-Gautier, *Appl. Organomet. Chem*, 1995, 9, 623.

[2]R. M. Olivas, C. R. Quetel and O. F. X. Donard, *J. Anal At Spectrom.*, 1995, 10, *865.*

[3]M. A. Quijano, M. Gutierrez, M. C. Perez-Conde and C. Camara, *J. Anal. At. Spectrom*, 1996, 11, 407.

[4]S. M. Bird, P. C. Uden, J. F. Tyson, E. Block and E. Denoyer, *J Anal. At Spectrom*, 1997, 12, 785.

[5]S. M. Bird, H. Ge, P. C. Uden, J. F. Tyson, E. Block and E. Denoyer, *J. Chromatogr. A,* 1997, 789, 349.

[6]C. Casiot, J. Szpunar, R. Lobinski and M. Potin-Gautier, *J Anal At. Spectrom*, 1999, 36, 645.

[7]H. M. Crews, P. A. Clarke, D. J. Lewis, L. M. Owen, P. R. Strutt and A. Izquierdo, *J. Anal. At. Spectrom.*, 1996, 11, 1177.

CHAPTER TEN

Conclusions

This project set out to design a robust and efficient interface for CE-ICP-MS and to investigate the application of the technique to elemental speciation studies. Much of the work in this Thesis has focused on the development and optimisation of the interface. The significant emphasis placed on the interface design reflects the recognition that the analytical characteristics of the hyphenated technique (i.e. sample dispersion, electrophoretic resolution, detection limits and analytical precision) are all directly influenced by the interface design.

The correct choice of nebuliser and spray chamber was fundamental in designing the interface. It was apparent from the initial investigation with the Meinhard nebuliser that, for effective compatibility with the low solution flow rates employed in CE, a low flow nebuliser was necessary. In terms of the spray chamber, a low volume rapid washout spray chamber was required in order to enhance the aerosol transport efficiency and minimise sample dispersion. During the development of the cyclonic spray chamber, liquid phase dispersion was identified as the fundamental process influencing the sample response and washout times. Aerosol phase dispersion was minimal compared to that in the liquid phase. For the cyclonic spray chamber, the combination of the smaller internal volume and centrifugal transport

mechanisms allowed a more rapid sample throughput than that obtained using a

Scott-type spray chamber.

The combination of a microconcentric nebuliser and cyclonic spray chamber

provided a simple interface which was as easy to assemble as any conventional

nebuliser/spray chamber configuration. The interface, with the use of an

optimised make-up flow or the application of a negative pressure, provided

efficient sample transport without degradation of electrophoretic resolution.

However, it was found that the MCN was prone to blocking which severely

limited its effectiveness as an analytically robust interface. By replacing the

MCN with the MicroMist nebuliser, the precision of the system was

significantly improved. The advantage of using an electroosmotic flow marker

to correct for drifts in migration time was demonstrated, with a migration time

repeatability of 0.5 % RSD. The MicroMist nebuliser did, however, provide a

lower sensitivity than that of the MCN which may be attributed to a difference

in the droplet size distribution of the primary aerosols. Despite the lower

sensitivity obtained with the MicroMist, it was preferred to the MCN interface

entirely on the basis of its reproducible suction. A sensitive system has little

value if analyses cannot be repeated due to poor precision. In addition, a great

deal of time was spent unblocking the MCN which was clearly not ideal for a

system intended for routine use.

Selenoamino acids and inorganic selenium species were separated by CE under

strong electroomotic flow conditions. The electrophoretic mobilities of the

four selenium species were sufficiently different and the nebuliser suction was

sufficiently low to allow an efficient separation without the need to apply a

negative pressure. Speciation analysis of the four yeast samples showed that

the predominant selenium species varied between samples. Since the

nutritional properties of selenium are highly species dependent, the yeast

samples will therefore offer differing nutritional benefits. For sample D, an

apparent matrix effect hindered the speciation analysis. The origin of the

matrix effect was not fully identified, alternative extraction procedures need to

be investigated to determine if the matrix effect was an inherent property of the

sample or due to a species formed during the extraction process.

Analysis of the yeast samples by anion exchange HPLC-ICP-MS gave an

interesting comparison of the two separation techniques. The efficiency and

resolution of the HPLC separation was significantly poorer than that for the

electrophoretic separation. Efficiencies for selenate were 1486 and 20000

theoretical plates for the HPLC and CE methods, respectively. Although

detection limits were not determined for the HPLC method, a comparison of

the relative peak intensities for the four selenium standards would indicate that

the HPLC method offered a considerable advantage in terms of sensitivity. For

samples B and C, the results from the two speciation methods agreed and there

was no evidence to suggest speciation changes during the chromatographic

process. For sample A, however, the two methods confirmed the major

selenium species to be selenomethionine but a second peak present in the

HPLC chromatogram was not observed by CE. A matrix effect was also

observed using the LC method and clearly demonstrated the difficulties

associated with the analysis of real samples.

CE-ICP-MS clearly offers a great deal of potential for elemental speciation

analysis and may find a variety of applications in the biological and

environmental sciences (see Appendix II, CE-ICP-MS study of metal-humic

acid complexes). As a result of the small samples volumes employed in CE,

detection limits will always be compromised with respect to other speciation

techniques, such as HPLC-ICP-MS. Thus, CE-ICP-MS would benefit in the

future from the development of an interface providing 100 % analyte transport

efficiency, for example an electrospray interface. In addition, the use of a

multi-capillary in place of the single bore separation capillary may also further

enhance the capabilities of the technique.

APPENDIX I

Calibration Curves
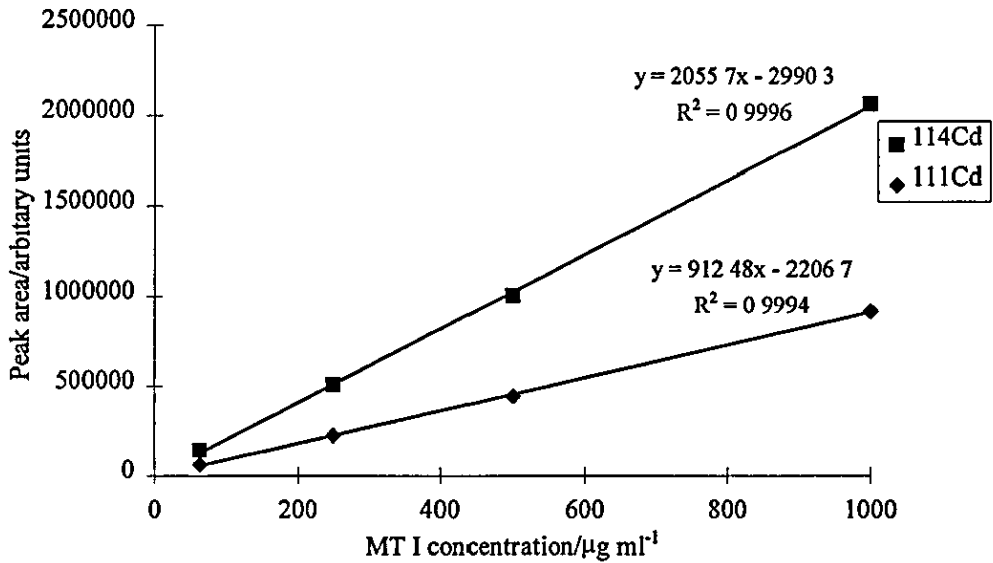
Figure I.1. *Calibration of ^{114}Cd and ^{111}Cd as a function of MT I concentration (MCN interface).*
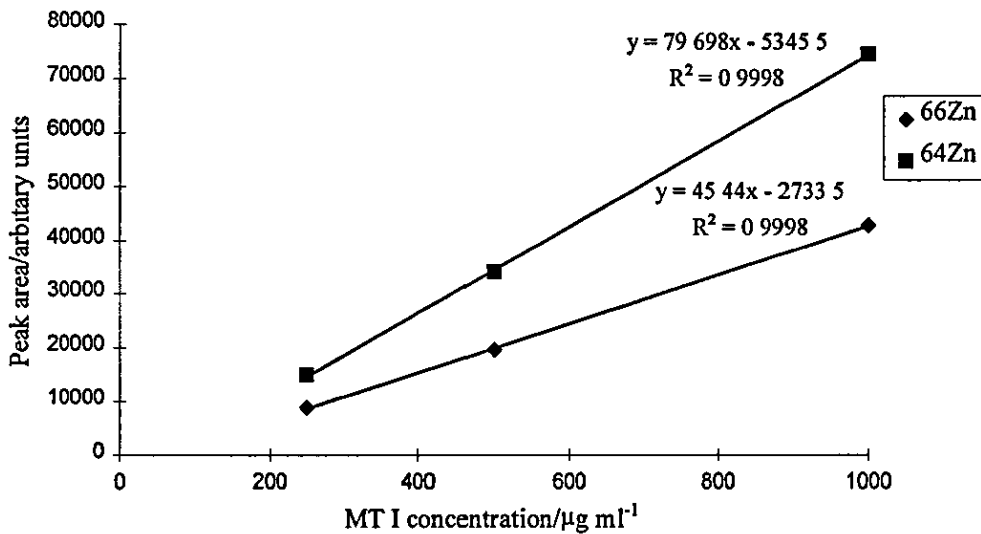
Figure I.2. *Calibration of ^{66}Zn and ^{64}Zn as a function of MT I concentration. No data points were included for the concentration 62.5 μg ml^{-1} since it was below the detection limits (MCN interface).*
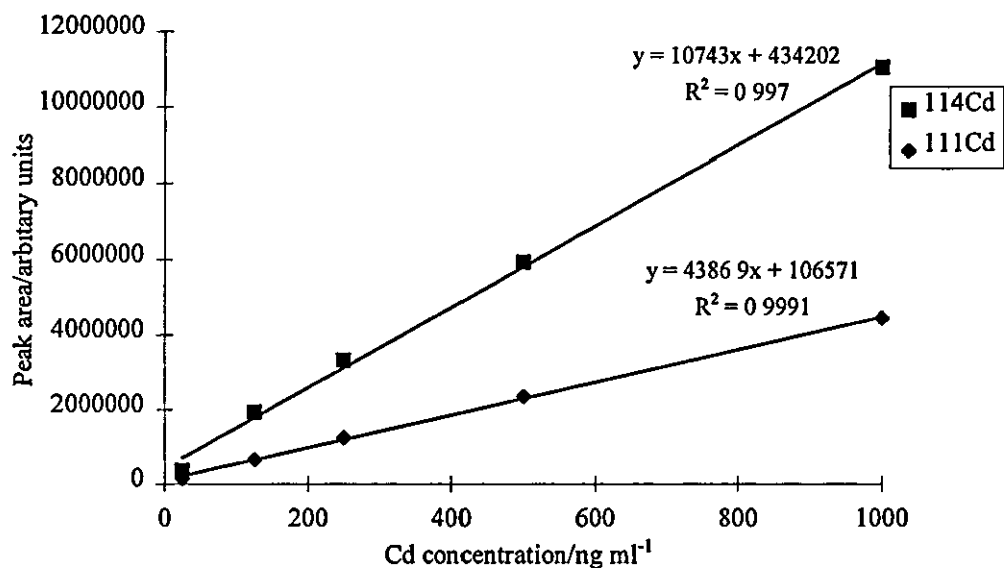
Figure I.3. ^{114}Cd *and* ^{111}Cd *calibration graphs for the determination of the*

total metal content in MT I (MCN interface).
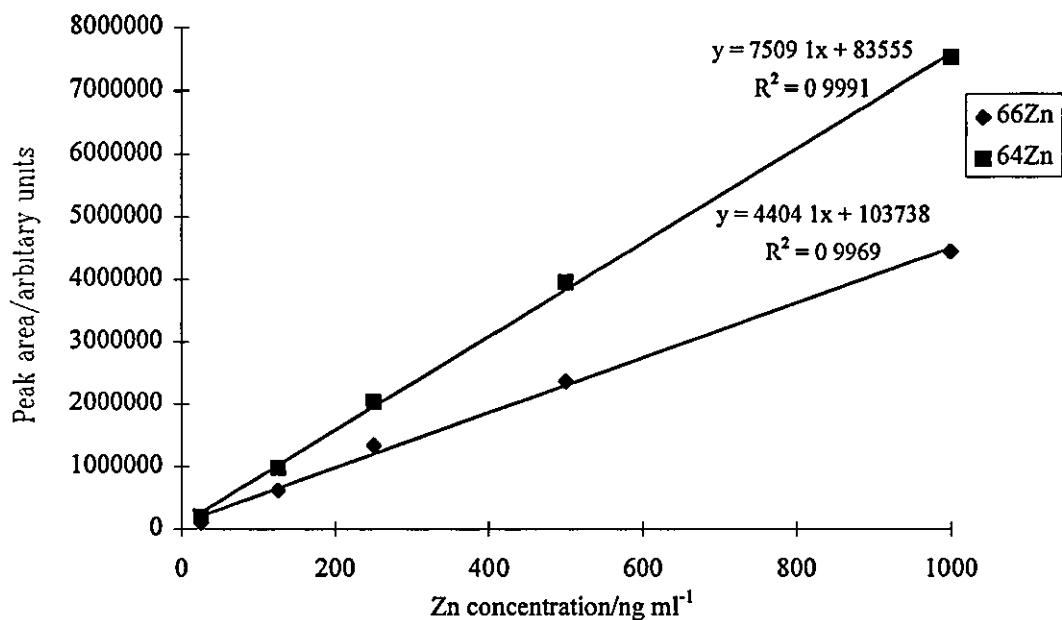
Figure I.4. ^{66}Zn *and* ^{64}Zn *calibration graphs for the determination of the*

total metal content in MT I (MCN interface).

174
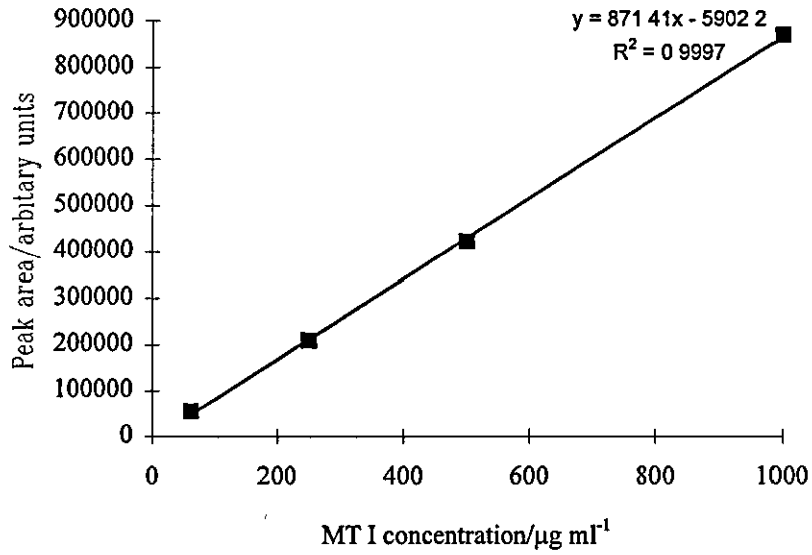
Figure I.5. Calibration of ^{114}Cd as a function of MT I concentration

(MicroMist interface).
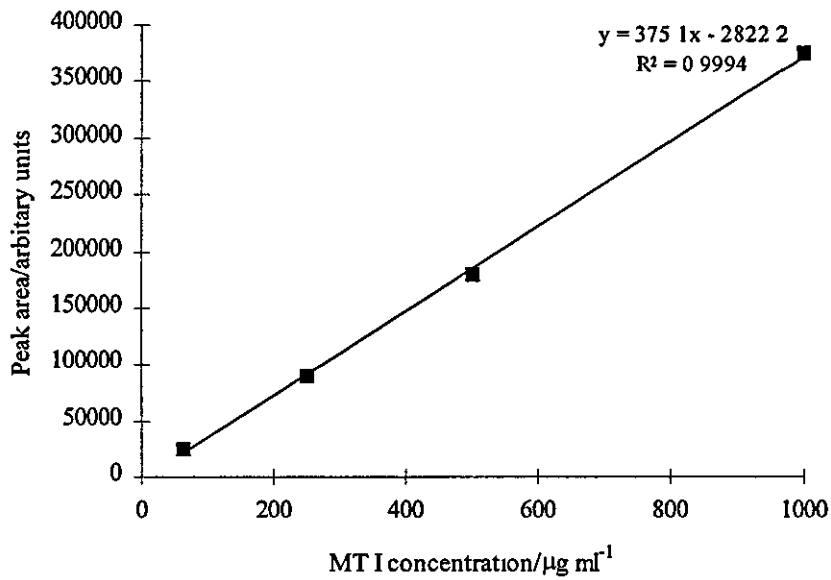
Figure I.6. Calibration of ^{111}Cd as a function of MT I concentration

(MicroMist interface).
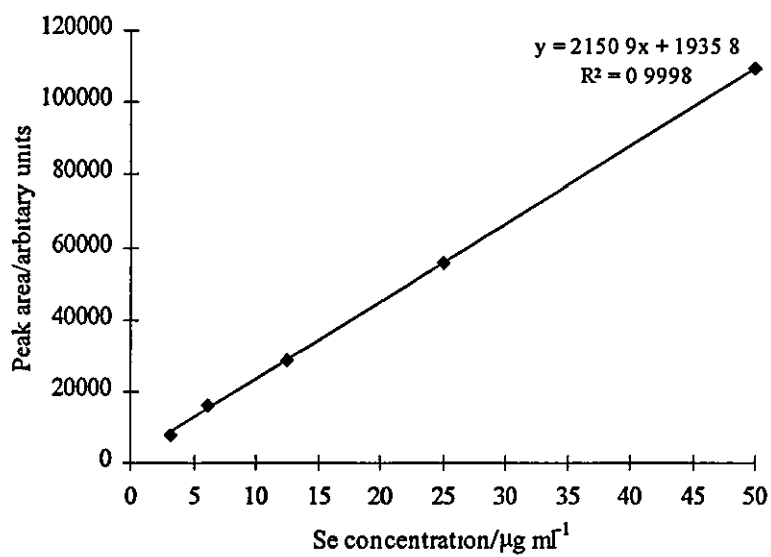
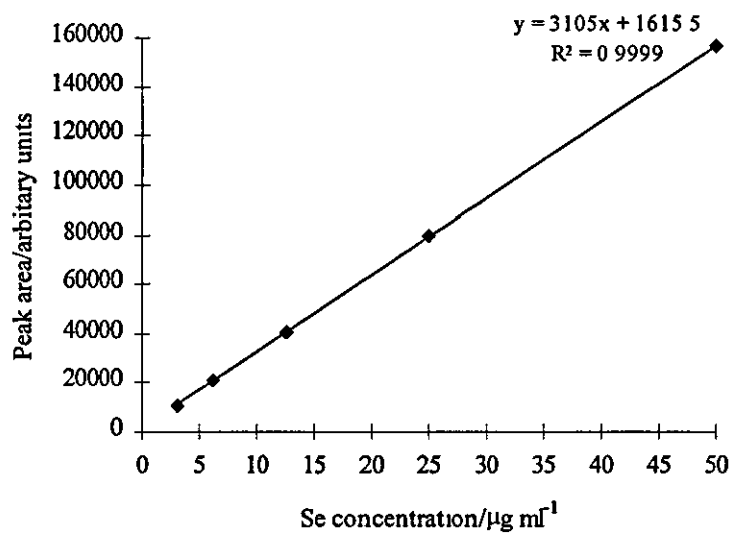*Figure I.7.* ^{82}Se *calibration curve for selenomethionine.*

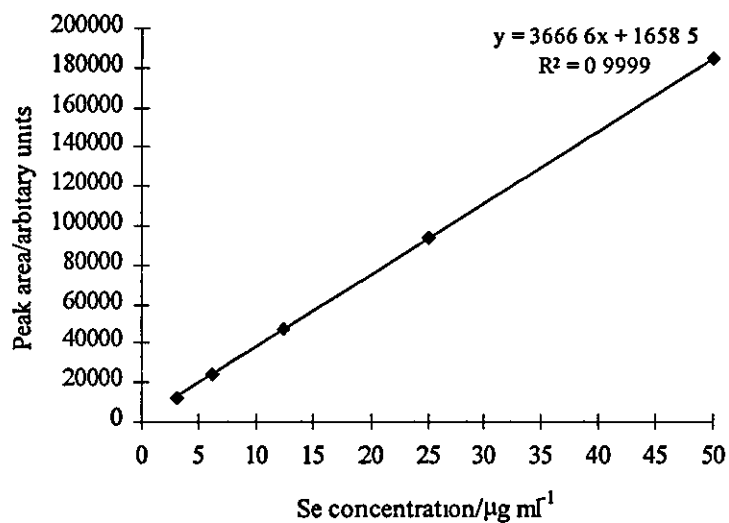*Figure I.8.* ^{82}Se *calibration curve for selenocystine.*

176

Figure I.9. ^{82}*Se calibration curve for selenite.*
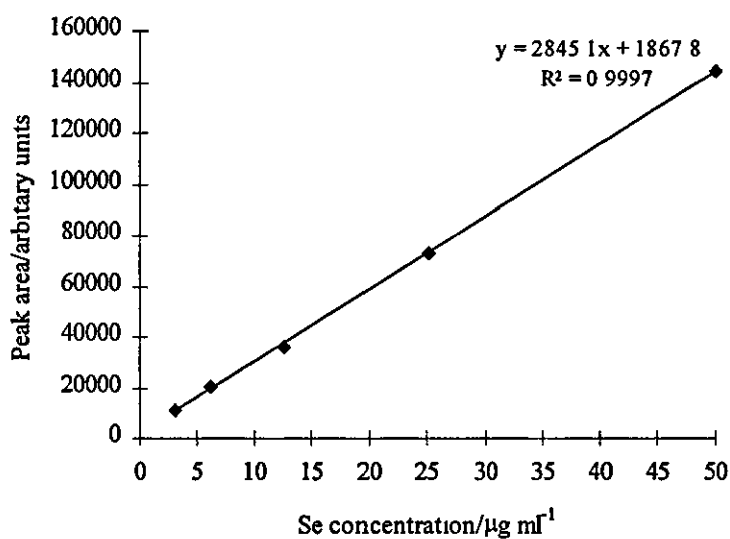

Figure I.10. ^{82}*Se calibration curve for selenate.*

APPENDIX II

CE-ICP-MS Study of Metal-Humic Acid Complexes

II.0 INTRODUCTION

Humic acids (HAs) are organic macromolecules exhibiting a wide variety of molecular mass distributions, substructures and functional groups.[1] They are found in all natural waters and soils and are composed mainly of the degradation products of living matter. Due to their polyfunctionality and high complexation capacity, humic acids are important in the environment since they have a direct influence on the bioavailability and transport of metals. Humic acids and metal-humic complexes have been separated and characterised using chromatographic[2-4] and electrophoretic techniques.[5-8] Because of the element specific detection and ability to separate cations, anions and neutral species, CE-ICP-MS appears an ideal technique for the characterisation of metal-humic complexes.

To demonstrate the potential of CE-ICP-MS, a number of Eu species were separated and detected.

II.1 EXPERIMENTAL

10 mM NH_4NO_3, 5 mM $(NH_4)_2CO_3$, 1 mM 1, 6 Diaminohexane-N,N,N',N' tetra acetic acid (HDTA) and $Eu(NO_3)_3$ were all prepared from standards (Sigma). The humic acid was a 500 μg ml^{-1} purified standard (Aldrich). $Co(gly)_3$ was used as an electroomotic flow marker.

The CE-ICP-MS system comprised of the MicroMist nebuliser interface, Prince

Crystal CE system and VG PQI ICP-MS. Eu species were separated in a 70

cm, 50 μm id fused silica capillary, using a 10 mM NH_4NO_3 buffer (pH 8 0)

and an applied voltage of 30 kV. All samples were prepared in 10mM NH_4NO_3

and mixed species were prepared by 1 + 1 dilution of the individual solutions.

II.2 RESULTS

Eight different Eu solutions were analysed (Table II.1) and the resulting

electropherograms can be seen in Fig II.1a - h.

| 1 - Eu, 2 - Eu/HA, 2 - Eu/HDTA, 4 - Eu/CO_3, |
| 5 - Eu/HA/HDTA, 6 - Eu/HA/CO_3, |
| 7 - Eu/HDTA/CO_3, 8 - Eu/HDTA/HA/CO_3 |

Table II.1. Eu samples analysed by CE-ICP-MS.

By monitoring the Eu isotopes, the distribution of Eu in the presence of the

different ligands could be seen. Free Eu and Eu carbonate were observed with

migration times very close to that of the EOF which would indicate that at pH

8.0 Eu was more likely to be present as Eu^+ than Eu^{3+}. In the presence of humic

acid, a broad Eu peak at 323 s was observed (Fig. II.1 b), and in the presence of

HDTA a peak at 248 s was detected (Fig. II.1 c). In the presence of both humic

acid and HDTA, the majority of the Eu was bound to the humic acid (Fig. II.1

e) A small shoulder on the humic acid peak was probably due to the EuHDTA

complex. When carbonate was added to a Eu/HA solution, a Eu/CO$_3$ peak was

not observed thus indicating that the Eu remained bound to the humic acid (Fig.

II.1 f). However, when carbonate was added to the Eu/HDTA solution the Eu

was distributed between both the carbonate and HDTA (Fig. II.1 g). It would

appear that carbonate suppressed, to some extent, the formation of the

EuHDTA complex. In the presence of humic acid, HDTA and carbonate, three

peaks corresponding to the Eu/CO$_3$, Eu/HA and Eu/HDTA complexes were

observed.

II.3 SUMMARY

Although very brief, this investigation has given an insight into the distribution

of Eu in the presence of various competing ligands and has clearly

demonstrated that CE-ICP-MS can be used to investigate the distribution of
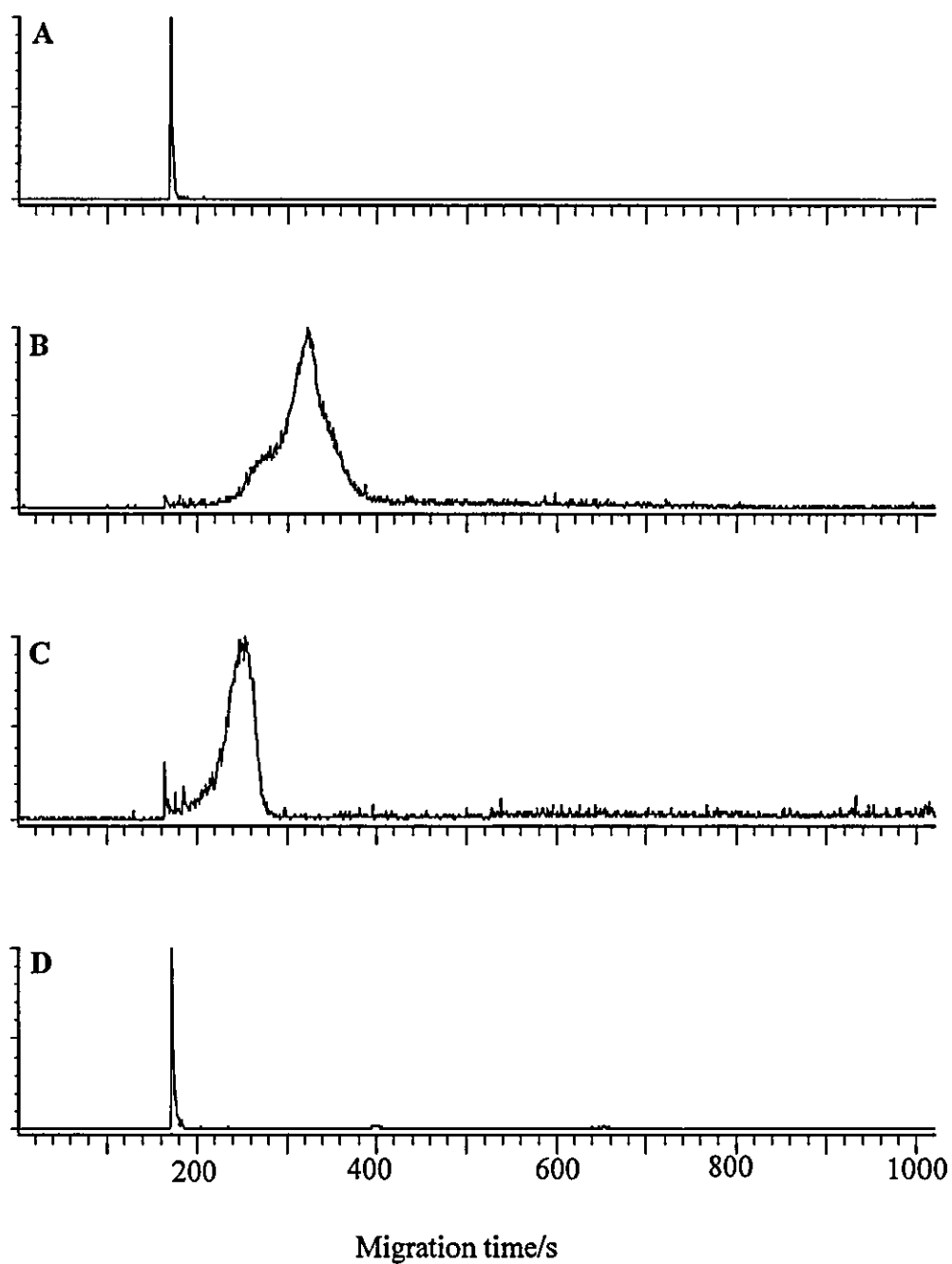
metals in the environment.

Migration time/s

Figure II.1 a - d. ^{153}Eu electropherograms. a - Eu, b - Eu/HA, c - Eu/HDTA,

d - Eu/CO$_3$. Conditions: 30 kV; 10 mM NH$_4$NO$_3$ buffer (pH 8.0); fused-silica

capillary, 50 µm id, 70 cm length; sample injection, 80 mbar for 12 s (19 nl);
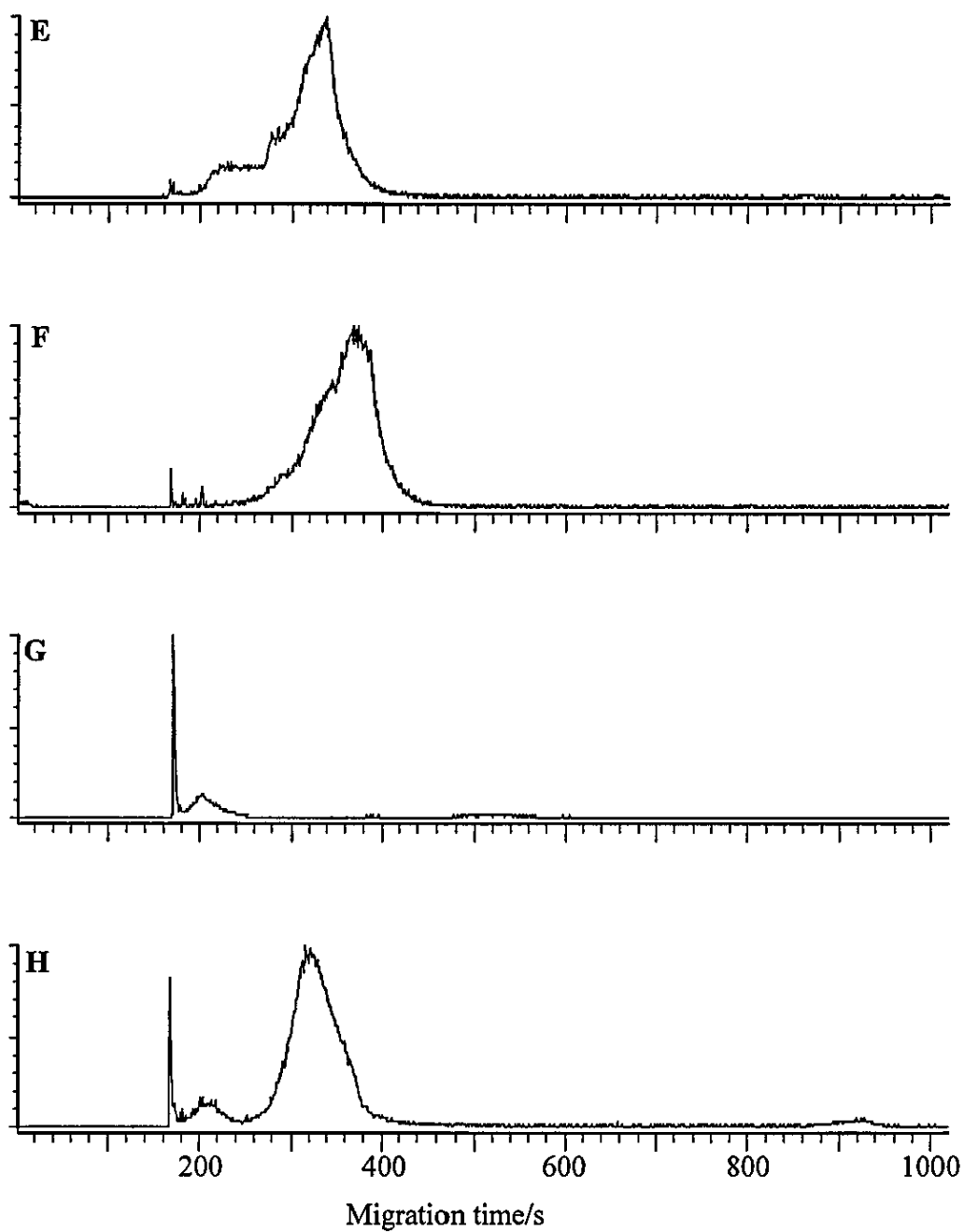
10 µl min^{-1} make-up flow rate; EOF ≈174 s.

Figure II.1 e - h. ^{153}*Eu electropherograms. e - Eu/HA/HDTA, f -*

Eu/HA/CO$_3$, g - Eu/HDTA/CO$_3$, h - Eu/HA/HDTA/CO$_3$.

REFERENCES

[1]A. Rigol, M. Vidal and G. Rauret, *J Chromatogr. A,* 1998, **807**, 275.

[2]G. Marx and K. G. Heumann, *Fresenius' J Anal. Chem,* 1999, **364**, 489.

[3]G. Woelki, S. Friedrich, G. Hanschmann and R. Salzer, *Fresenius' J. Anal Chem.,* 1997, **357**, 548.

[4]G. C. Butler and D. K. Ryan, *Abstracts of the papers of the American Chem. Soc.,* 1998, **216**, 61.

[5]D. Fetsch, M. Hradilova, E. M. P. Mendez and J. Havel, *J. Chromatogr. A,* 1998, **817**, 313.

[6]P. Schmitt-Kopplin, N. Hertorn, A. W. Garrison, D. Freitag and A. Kettrup, *Anal. Chem,* 1998, **70**, 3798.

[7]M. Norden and E. Dabek-Zlotorzynska, *Electrophoresis,* 1997, **18**, 292.

[8]D. Fetsch, M. Fetsch, E. M. P. Mendez and J. Havel, *Electrophoresis,* 1998, **19**, 2465.

APPENDIX III

Presentations and Publications

Presentations

[1]*Capillary Electrophoresis-Inductively Coupled Plasma Mass Spectrometry.*

CSL Food Science Laboratory, Norwich, 24 December 1997.

[2]*An Interface for Capillary Electrophoresis-Inductively Coupled Plasma Mass Spectrometry.*

Research and Development Topics in Analytical Chemistry meeting, Durham, 6 - 9 April 1998.

[3]*The Development of an Interface for Coupling Capillary Electrophoresis and Inductively Coupled Plasma Mass Spectrometry.*

Ninth BNASS, Bath, 8 - 10 July 1998.

[4]*Elemental Speciation By Capillary Electrophoresis-ICP-MS.*

European Winter Conference on Plasma Spectrochemistry, Pau, France, 10 - 15 January 1999.

Publications

[1]*Design and Characterisation of a Microconcentric Nebuliser Interface for Capillary Electrophoresis-Inductively Coupled Plasma Mass Spectrometry.*

J. Anal. At. Spectrom., 1998, 13, 1095-1100.

[2]*The Speciation of Selenium in Selenium Enriched Yeasts by Capillary*

Electrophoresis-Inductively Coupled Plasma Mass Spectrometry (In preparation).

Design and characterisation of a microconcentric nebuliser interface for capillary electrophoresis-inductively coupled plasma mass spectrometry

Karen A. Taylor,[a] Barry L. Sharp,*[a] D. John Lewis[b] and Helen M. Crews[b]

[a] *Department of Chemistry, Loughborough University, Loughborough, UK LE11 3TU*
[b] *CSL Food Science Laboratory, Norwich Research Park, Colney, Norwich, UK NR4 7UQ*

An interface for capillary electrophoresis (CE) and inductively coupled plasma mass spectrometry (ICP-MS) is reported. The interface was constructed using a commercial microconcentric nebuliser and home-built cyclonic spray chamber. Isoforms of the heavy metal binding protein, metallothionein, were separated and the bound metals detected to characterise the interface. Nebuliser suction was identified as the principal factor controlling separation resolution in the CE-ICP-MS system. Two methods for counterbalancing the nebuliser suction were investigated: in the first method an optimised make-up flow was employed, and in the second a negative pressure was applied to the inlet vial. Negative pressure was the preferred method for counterbalancing the nebuliser suction because sensitivity was not compromised. Separation resolution, under negative pressure conditions, was improved compared with that achieved using on-capillary UV detection. Absolute metal detection limits for ^{114}Cd, ^{111}Cd, ^{66}Zn and ^{64}Zn were 2.09, 3 42, 8 93 and 9 12 fg, respectively.

Introduction

The essentiality of trace elements in plant, animal and human nutrition has long been known. Yet it is only in the last decade that research has highlighted the importance of elemental speciation. Elemental speciation can be termed as the separation and quantification of the different oxidation states and/or chemical forms of a particular element. Its importance derives from the fact that the toxicity and nutritional benefit of many trace elements is dependent upon oxidation state and chemical form. Elemental speciation also has an important role in the environment where the absorption, transport and removal of pollutants is highly species-dependent.

One of the most popular approaches to elemental speciation analysis has been the coupling of chromatographic separation techniques with the element-specific detection of inductively coupled plasma mass spectrometry (ICP-MS) and inductively coupled plasma atomic emission spectrometry (ICP-AES) Several reviews on the use of chromatography hyphenated with ICP-MS[1–5] and ICP-AES[3,5] for speciation studies have been published. Without doubt, the most versatile hyphenated technique for elemental speciation analysis is HPLC-ICP-MS which has been widely used for the determination of trace elements in biological fluids[6–12] and for the speciation of metals in environmental media.[13–18]

Recently, capillary electrophoresis (CE) coupled to ICP-MS has received attention as a potential elemental speciation technique. CE is a powerful and versatile separation technique that has been applied to the determination of a wide variety of analytes, from small inorganic ions[19–24] to proteins.[25–29] Often utilised as a technique complementary to HPLC, CE is superior in terms of separation efficiency (particularly for high molecular mass species), sample volume required (typically 1–30 nl), analysis time, reagent consumption and analyte applicability. CE also shows unique promise for speciation purposes by exerting minimal disturbance on the existing equilibrium between different analytes. In HPLC, interactions

between the analytes and stationary phase may destroy or shift the equilibrium, resulting in inaccurate quantitative speciation information.[30]

Olesik and co-workers[31] published the first research on CE-ICP-MS in 1995 It was evident from this first publication that the key to the analytical success of CE-ICP-MS was in the design of the interface. Subsequent research published on CE-ICP-MS has therefore focused on interface design. Interfaces based on glass concentric,[31–34] glass frit,[35] high efficiency,[33] direct injection[36] (DIN), ultrasonic[37] and microconcentric[38] (MCN) nebulisers have been developed with varying degrees of success.

This paper describes a CE-ICP-MS interface based on a commercial MCN and home-built cyclonic spray chamber. The principal goal of this work was to design an interface that not only facilitates efficient sample transport without loss of electrophoretic resolution, but also is robust, simple, easily assembled and relatively inexpensive. The design of the interface and its performance characteristics, in terms of separation resolution, precision and limits of detection, will be discussed The heavy metal binding protein, metallothionein, was used to characterise the interface. Metallothionein is a low molecular mass sulfhydryl-rich protein which has a high affinity for essential (Zn, Cu) and toxic (Cd) trace metals. The suggested role of metallothionein in heavy metal metabolism and detoxification has led to numerous investigations into its unique chemical and physical properties.[39–42]

Experimental

Reagents and materials

Metallothioneins containing isoforms I and II (M7641, rabbit liver) and single isoform I (M5267, rabbit liver) were purchased from Sigma (Poole, UK). Metallothionein samples were prepared by dilution of the appropriate mass of standard with ultrapure (18.2 MΩ) Milli-Q water (Millipore, Bedford, MA, USA). The electrophoresis buffer was 20 mM Tris (Merck,

Poole, UK) adjusted to pH 7.8 with Aristar hydrochloric acid [HCl (FSA Laboratory Supplies, Loughborough, UK)]. A 10 mM ammonium nitrate [NH₄NO₃ (Merck)] solution was used as the make-up flow. The electro-osmotic flow marker was 1% mesityl oxide (Sigma) prepared by 1% (v/v) dilution in 50% methanol (Rathburn Chemicals, Walkerburn, UK).

Individual stock standard solutions of Cd, Zn, In and Ce at 1000 µg ml⁻¹ were obtained from Merck. For the total metal determination in metallothionein I (MT I), solutions containing Cd and Zn at 1000, 500, 250, 125 and 25 ng ml⁻¹ were prepared by dilution of the 1000 µg ml⁻¹ stock standard solutions in Milli-Q water. The ICP-MS instrument was tuned and optimised using a multi-element solution containing Be, Mg, Co, Ni, In, Ce, Pb, Bi and U at 25 ng ml⁻¹ per metal, prepared by dilution of a stock standard solution [ICP-MS 100 solution (SPEX Industries, Edison, NJ, USA)] in 1% Aristar nitric acid [HNO₃ (Merck)].

Fused-silica capillaries (50 µm id, 375 µm od) were purchased from Composite Metal Services (Worcester, UK). Capillaries were pre-conditioned using 0 5 M NaOH (Merck) prior to their first use.

Instrumentation

CE system. Separations were performed using a Prince Technologies Crystal 310 CE system (Prince Technologies, Sunderland, UK) The Crystal 310 CE system has a double piston arrangement that allows both positive and negative pressures to be applied to the inlet vial. A 4225 variable UV/VIS detector (Thermo Separation Products, Hemel Hempstead, UK) was used for on-capillary UV detection. A fused-silica capillary (total length 77 cm, 60 cm to window) was used and an absorbing wavelength of 200 nm was monitored. The separation voltage (that yielding the best resolution of the metallothionein isoforms) was optimised at 25 kV Samples were injected hydrostatically (80 mbar for 6 s) and the capillary was rinsed with buffer for 2 min between each run. Electropherograms were recorded using a Dell OptiPlex Gs computer and ProGC software (Thermo Unicam, Cambridge, UK).

ICP-MS. A VG PlasmaQuad (PQ II Turbo Plus) inductively coupled plasma mass spectrometer (VG Elemental, Winsford, UK) was used throughout this work. Data acquisition and interpretation was performed using Time Resolved Analysis (TRA) and Masslynx software (VG Elemental). The ICP-MS operating conditions are summarised in Table 1.

CE-ICP-MS interface. The CE-ICP-MS interface incorporated a commercial MCN M2S (CETAC Technologies, Cheshire, UK), a 1/16 in PTFE T-piece (Omnifit, Cambridge, UK) and a small cyclonic spray chamber (fabricated locally). A schematic diagram of the interface is presented in Fig. 1.

The separation capillary was passed through a hole in the side of the Crystal CE system and was inserted through the T-piece and into a Pt-Ir tube [0.65 mm id (Johnson Matthey, Reading, UK)]. The Pt-Ir tube and capillary were then connected directly into the back of the MCN using a standard

Table 1 ICP-MS operating conditions

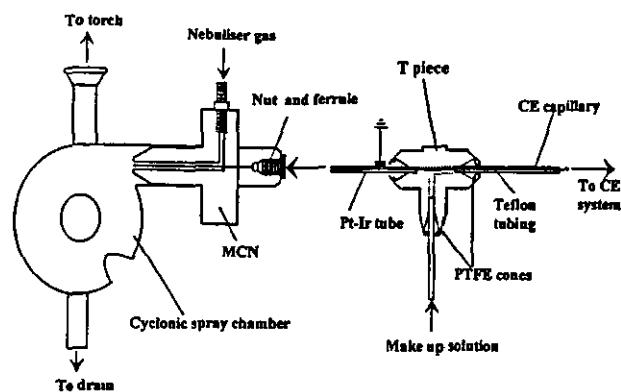| Rf power	1350 W
Reflected power	0 W
Coolant gas flow	13 5 l min⁻¹
Auxiliary gas flow	1 45 l min⁻¹
Nebuliser gas flow	0 90 l min⁻¹
Sampler cone	Ni, 1 0 mm orifice
Skimmer cone	Ni, 0 7 mm orifice
Measurement mode	Peak jump (dwell time 10 24 ms)
Isotopes monitored	¹¹⁴Cd, ¹¹¹Cd, ⁶⁶Zn, ⁶⁴Zn

Fig. 1 Schematic diagram of the CE-ICP-MS interface.

nut and ferrule. The capillary was sheathed, up to the point of entering the T-piece, using Teflon tubing (0.03 in id, 0.063 in od). The capillary sheath was necessary in order to maintain a constant temperature, and current, within the capillary and therefore provide reproducible results Grounding of the capillary was achieved by the use of a coaxial sheath of electrolyte solution which was pumped through the vertical arm of the T-piece using a Gilson Minipuls 3 peristaltic pump (Gilson Medical Electronic, Villiers-Le-Bel, France). Undesirable pulsing of the peristaltic pump at low flow rates was minimised by using microbore pump tubing (0.19 mm bore) and higher pump rotation rates. A microbore HPLC pump (Dionex GP40 Microbore Gradient Pump, Dionex, Camberley, UK) and self-aspiration were investigated as possible alternatives to the peristaltic pump The HPLC pump was deemed unsuitable because of irregular pulsing at low flow rates and self-aspiration was found to give a more stable baseline but was practically difficult to adopt. To complete the electrical circuit the Pt-Ir tube was connected to the ground electrode of the CE system via a crocodile-type clip. The nebuliser was inserted into a small cyclonic spray chamber which was connected to the ICP torch via a flexible Teflon tube.

The cyclonic spray chamber was designed specifically for use in the CE-ICP-MS interface. It was fabricated from glass and had a general spherical shape with a drain at the base and a horizontal mounting for the MCN on the side The internal volume was 21.0 ml. A schematic diagram and photograph of the spray chamber are shown in Fig 2a and b, respectively. Sample aerosol from the nebuliser was directed horizontally and intersected the chamber wall tangentially This arrangement resulted in the sample aerosol experiencing a centrifugal force which served to remove larger droplets. A dimple of 2.5 cm diameter was impressed into one side of the spray chamber and had the effect of disrupting the circulating flow of aerosol, thereby generating turbulence and forcing larger droplets to collide with the dimple and with the outer wall of the chamber. The design of the dimple was based upon those incorporated in small vertical rotary spray chambers described by Wu and Hieftje[43] and Wu et al.[44] A flow spoiler was also impressed into the body of the spray chamber and was designed to stall the circulating flow of aerosol, thus preventing recirculation. Recirculation can lead to sample dispersion, increased sample washout times and band broadening,[45] and is therefore undesirable in a spray chamber intended for CE-ICP-MS.

Results and discussion

Cyclonic spray chamber

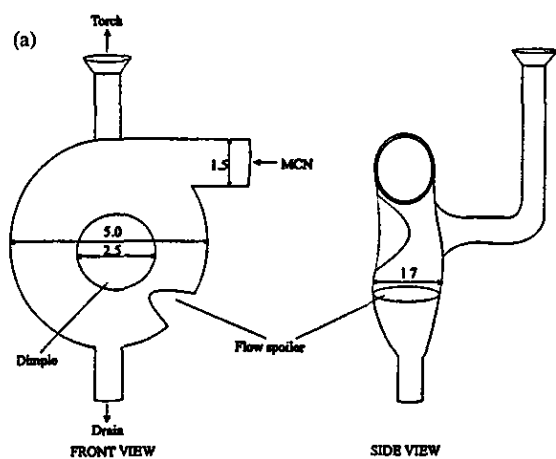The analytical performance of the cyclonic spray chamber was assessed by measurement of sample response and washout

Fig. 2 a, Diagram of the cyclonic spray chamber illustrating front and side views All units in cm. b, Photograph of the cyclonic spray chamber

times These criteria are critical in CE-ICP-MS since they have a direct influence on band broadening. A test solution, containing In and Ce at 25 ng ml^{-1}, was introduced directly into the nebuliser using a peristaltic pump and the ^{115}In signal was monitored using TRA. The response time was defined as the time taken for the signal to equilibrate at its maximum value. Sample washout times were measured by replacing the test solution with a 1% HNO$_3$ blank and monitoring the signal decay. Washout time was defined here as the period required for a signal to fall to 1% of its initial value [46] For comparative purposes the measurements were repeated using an MCN/Scott-type double pass spray chamber and cross-flow/Scott-type spray chamber combination. In addition, a cyclonic spray chamber identical in design with that described but with a smaller internal volume (6 5 ml) was assessed. The nMCN was operated at 100 µl min^{-1} which was close to its natural aspiration rate and the cross-flow nebuliser was run at 0.7 ml min^{-1}, the standard flow rate of routine analysis. For the MCN, a reduction in the solution flow rate, at least to 10 µl min^{-1}, did not significantly affect sample response and washout times.

The data compiled in Table 2 demonstrate that the cyclonic spray chamber is superior to the conventional Scott-type chamber with respect to sample response and washout times. Both the 21.0 and 6.5 ml cyclonic spray chambers have sample response and washout times of 6 and 8 s, respectively. In contrast, the response and washout times for the Scott-type

chamber were 15 and 28 s, respectively. Thus, the cyclonic chamber offers a sample throughput that is 3.5 times faster than that provided by the conventional Scott-type chamber.

Separation resolution and precision

CE is capable of achieving a high separation resolution and it is therefore crucial that this resolution is not degraded when the sample components are transported through the interface to the plasma. To assess whether the interface adversely affected separation resolution, rabbit liver metallothionein was separated and detected on-capillary using a UV detector. This separation was then repeated using CE-ICP-MS and the corresponding separation resolutions were compared. Separation resolution (Rs) was calculated using the following equation:[47]

$$Rs = \frac{1}{4}\left(N^{1/2}\frac{\Delta t}{\bar{t}}\right)$$

where N is the efficiency, Δt is the difference in migration time of MT I and MT II (s) and $\bar{t}$ is the mean migration time (s).

The UV detected electropherogram of rabbit liver metallothionein is illustrated in Fig. 3. The two predominant peaks were identified as the two major isoforms of metallothionein, MT I and MT II The isoforms were well resolved with $Rs = 2.45$ The identity of the four smaller peaks observed in the electropherogram is not known. It is probable, however, that these peaks are other isoforms of metallothionein. It has been reported that rabbit liver metallothionein may consist of up to six individual isoforms, although only MT I and MT II have been identified.[39,40]

For CE-ICP-MS, it was necessary to optimise the make-up flow rate in order to minimise the nebuliser suction and allow a good resolution of the two isoforms. Suction from self-aspirating concentric nebulisers has a detrimental effect upon separation resolution by inducing laminar flow within the separation capillary. Kinzer et al.[33] reported that this suction can be offset by pumping make-up solution, at a sufficient flow rate, to the nebuliser.

Rabbit liver metallothionein separations were performed using make-up flow rates between 10 and 100 µl min^{-1} A flow rate of 80 µl min^{-1} was found to provide the optimum resolution of the two isoforms (Fig. 4) The separation resolution of MT I and MT II for ^{114}Cd was 2.52. This was marginally superior to that obtained by UV detection. At make-up flow rates below the optimum, separation resolution deteriorated as a result of increased suction from the MCN. This is illustrated in Fig. 5, which shows the CE-ICP-MS electropherogram obtained using a make-up flow rate of 10 µl min^{-1}. At 10 µl min^{-1}, inadequate compensation for the nebuliser suction was achieved and consequently the sample components were drawn through the capillary, resulting in a complete loss of resolution of the two isoforms.

To prevent air bubbles and excess of sample being loaded into the capillary, as a result of the nebuliser suction, the make-up flow rate was increased (to the natural aspiration rate of the MCN) after the buffer rinse and was resumed to the experimental rate immediately upon application of the voltage In previous interfaces,[32,33] the nebuliser gas flow has been turned off during sample injection to prevent such problems. However, we have found that this method reduced the overall precision of the system because of the time taken in resuming the gas flow to its original value. The nebuliser gas flow rate must be increased slowly to prevent possible extinction of the plasma; consequently, the probability of associated irreproducibilities was enhanced.

Negative pressure. Under optimum conditions, the CE-ICP-MS interface did not adversely affect the separation

Table 2 Comparison of the analytical performance of various nebuliser/spray chamber combinations (all values are the mean of three replicates) Test solution delivered at 100 µl min^{-1} to MCN and 0 7 ml min^{-1} to cross-flow nebuliser

Nebuliser/ spray chamber	Response time/s	Washout time/s	^{115}In response/ counts s^{-1}	CeO$^+$/ Ce$^+$ (%)	Ce^{2+}/ Ce$^+$ (%)
Cross-flow/Scott	13	25	2.4 × 10^5	0 9	0 8
MCN/Scott	15	28	1 6 × 10^5	0.7	0 6
MCN/cyclonic (21 0 ml)	6	8	1 8 × 10^5	0 7	0 6
MCN/cyclonic (6 5 ml)	6	8	1 3 × 10^5	0 6	0 6

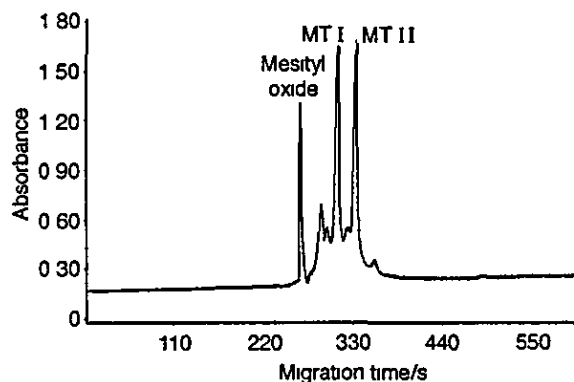
Fig. 3 UV detected electropherogram of rabbit liver metallothionein (1000 µg ml^{-1}) Conditions UV wavelength, 200 nm, 25 kV applied voltage, fused-silica capillary, 50 µm id, 77 cm total length, 60 cm to window; sample injection, 80 mbar for 6 s (19 nl ; 20 mM Tris HCl buffer (pH 7 8), neutral marker, 1% mesityl oxide, marker injection, 15 mbar for 3 s.
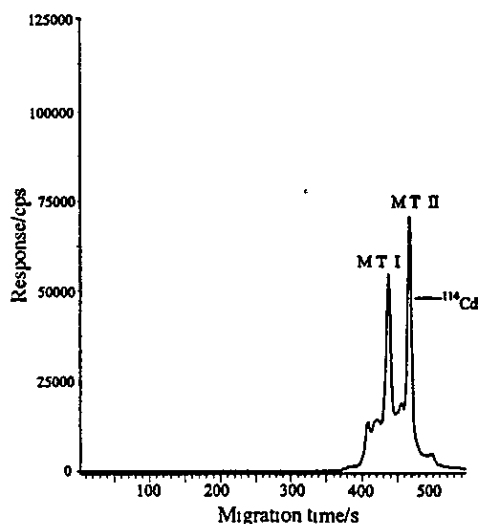

Fig. 4 CE-ICP-MS electropherogram (for ^{114}Cd) of rabbit liver metallothionein (1000 µg ml^{-1}) Conditions 25 kV applied voltage, fused-silica capillary, 50 µm id, 77 cm length, sample injection, 80 mbar for 6 s (19 nl), 20 mM Tris HCl buffer (pH 7 8), 80 µl min^{-1} make-up flow rate (0 01 M NH$_4$NO$_3$).

resolution of the two metallothionein isoforms. In fact, the resolution was marginally improved compared with that obtained by UV detection. However, as a consequence of employing a make-up flow rate of 80 µl min^{-1}, the sample was significantly diluted and sensitivity reduced. With an injected sample volume of 19 nl and an analyte peak width of 7 s, the dilution factor was 491. Clearly, this was not ideal since separation resolution compromised sensitivity To ensure that neither separation resolution nor sensitivity was compromised, a method of overcoming nebuliser suction without employing a high make-up flow rate was required In a previous concentric nebuliser interface, Lu et al.[32] applied a negative pressure to
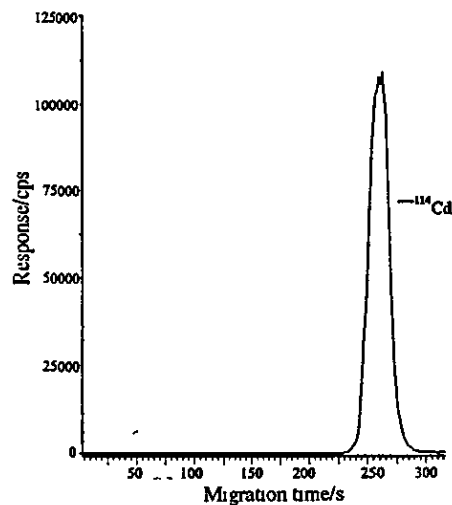

Fig. 5 CE-ICP-MS electropherogram of rabbit liver metallothionein (1000 µg ml^{-1}) Conditions as in Fig 4, except that a 10 µl min^{-1} make-up flow rate was used.

the inlet vial to counterbalance the nebuliser suction and, under negative pressure, an improvement in separation resolution was reported.

The effect of applying a negative pressure to the inlet vial during the separation of rabbit liver metallothionein can be seen in the electropherogram presented in Fig 6. This separation was performed using a make-up flow rate of 10 µl min^{-1} and a pressure of −130 mbar (applied by the CE system) At a make-up flow rate of 10 µl min^{-1}, suction from the MCN was prominent, but the applied negative pressure was sufficient to counterbalance this suction and the result was an excellent separation of the two isoforms ($Rs = 3$). The migration times
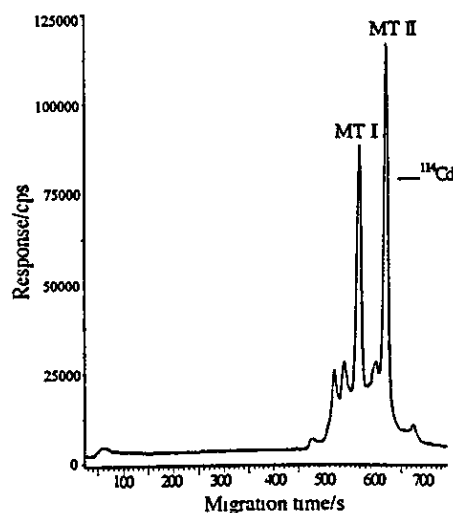

Fig. 6 CE-ICP-MS electropherogram of rabbit liver metallothionein (1000 µg ml^{-1}) Conditions as in Fig. 4, except that a 10 µl min^{-1} make-up flow rate and −130 mbar applied pressure were used

and resolution values listed in Table 3 demonstrate the effect of employing a negative pressure Resolution, under negative pressure, was improved compared with that obtained using a high make-up flow rate This indicated that, even at an 80 µl min^{-1} make-up flow rate, suction from the nebuliser was present and had a detrimental effect upon resolution The presence of nebuliser suction at an 80 µl min^{-1} make-up flow rate was also indicated by the shorter migration times. The resolution achieved using a negative pressure was also superior to that observed with UV detection This increase in resolution was largely due to a change in the capillary length but may also be related to the element-specific detection. The length of capillary used with the CE-ICP-MS interface was 17 cm greater than that employed with the UV detector. Separation resolution is directly related to capillary length (although a maximum length limit exists above which resolution deteriorates due to molecular diffusion). The expected increase in sensitivity associated with reducing the make-up flow rate to 10 µl min^{-1} was not achieved, with a factor of 2 improvement. This may be an indication that the MCN was beginning to show marginal performance at such low solution flow rates.

Precision. The precision of the CE-ICP-MS system was assessed by measurement of the migration time, peak area and peak height reproducibilities of MT I and MT II. Ten repetitive separations of rabbit liver metallothionein (1000 µg ml^{-1}) were performed and ^{114}Cd peak areas were integrated using Masslynx. Precision values were between 8 and 15% RSD (Table 4)

Detection limits

CE-ICP-MS detection limits for the isotopes ^{114}Cd, ^{111}Cd, ^{66}Zn and ^{64}Zn were determined, under negative pressure conditions, using rabbit liver MT I. The ICP-MS peak areas were integrated using Masslynx and calibrated as a function of MT I concentration. Signals for the four isotopes were linear (for the concentration range 1000–62 5 µg ml^{-1} MT I) with correlation coefficients of 0.9996, 0.9994, 0 9998 and 0.9998 for ^{114}Cd, ^{111}Cd, ^{66}Zn, and ^{64}Zn respectively. MT I concentration detection limits were determined from 3σ of the blank signal. To determine the concentration detection limits of metals bound to MT I, it was necessary to quantify the total metal content in MT I. A 1000 µg ml^{-1} solution of MT I was diluted with Milli-Q water to 5 µg ml^{-1} and the metal concentration in this sample was measured against an aqueous standard calibration The percentage by mass of metallothionein was 7.28, 7.20, 0 68 and 0 66% for ^{114}Cd, ^{111}Cd, ^{66}Zn and ^{64}Zn, respectively.

The CE-ICP-MS concentration detection limits of MT I, the concentration detection limits of the metals bound to MT

Table 3 Effect of negative pressure upon separation resolution

| Make-up flow rate/ µl min^{-1} | Applied negative pressure/mbar | Migration time/s | | Resolution |
		MT I	MT II	
80^a	0	438	468	2 52
10^a	−130	568	619	3 00
0^b	0	313	333	2 45

^{a}ICP-MS detection. ^{b}UV detection

Table 4 CE-ICP-MS precision data

	MT I RSD (%)	MT II RSD (%)
Migration time	8	9
Peak area	15	13
Peak height	11	12

Table 5 CE-ICP-MS detection limits (determined using a make-up flow rate of 10 µl min^{-1} and −130 mbar applied pressure)

	^{114}Cd	^{111}Cd	^{66}Zn	^{64}Zn
MT I concentration LOD/ µg ml^{-1} solution	1 52	2 52	68.74	71 97
Metal concentration LOD/ µg g^{-1} MT	0 11	0 18	0 47	0 48
Metal absolute LOD/fg	2 09	3 42	8 93	9 12

I and the absolute metal detection limits, based on a 19 nl injection volume, are presented in Table 5. The detection limits varied with the amount of specific metal bound to MT I and with the instrumental sensitivity for each metal. The detection limit for ^{114}Cd was a factor of 2 lower than that previously reported for a concentric nebuliser interface.[32] Compared with the ultrasonic nebuliser interface reported by Lu and Barnes,[37] detection limits for Cd were higher (by < factor of 2) but were lower for Zn (by a factor of 4). The poorer sensitivity for Cd, compared with that for the ultrasonic nebuliser interface, is compensated by the simplicity, ease of use and financial cost of the MCN interface.

Conclusions

There is no doubt that the key to the analytical success of CE-ICP-MS lies in the design of the interface. Efficient sample transport without degradation of separation resolution is the principal function of the interface, but for viable routine use the interface must also be robust and relatively simple. The CE-ICP-MS interface described here is robust, simple, easily assembled and relatively inexpensive. Degradation of separation resolution resulting from nebuliser suction is overcome, without compromising sensitivity, by applying a negative pressure to the inlet vial. This study has demonstrated that the CE-ICP-MS system is suitable for the separation and quantification of metals bound to metallothionein isoforms The challenge now must be to establish unique elemental speciation applications for CE-ICP-MS.

References

1 G K. Zoorob, J. W McKiernan and J. A Caruso, *Mikrochim. Acta*, 1998, **128**, 145.
2 K. Sutton, R. M. C Sutton and J A. Caruso, *J Chromatogr A*, 1997, **789**, 63.
3 L. A. Ellis and D. J Roberts, *J Chromatogr A*, 1997, **774**, 3
4 F. A Byrdy and J A Caruso, *Environ. Sci. Technol.*, 1994, **28**, 528A.
5 S. J. Hill, M. J Bloxham and P. J. Worsfold, *J. Anal. At Spectrom.*, 1993, **8**, 499
6 S C. K. Shum, H Pang and R S. Houk, *Anal. Chem.*, 1992, **64**, 2444.
7 K. Takatera and T. Watanabe, *Anal. Chem.*, 1993, **65**, 759
8 G Zoorob, M. Tomlinson, J. Wang and J Caruso, *J Anal. At Spectrom.*, 1995, **10**, 853
9 B Gerken and R. M Barnes, *Anal. Chem.*, 1991, **63**, 283
10 U. Kumar, J. G Dorsey, J A. Caruso and E H. Evans, *J Chromatogr Sci.*, 1994, **32**, 282
11 S C K. Shum and R S Houk, *Anal. Chem.*, 1993, **65**, 2972
12 L. M W. Owen, H. M. Crews, R C Hutton and A. Walsh, *Analyst*, 1992, **117**, 649
13 H. Yang, S Jiang, Y. Yang and C Hwang, *Anal. Chim. Acta*, 1995, **312**, 141.
14 P Thomas and K. Sniatecki, *J Anal. At Spectrom.*, 1995, **10**, 615
15 C. Huang and S. Jiang, *J Anal At Spectrom.*, 1993, **8**, 681
16 A. Al-Rashdan, N. P Vela, J. A. Caruso and D T Heitkemper, *J Anal. At Spectrom.*, 1992, **7**, 551

17 J W. McLaren, K. W M Siu, J. W Lam, S N Willie, P. S Maxwell, A Palepu, M Koether and S S Berman, *Fresenius' J. Anal. Chem.*, 1990, 337, 721.
18 J Wang, M J Tomlinson and J. A. Caruso, *J Anal. At. Spectrom.*, 1995, 10, 601
19 M J Thornton and J S Fritz, *J Chromatogr, A*, 1997, 770, 301.
20 E Simunicova, D Kaniansky and K. Loksikova, *J Chromatogr, A*, 1994, 665, 203
21 Y Shi and J S Fritz, *J Chromatogr*, 1993, 640, 473.
22 M Chen and R. M. Cassidy, *J. Chromatogr*, 1993, 640, 425
23 P Jandik, W R. Jones, A. Weston and P R Brown, *LC-GC*, 1991, 9, 634
24 K. Ito and T Hirokawa, *J Chromatogr A*, 1996, 742, 281
25 M A. Jenkins and M D Guerin, *J Chromatogr B*, 1996, 682, 23
26 E. Jellum, H. Dollekamp and C Blessum, *J Chromatogr B*, 1996, 683, 55
27 K. A. Denton and S. A. Tate, *J Chromatogr B*, 1997, 697, 111.
28 P. A. McDonnell, G W Caldwell and J. A. Masucci, *Electrophoresis*, 1998, 19, 448
29 M. Rabiller Baudry, A. Bouguen, D Lucas and B. Chaufer, *J. Chromatogr B*, 1998, 706, 23
30 E Dabek-Zlotorzynska, E. P C. Lai and A. R. Timerbaev, *Anal. Chim. Acta.*, 1998, 359, 1.
31 J. W Olesik, J. A. Kinzer and S V Olesik, *Anal. Chem.*, 1995, 67, 1.
32 Q Lu, S M Bird and R. M. Barnes, *Anal. Chem.*, 1995, 67, 2949.
33 J A. Kinzer, J W. Olesik and S V Olesik, *Anal. Chem.*, 1996, 68, 3250
34 B Michalke and P Schramel, *Fresenius' J Anal. Chem.*, 1997, 357, 594
35 M J. Tomlinson, L Lin and J. A Caruso, *Analyst*, 1995, 120, 583
36 Y Liu, V Lopez-Avila, J. J Zhu, D R Wiederin and W. F Beckert, *Anal. Chem.*, 1995, 67, 2020
37 Q. Lu and R M. Barnes, *Microchem. J.*, 1996, 54, 129
38 E. Mei, H. Ichihashi, W Gu and S. Yamasaki, *Anal. Chem.*, 1997, 69, 2187
39 V Virtanen, G Bordin and A-R. Rodriguez, *J Chromatogr A*, 1996, 734, 391.
40 M. P Richards and J H Beattie, *J Chromatogr B*, 1995, 669, 27
41 J. H. Beattie and M P. Richards, *J Chromatogr A*, 1995, 700, 95.
42 G Liu, W Wang and X. Shan, *J Chromatogr B*, 1994, 653, 41
43 M. Wu and G. M Hieftje, *Appl Spectrosc*, 1992, 46, 1912.
44 M. Wu, Y. Madrid, J. A. Auxier and G. M. Hieftje, *Anal. Chim. Acta*, 1994, 286, 155
45 J. A. Koropchak, S Sadain and B Szostek, *Spectrochim. Acta, Part B*, 1996, 51, 1733.
46 B L. Sharp, *J Anal. At. Spectrom.*, 1988, 3, 939.
47 *Capillary Electrophoresis Theory and Practice*, ed. P. D Grossman and J. C. Colburn, Academic Press, San Diego, CA, 1992.

Paper 8/03822H